Engineering with Computers (2023) 39:1935–1979
https://doi.org/10.1007/s00366-021-01542-0

ORIGINAL ARTICLE

Boosting whale optimization with evolution strategy and Gaussian random walks: an image segmentation method

Abdelazim G. Hussien[1,2] · Ali Asghar Heidari[3] · Xiaojia Ye[4] · Guoxi Liang[5] · Huiling Chen[3] · Zhifang Pan[6]

Received: 18 January 2021 / Accepted: 27 October 2021 / Published online: 27 January 2022

Abstract
Stochastic optimization has been found in many applications, especially for several local optima problems, because of their ability to explore and exploit various zones of the feature space regardless of their disadvantage of immature convergence and stagnation. Whale optimization algorithm (WOA) is a recent algorithm from the swarm-intelligence family developed in 2016 that attempts to inspire the humpback whale foraging activities. However, the original WOA suffers from getting trapped in the suboptimal regions and slow convergence rate. In this study, we try to overcome these limitations by revisiting the components of the WOA with the evolutionary cores of Gaussian walk, CMA-ES, and evolution strategy that appeared in Virus colony search (VCS). In the proposed algorithm VCSWOA, cores of the VCS are utilized as an exploitation engine, whereas the cores of WOA are devoted to the exploratory phases. To evaluate the resulted framework, 30 benchmark functions from IEEE CEC2017 are used in addition to four different constrained engineering problems. Furthermore, the enhanced variant has been applied in image segmentation, where eight images are utilized, and they are compared with various WOA variants. The comprehensive test and the detailed results show that the new structure has alleviated the central shortcomings of WOA, and we witnessed a significant performance for the proposed VCSWOA compared to other peers.

Keywords Exploration and exploitation · Nature-inspired method · Metaheuristic · Optimization algorithms · Engineering problems

1 Introduction

In the last 2 decades, many metaheuristic algorithms have been proposed by researchers due to their advantages like flexibility, bypassing local optima, and they did not need gradient information [1]. Metaheuristics algorithms have gained huge attention and a significant interest as they can solve real-world optimization problems by mathematically simulating physical/biological phenomena. They have been applied to many problems [2, 3]. These algorithms can be divided into four major categories: l(EAs), Swarm Intelligence-based algorithm (SI-based), physics & chemistry algorithms, and Human-based Algorithm. The first category (evolutionary algorithms) contains algorithms inspired by natural evolution. In EAs, there is a randomly generated population at first to start. Then, all individuals are evaluated

✉ Guoxi Liang
guoxiliang2017@gmail.com

✉ Huiling Chen
chenhuiling.jlu@gmail.com

✉ Zhifang Pan
panzhifang@wmu.edu.cn

Abdelazim G. Hussien
abdelazim.hussien@liu.se; aga08@fayoum.edu.eg

Ali Asghar Heidari
aliasghar68@gmail.com

Xiaojia Ye
yxj@lixin.edu.cn

1 Department of Computer and Information Science, Linköping University, Linköping, Sweden

2 Faculty of Science, Fayoum University, Fayoum, Egypt

3 Department of Computer Science and Artificial Intelligence, Wenzhou University, Wenzhou 325035, People's Republic of China

4 Shanghai Lixin University of Accounting and Finance, Shanghai 201209, People's Republic of China

5 Department of Information Technology, Wenzhou Polytechnic, Wenzhou 325035, People's Republic of China

6 The First Affiliated Hospital of Wenzhou Medical University, Wenzhou 325000, People's Republic of China

over a generation to produce new individuals using crossover and mutation processes. This category includes genetic algorithms (GA) [4], evolution simulation strategy (ES) [5], genetic programming (GP) [6], and biogeography-based optimizer (BBO) [1].

The second category is SI-based algorithms inspired by swarms' social behavior [7], a collection of living beings in nature. Examples of SI algorithms are particle swarm algorithm (PSO) [8], ant colony optimization [9], Harris hawks optimizer (HHO) [10], virus colony search [11], slime mould algorithm (SMA) [12], Hunger games search (HGS) [13], and Runge–Kutta (RUN) optimizer [14]. The third class includes algorithms that simulate physical or chemical phenomena. Examples of this class are simulated annealing (SA) [15], and gravitational search algorithm (GSA) [16]. The last class includes algorithms, which are inspired by human behavior like teaching learning-based optimization (TLBO) [17] and tabu (Taboo) search (TS) [18]. In addition to engineering optimization problems [19, 20], these stochastic methods have found their applications and contributions in more complex problems and attracted many works in science and engineering fields such as medical data classification [21–24], scheduling problems [25, 26], feature selection [27–29], wind speed forecast [30], engineering design problems [31–33]. Furthermore, potential of metaheuristics is not limited to such problems and still much room to discover in the fields of hard maximum satisfiability problem [34, 35], bankruptcy prediction [36, 37], parameter optimization [38–40], PID control [41–43], detection of foreign fiber in cotton [44, 45], surveillance [46], service ecosystem [47, 48], micro-expression spotting [49, 50], and prediction problems in educational ground [51, 52].

WOA is a recent algorithm developed by the author in [53] that has gained huge attention due to its simple code and high similarity with grey wolf optimizer (GWO). This algorithm can outperform many state-of-the-art algorithms such as GSA, PSO, and GA. This algorithm is based on the humpback special hunting behavior, which is called the bubble net method. WOA has received huge interest and global attention since its inception, as it shows a good performance in handling many optimization tasks. Consequently, some modifications have been made by many researchers. In [54], they proposed a binary version of WOA using two transfer functions. The new versions applied to solve travel salesman problem (TSP). In [55], Aljarah et al. used WOA to find the optimal connecting weights in a neural network. Also, Elaziz et al. [56] developed a hyper-heuristic algorithm by using DE to improve the initial WOA population. In [57], Emary et al. tried to study the impact of levy flight in WOA and SCA. Likewise, Oliva et al. [58] proposed a new version of WOA using chaotic maps and applied it to estimate photovoltaic cell parameters. In [59], Xiong et al. proposed an improved version of WOA by developing two prey search strategies. In [60], Chen et al. proposed two strategies based on Lévy flight and chaotic local search to have a good balance between the core capacities. Also, authors in [61] introduced a hybrid version of WOA and SA by embedding SA in WOA as a local search strategy. In [62], Abdel-Basset et al. designed a new version of WOA and used it in Cryptanalysis in Merkle–Hellman Cryptosystem. Another hybrid version between WOA and GWO called WGC is introduced to cluster data [63]. Agrawal et al. [64] applied embedded quantum operators in WOA and used it in the feature selection problem. Authors in [65] proposed a new version using an opposition-based technique to prevent the basic whale method on from getting trapped in local optima. Also, in works of [66, 67], the proposed approach was applied to the feature selection problem. In [68], Hemasian-Etefagh et al. tried to prevent the classical WOA from trapping into local optima by introducing a new version called group WOA (GWOA), in which the population was divided into many groups based on their fitness value. In [69], Hassib et al. proposed a novel classification framework for big data using the WOA. To solve job shop scheduling problems (JSSP), [70] tried to solve it by introducing a hybrid algorithm called (WOA-LFDE) in which differential evolution (DE), and Lévy flight are hybridized with WOA. Also, in [71], Jiang et al. introduced an enhanced WOA by embodying two approaches: introducing an armed force program and adjusting beneficial strategy. In [72], Guo et al. used a modified version of WOA by using the adaptive strategy of the neighborhood to forecast the demand for water resources. Also, in [73], Got et al. introduced an enhanced multi-objective version of WOA called guided population archive WOA (GPAWOA) to solve multi-objective problems.

WOA has been applied to many medical applications. Authors in [39] developed a chaotic multi-swarm WOA version called CMWOA using a support vector machine (SVM) and applied it to perform feature selection to many well-known and common medical diseases problems such as breast cancer, erythemato-squamous, and diabetes. Also, in [74], Abdel-Basset et al. integrated the basic WOA with TS and employed it to solve the quadratic assignment problem (Locating departments of the hospital). In [75], Tharwat et al. used WOA with SVM to be able to classify the biotransformed toxicity effects of hepatic drugs. Also, in [76], Zhao et al. mixed SVM kernel function with WOA to classify colorectal cancer diagnosis.

Gharehchopogh and Gholizadeh listed all WOA variants and applications with details in a comprehensive survey [77]. Despite the original WOA success, many works showed that its performance might degrade when solving some optimization tasks.

On the other hand, another recent metaheuristic called virus colony search (VCS) was developed [11]. VCS simulates viruses diffusion and infection behavior in attacking cells. VCS has been applied to many power optimization problems such as unit commitment [78], resource allocation [79], and distributed generators placement [80].

In this study, a new enhanced WOA-based algorithm is designed that embedded the core mechanisms of VCS into the main method. It aims to overcome these limitations by revisiting the WOA based on the core components of the Gaussian walk, CMA-ES, and evolution strategy that appeared in the VCS. This could prevent WOA from getting trapped into local optima by maintaining a better balance among the exploration and exploitation capabilities. To evaluate the resulted framework, 30 benchmark cases from IEEE CEC2017 were employed in addition to four different constrained engineering problems. Besides, the enhanced WOA-based variant has been applied to image segmentation, where eight images are utilized, and they are compared with various WOA variants. The attained results show that the new structure has alleviated the central shortcomings of WOA, and we saw a significant performance for the proposed VCSWOA compared to other peers.

This paper is organized as follows. Sections 2 and 3 give a detailed description and mathematical equations to the WOA and VCS, respectively. Sections 4 and 5 show the proposed method and results discussions. Section 6 concludes the paper.

2 Whale optimization algorithm

In this section, we present the basics of the WOA by describing its main components, such as inspiration, its mathematical model, and how it deals with exploration and exploitation. The WOA [53] introduced by Mirjalili et al. in 2016, which mimics the foraging of humpback whales. Whales are beautiful creatures that have a special hunting technique called bubble-net feeding or 9-shape. Then, other agents attempt to change their location vector to attain the best position according to Eq. (1).

$$\mathbf{D} = |\mathbf{C}.\mathbf{X}^*(t) - \mathbf{X}(t)| \tag{1}$$

$$\mathbf{X(t+1)} = \mathbf{X}^*(t+1) - \mathbf{A}.\mathbf{D} \tag{2}$$

where t denotes the counter of iteration, $\mathbf{C}$ and $\mathbf{A}$ are coefficient vectors, $\mathbf{X}^*$ means the position vector of the best agent, and $\mathbf{X}$ is the location vector. $\mathbf{A}$ and $\mathbf{C}$ values are obtained from the following rules:

$$\mathbf{A} = 2.\mathbf{a}.\mathbf{r} - \mathbf{a} \tag{3}$$

$$\mathbf{C} = 2.\mathbf{r}, \tag{4}$$

where a is linearly decreased from 2 to 0 over iterations and r randomly bounded in [0,1]. To mathematically simulate the exploitation phase, we have two approaches (1) Shrinking encircling: attained by decreasing a value's with regard to Eq. (4). Note that $\mathbf{A}$ is a random value between $[-a, a]$. (2) Spiral updating: this phase realizes the distance between the whale and the prey. Equation (5), calculates the spiral that mimics the helix-shaped movement as follow:

$$\mathbf{X}(t+1) = \mathbf{D}^l e^{bl}.\cos(2\pi l)) + \mathbf{X}^*(t), \tag{5}$$

where b is constant, l is a random number in $[-1, 1]$. To select either spiral moves or shrinking encircling phase, a chance of 50% is assumed as follow:

$$\mathbf{X}(t+1) = \begin{cases} \mathbf{X}^*(t) - \mathbf{A}.\mathbf{D} & if\ p < 0.5 \\ \mathbf{D^l}.e^{bl}.\cos(2\pi l) + \mathbf{X}^*(t) & if\ p \geq 0.5, \end{cases} \tag{6}$$

where p is a random number in a uniform distribution. In other hand side, in exploration (diversification) stage, $1 \prec A \prec -1$ is used to force the solution to move away from this location. Equations (7) and (8), represent the mathematical for exploration phase as follow:

$$\mathbf{D} = |\mathbf{C}.\mathbf{X}_{rand} - \mathbf{X}| \tag{7}$$

$$\mathbf{X}(t+1) = X_{rand} - \mathbf{A}.\mathbf{D} \tag{8}$$

The general pseudo-code steps of WOA are presented in Algorithm 1.

Algorithm 1 Whale Optimization Algorithm.

```
Input: n Number of whales in the population.
MaxIter Number of iteration for Optimization
Output: Optimal whale position
Initialize a the population of n whales
Find X* = best search agent threads
while stopping criteria not meet to  do
    for whale_i belong to whales do
        Calculate and Update a; A, C, p and l.
        if p < 0.5 then
            if (|A|< 1) then
                Update position by Eq. (2)
            else(|A|≥ 1)
                Select a random search agent (X_rand)
                Update position by Eq. (8)
            end if
        else(p ≥ 0.5)
            Update position by Eq. (4)
        end if
        Update X(t + 1) from Eq. (5)
    end for
    Check if any search agent goes beyond the search space
    Calculate the fitness of each search agent
    Update X* if there is a better solution
end while
```

3 Virus colony optimization algorithm

Virus colony search (VCS) is a novel population algorithm inspired by nature, which simulates infection and diffusion techniques. VCS mainly depends on three strategies: (1) Gaussian walk, (2) CMA-ES, and (3) evolution strategy.

The population is divided into two groups: V_{pop} which refers to virus colony, and H_{pop}, which refers to host cell colony. A host cell is infected by one virus. Then, the virus must obtain nutrients by destroying the host cell to be able to reproduce. Finally, the few best viruses remain in the next generation, and the other viruses are evolved. The following subsections simulate these steps mathematically.

3.1 Viruses diffusion

A random walk is needed in this phase to simulate virus moving. Gaussian random walk (GRW) is used since it has a good performance as given in Eq. (9).

$$Vpop_i = \text{Gaussian}(G^g_{best}, \tau) + (r_1.G^g_{best} - r_2.V_{pop_i}), \tag{9}$$

where i refers to a random value and equals $1, 2, 3, \dots, N$ where N is the size of the population, $r_1\&r_2$ are random variables and falls in the interval [0, 1], and τ refers to the standard deviation and can be calculated as follows:

$$\tau = \log(g)/g.(V_{pop_i} - G^g_{best}). \tag{10}$$

In Eq. (9), the term $(r_1.G^g_{best} - r_2.V_{pop_i})$ is used as a search direction in order to prevent direction from getting trapped in a local optimum. Also, the term $log(g)/g$ is used to decrease Gaussian jump size over generations to improve the local search performance.

3.2 Host cells infection

In this stage, the virus invades the host cell and tries to destroy it until its death. Then, the virus interacts with the host cell by absorbing essential nutrition and metabolizing harmful substances. Then, the host cell will be converted into a new virus. This process is used to improve the capabilities of the exploration process and observe the exchange of information. Hence, covariance matrix adaptation evolution strategy (CMA-ES) can be used to model derivative-free and stochastic optimization. The main steps to mathematically simulate this stage is as follows:

Step 1: H_{pop} updating process using Eq. (11).

$$Hpop^g_i = \left(\frac{\sum_i^N V_{pop_i}}{N}\right) + \sigma^g_i \times N_i(0, c_g) \tag{11}$$

where $N_i(0, c_g)$ refers to the normal distribution with mean 0 and$D\times D$ covariance matrix c_g. D refers to problem dimension, g refers to the current iteration.
Step 2: Selection of the best λ from the previous stage as a parental vector. The selected vector center can be calculated as follow:

$$X_{\text{mean}}^{g+1} = \frac{1}{\lambda}\sum_{i=1}^{\lambda} w_i Vpop_i^{\lambda best}|wi = \ln(\lambda+1) \times \left(\sum_{j=1}^{\lambda}(\ln(\lambda+1) - \ln(j))\right), \tag{12}$$

where λ can be calculated as $\lfloor \frac{N}{2} \rfloor$, i refers to the individual index, w_i refers to recombination weight. Here, two evolution paths can be computed to track the population mean changes with an exponential decay of the past.

$$p_\sigma^{g+1} = (1-c_\sigma)p_\sigma^g + \sqrt{c_\sigma(2-c_\sigma)\lambda_w} \frac{1}{\sigma^g}(c^g)^{-1/2}(X_{\text{mean}}^{g+1} - X_{\text{mean}}^g) \tag{13}$$

$$p_c^{g+1} = (1-c_c)p_c^g + h_\sigma\sqrt{c_c(2-c_c)\lambda_w} \frac{1}{\sigma^g}(X_{\text{mean}}^{g+1} - X_{\text{mean}}^g) \tag{14}$$

where $\lambda_w^{-1} = \sum_{i=1}^{\lambda} w_i^2$, $c_\sigma = (\lambda_w + 2)/(N + \lambda_w + 3)$, $c_c = 4/(N+4)$, $h_\alpha = 1$ if $||p_\sigma^{g+1}||$ is large.

Step 3: Updating the step size

σ^{g+1} can be updated using Eq. (15).

$$\sigma^{g+1} = \sigma^g \times \exp\left(\frac{c_\sigma}{d_\sigma}\left(\frac{||p_\sigma^{g+1}||}{E||N(0,I)||} - 1\right)\right) \tag{15}$$

Also, covariance matrix c^{g+1} is constructed using Eq. (16).

$$c^{g+1} = (1-c_1-c_\lambda)c^g + c_1 p_c^{g+1}(p_c^{g+1})^{\mathrm{T}} + c_\lambda \sum_{i=1}^{\lambda} w_i \frac{vpop_i^{\lambda best} - X_{\text{mean}}^g}{\sigma^g} . \frac{(Vpop_i^{\lambda best} - X_{\text{mean}}^g)^{\mathrm{T}}}{\sigma^g} \tag{16}$$

where c_1, c_2 have

$$d_\sigma = 1 + c_\sigma + 2\max\{0, (\sqrt{\lambda_w - 1}/\sqrt{N+1}) - 1\} \tag{17}$$

$$c_1 = \frac{1}{\lambda_w}\left(\left(1 - \frac{1}{\lambda_w}\right)\min\left\{1, \frac{2\lambda_w - 1}{(N+2)^2 + \lambda_w} + \lambda_w\right\} + \frac{1}{\lambda_w} . \frac{2}{\lambda_w}(N + \sqrt{2})^2\right) \tag{18}$$

$$C_\lambda = (\lambda_w - 1)C_1 \tag{19}$$

3.3 Immune response

According to the host cell immune influence system, only the highest performance virus will retain its properties to the next generation and the others are killed by the immune system. Hence, following steps are used to model the virus evolution.

Step 1: Performance rank evaluation

$Pr_{rank(1)}$ can be calculated as follow.

$$Pr_{rank(1)} = \frac{(N - i + 1)}{N} \tag{20}$$

Step 2: Evolution of individuals

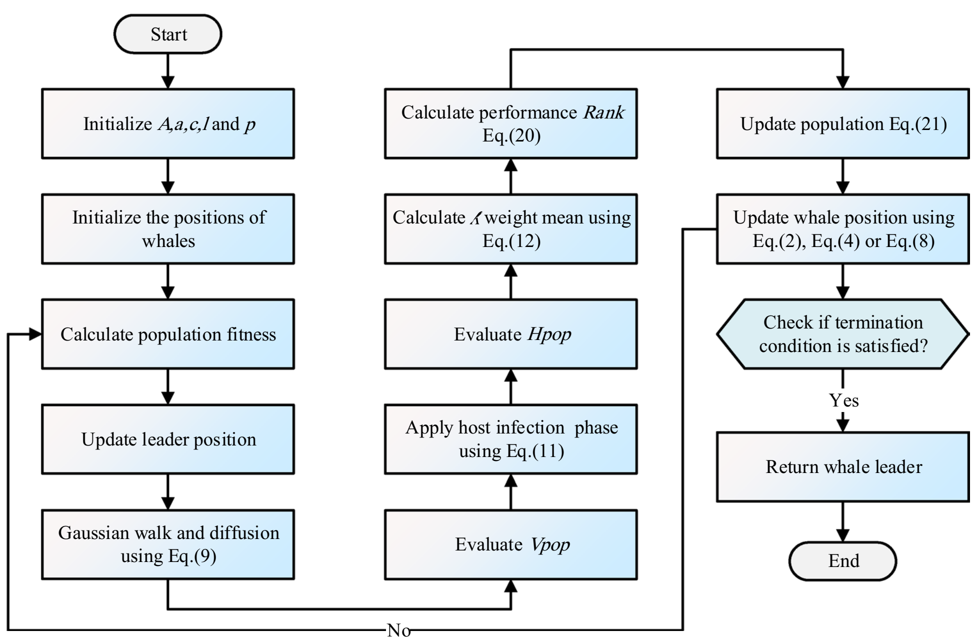

Fig. 1 The flowchart of the proposed method

$$\begin{cases} Vpop_{i,j} = Vpop_{k,j} - rand \times \\ (Vpop_{h,j} - Vpop_{i,j}) & r > Pr_{rank(i)} \\ \\ Vpop_{i,j} = Vpop_{i,j} & \text{otherwise} \end{cases} \tag{21}$$

where the 3 variables k, i, h are chosen randomly from $[1, 2, 3, \ldots, N]$ such that $i \neq k \neq h$, and $j \in 1, 2, 3, \ldots, d]$ and rand and r are the random values ∈ [0, 1].

4 Proposed algorithm

In this section, the structure of the proposed WOA-based method is explained in detail, as given in Fig. 1. The basic WOA has some core limitations, especially in solving complex problems, mainly the multimodal functions and high dimensional ones. The main WOA's limitations are dropping into local optima and the problem of the slow convergence.

VCSWOA aims to overcome these limitations by revisiting the WOA based on the core components of Gaussian walk, CMA-ES, and evolution strategy that appeared in the VCS. These ideas are to enhance the convergence speed and local optima avoidance of the WOA method. Here, the components of the VCS algorithm are devoted to performing intensification drifts to make the WOA algorithm more capable of avoiding local optima, which will reflect an improvement in exploitation abilities. On the other hand, the conventional cores of the WOA are utilized to handle exploratory patterns we need during a well-organized searching around the regions of the feature domain. In this way, we can reach a well-harmonized balance between exploitation and exploration procedures.

The pseudo-code of VCSWOA is shown in Algorithm , and it works as follows: An initial whale population is generated randomly at the initial state. Then, the three phases of Gaussian walk, CMA-ES, and evolution strategy are performed to further evolve the immature population: i.e., viruses diffusion, host cell infection, and immune response in VCS. After that, the updating phase of each search agent's position is done based on p and $|A|$ values.

Table 1 CEC2017 benchmark functions

No.	Types	Name	Opt
F1	Unimodal	Shifted and rotated bent cigar function	100
F2		Shifted and rotated sum of different power function	200
F3		Shifted and rotated Zakharov function	300
F4	Multimodal	Shifted and rotated Rosenbrock's function	400
F5		Shifted and rotated Rastrigin's function	500
F6		Shifted and rotated expanded Scaffer's F6 function	600
F7		Shifted and rotated Lunacek bi-Rastrigin function	700
F8		Shifted and rotated non-continuous Rastrigin's function	800
F9		Shifted and rotated Lévy function	900
F10		Shifted and rotated Schwefel's function	1000
F11	Hybrid	Hybrid function 1 ($N = 3$)	1100
F12		Hybrid function 2 ($N = 3$)	1200
F13		Hybrid function 3 ($N = 3$)	1300
F14		Hybrid function 4 ($N = 4$)	1400
F15		Hybrid function 5 ($N = 4$)	1500
F16		Hybrid function 6 ($N = 4$)	1600
F17		Hybrid function 6 ($N = 5$)	1700
F18		Hybrid function 6 ($N = 5$)	1800
F19		Hybrid function 6 ($N = 5$)	1900
F20		Hybrid function 6 ($N = 6$)	2000
F21	Composition	Composition function 1 ($N = 3$)	2100
F22		Composition function 2 ($N = 3$)	2200
F23		Composition function 3 ($N = 4$)	2300
F24		Composition function 4 ($N = 4$)	2400
F25		Composition function 5 ($N = 5$)	2500
F26		Composition function 6 ($N = 5$)	2600
F27		Composition function 7 ($N = 6$)	2700
F28		Composition function 8 ($N = 6$)	2800
F29		Composition function 9 ($N = 3$)	2900
F30		Composition function 10 ($N = 3$)	3000

Algorithm 2 VCSWOA

Input:
Number of whales in the population (n)
Maximum function evaluation number ($MaxFEs$)
Number of dimensions (dim)
selected best individuals number ($\lambda = \left\lfloor \frac{N}{2} \right\rfloor$)
Output:
Optimal whale Position
Positions=Initialize a the population of n whales
Find $X* = best$ search agent threads
EFs=0
while $FEs < MaxFEs$ **do**
  Check the boundary
  Apply Gaussian random walk and diffusion phase Eq. (9)
  FEs=FEs+N
  Evaluate V_{pop}
  Host infection phase using Eq. (11)
  FEs=FEs+N
  Evaluate H_{pop}
  select λ best solution
  calculate λ weight means using Eq. (15)
  update population using Eq. (21)
  if Best score < Leader score **then**
    Leader pos=Best pos
    Leader score=Best score
  end if
  for $whale_i$belong to whales **do**
    Calculate and Update $a; A, C, p$ and l
    FEs=FEs+1
    if $p < 0.5$ **then**
      if ($|A|< 1$) **then**
        Update position by Eq. (2)
      else($|A|\geq 1$)
        Select a random search agent (X_{rand})
      end if
    else($p \geq 0.5$)
      Update position by Eq. (4)
    end if
    Update $\mathbf{X}(t+1)$ from Eq. (5)
  end for
  Check if any search agent goes beyond the search space
  Calculate the fitness of each search agent
  Update X^* if there is a better solution
  t=t+1
end while

5 Experiment

In this section, many experiments have been performed to prove the efficiency of the proposed algorithm: benchmark functions, Engineering problems, and image segmentation problems.

5.1 Benchmark functions

Thirty functions from the IEEE CEC2017 benchmark have been used. Table 1 defines these functions and their type including unimodal, multimodal, hybrid, and composite. VCSWOA has been compared with other eight WOA variants namely: chaotic WOA (CWOA) [81], Opposition learning-based WOA (OBWOA) [82], A-C parametric WOA (ACWOA) [83], Enhanced associative learning-based exploratory WOA (BMWOA), improved WOA (IWOA) [84], Balanced WOA with levy flight and chaotic local search (BWOA) [60], Multi-strategy boosted mutative WOA (CCMWOA) [], and Levy flight-based WOA (LWOA) [57]. The parameter settings for each algorithm are given in Table 2. The number of individuals, number of dimensions, and the maximum number of function evaluations (*MaxFEs*) are given in Table 3. We used same conditions as per fair comparisons settings in artificial intelligence community [85, 86].

Table 4 shows the experiment results in terms of average (mean), standard deviation (std), best (min), and worst

Table 2 The parameter settings for the algorithms

Algorithm	Parameters
CWOA	$cindex = 5; a_1 = [0, 2]; a_2 = [-2, -1]; A = [-a_1, a_1]; C = [0, 2]; b = 1; l = [1, a_2]; p = [0, 1]$
OBWOA	$a_1 \in [0, 2]; a_2 \in [-2, -1]; A \in [-a1, a1]; C \in [0, 2]; b = 1; l \in [1, a2]; p \in [0, 1]$
ACWOA	$w \in [0.5, 1]; a_1 \in [0, 2]; a_2 \in [-2, -1]; A \in [-a1, a1]; C \in [0, 2]; b = 1; l \in [1, a2]; p \in [0, 1]$
BMWOA	$bw = 0.001; beta = 0.1; a_1 \in [0, 2]; a_2 \in [-2, -1]; A \in [-a1, a1]; C \in [0, 2]; b = 1; l \in [1, a2]; p \in [0, 1]$
IWOA	$CR = 0.9; a_1 \in [0, 2]; a_2 \in [-2, -1]; A \in [-a_1, a_1]; C \in [0, 2]; b = 1; l \in [1, a_2]; p \in [0, 1]$
BWOA	$m = 2500; a_1 \in [0, 2]; a_2 \in [-2, -1]; A \in [-a_1, a_1]; C \in [0, 2]; b = 1; l \in [1, a_2]; p \in [0, 1]$
CCMWOA	$m = 1500; setCan \in [0, 1]; a_1 \in [0, 2]; a_2 \in [-2, -1]; A \in [-a_1, a_1]; C \in [0, 2]; b = 1; l \in [1, a_2]; p = [0, 1]$
LWOA	$S \in [lb, ub], s = [0, S]; a_1 \in [0, 2]; a_2 \in [-2, -1]; A \in [-a_1, a_1]; C \in [0, 2]; b = 1; l \in [1, a_2]; p \in [0, 1]$

(max). From this table, it can be noticed that VCSWOA ranked first in all unimodal functions (F1–F3) in Avg and Std values. However, in multimodal ones, VCSWOA has ranked first in avg at five functions (F4, F6, F8, F9, and F10), and ranked second in the other 3 functions. For both composite and hybrid functions, VCSWOA achieved the highest value in 7 functions and the second highest in other 8 functions. Also, Table 5 shows the Wilcoxon signed-rank [87] results in which VCSWOA has considered superior compared with other algorithms with a p value smaller than 5%. Figure 2 shows the convergence curve for 10 selected functions.

5.2 Engineering problems

In this subsection, four different engineering problems have been used: pressure vessel design problem, welded beam design problem, tension/compression spring design problem, and cantilever beam design problem.

5.2.1 Pressure vessel design problem

Pressure vessel design problem is considered as a one of the wide engineering design problems which aims to find the lowest materials cost of the pressure vehicle. It's consist of 4 parameters(Shell thickness T_s, Cylindrical length L, head thickness T_k and Radius R). The mathematical design can be formulated as:

Table 3 The parameter settings

No.	Parameter name	Value
1	Population size	30
2	No of dim	30
3	MaxFEs	dim*10,000

Minimize: $f(x) = 0.6224x_1x_3x_4 + 1.7781x_2x_3^2 + 3.1661x_1^2x_4 + 19.84x_1^2x_3$

Subject to: $g_1(x) = -x_1 + 0.0193x$

$g_2(x) = -x_2 + 0/00954x_3 \le 0$

$g_3(x) = -\pi x_3^2 x_4 - (4/3)\pi x_3^3 + 1,296,000 \le 0$

$g_4(x) = x_4 - 240 \le 0$

Variable Range $0 \le x_i \le 100, \quad i = 1,2$

$0 \le x_i \le 200, \quad i = 3,4$

Table 6 shows the results of VCSWOA compared with SMA, WOA, GWO, MFO, ACO, HPSO, and BA. It's obvious that the proposed algorithm has less cost.

5.2.2 Welded beam design problem

This problem has 4 parameters: bar length(l), bar height(t), Thickness of welded(h), and thickness of bar(b). Its mathematical equations can be shown as below:

Minimize:

$f_1(x) = 1.10471 * x(1)^2 * x(2) + 0.04811 * x(3) * x(4) * (14.0 + x(2))$

Subject to:

$g_1(x) = \tau - 13,600$

$g_2(x) = \sigma - 30,000$

$g_3(x) = x(1) - x(4)$

$g_4(x) = 6000 - p$

Variable Range

$0.125 \le x_1 \le 5$

$0.1 \le x_2 \le 10$

$0.1 \le x_3 \le 10$

$0.125 \le x_4 \le 5$

The results in Table 7 shows that VCSWOA has reach the most near optimal solution against many metaheuristic algorithms.

5.2.3 Tension/compression spring design problem

The third problem used is Tension/Compression Spring problem which has 3 parameters :coil diameter(D), wire diameter(d), and number of active soils(N). The mathematical formulation is shown below:

Minimize:

$f(x) = (x_3 + 2)x_2x_1^2$

Subject to:

$g_1(x) = 1 - (x_2^3x_3/71,785x_1^4) \le 0$

Table 4 The comparison results of all algorithms over 30 functions

	F1				F2			
	Avg	Std	Min	Max	Avg	Std	Min	Max
VCSWOA	**3.05E+03**	**4.94E+03**	**2.57E+02**	**2.01E+04**	**4.12E+05**	**1.75E+06**	**2.00E+02**	**9.52E+06**
CWOA	3.37E+09	2.91E+09	6.02E+07	1.32E+10	4.02E+31	1.09E+32	2.65E+19	5.12E+32
OBWOA	4.41E+07	3.44E+07	8.56E+06	1.25E+08	2.75E+24	8.49E+24	7.17E+17	4.17E+25
ACWOA	5.10E+09	2.20E+09	2.01E+09	1.02E+10	4.47E+34	2.25E+35	1.86E+22	1.23E+36
BMWOA	2.29E+08	1.11E+08	6.01E+07	5.35E+08	1.88E+24	7.42E+24	1.63E+18	3.88E+25
IWOA	1.88E+06	1.83E+06	2.20E+05	7.13E+06	6.23E+19	3.16E+20	1.51E+13	1.73E+21
BWOA	1.78E+08	9.60E+07	4.78E+07	4.59E+08	1.07E+27	5.81E+27	2.74E+18	3.19E+28
CCMWOA	1.87E+10	5.73E+09	6.95E+09	3.16E+10	8.21E+38	3.01E+39	1.43E+25	1.54E+40
LWOA	4.93E+05	1.24E+05	3.32E+05	8.56E+05	4.33E+06	2.27E+07	1.08E+03	1.24E+08
	F3				F4			
	Avg	Std	Min	Max	Avg	Std	Min	Max
VCSWOA	**3.11E+02**	**7.18E+00**	**3.03E+02**	**3.29E+02**	**4.93E+02**	2.65E+01	4.23E+02	**5.44E+02**
CWOA	1.57E+05	4.61E+04	8.07E+04	2.60E+05	7.00E+02	1.90E+02	5.27E+02	1.41E+03
OBWOA	5.41E+04	1.87E+04	3.82E+04	1.43E+05	5.63E+02	4.40E+01	4.95E+02	6.94E+02
ACWOA	4.98E+04	1.28E+04	3.90E+04	8.17E+04	1.23E+03	6.22E+02	6.64E+02	4.24E+03
BMWOA	7.17E+04	9.13E+03	4.98E+04	8.45E+04	6.13E+02	4.17E+01	5.42E+02	7.15E+02
IWOA	8.44E+04	3.18E+04	3.89E+04	1.49E+05	5.30E+02	4.24E+01	**4.10E+02**	6.38E+02
BWOA	5.85E+04	1.15E+04	3.70E+04	8.60E+04	6.00E+02	4.83E+01	5.38E+02	7.44E+02
CCMWOA	7.82E+04	4.33E+03	6.71E+04	8.70E+04	3.50E+03	1.13E+03	1.42E+03	5.91E+03
LWOA	5.14E+02	1.50E+02	3.64E+02	1.16E+03	4.99E+02	**2.18E+01**	4.67E+02	5.55E+02
	F5				F6			
	Avg	Std	Min	Max	Avg	Std	Min	Max
VCSWOA	7.65E+02	4.59E+01	6.37E+02	**8.29E+02**	**6.55E+02**	7.06E+00	6.41E+02	**6.70E+02**
CWOA	8.14E+02	5.99E+01	7.28E+02	1.01E+03	6.72E+02	9.69E+00	6.52E+02	6.87E+02
OBWOA	8.01E+02	3.21E+01	7.24E+02	8.44E+02	6.64E+02	6.66E+00	6.52E+02	6.76E+02
ACWOA	7.97E+02	3.35E+01	7.26E+02	8.56E+02	6.66E+02	**6.40E+00**	6.55E+02	6.79E+02
BMWOA	7.86E+02	4.95E+01	6.96E+02	8.79E+02	6.65E+02	9.27E+00	6.39E+02	6.78E+02
IWOA	**7.46E+02**	5.37E+01	**6.29E+02**	8.88E+02	**6.55E+02**	9.43E+00	**6.30E+02**	6.73E+02
BWOA	7.68E+02	**3.30E+01**	7.11E+02	8.17E+02	6.63E+02	7.21E+00	6.46E+02	6.74E+02
CCMWOA	8.33E+02	3.41E+01	7.22E+02	8.71E+02	6.74E+02	6.05E+00	6.65E+02	6.84E+02
LWOA	7.51E+02	5.35E+01	6.57E+02	8.76E+02	6.63E+02	1.11E+01	6.49E+02	6.96E+02
	F7				F8			
	Avg	Std	Min	Max	Avg	Std	Min	Max
VCSWOA	1.26E+03	**6.40E+01**	1.14E+03	1.36E+03	**9.69E+02**	2.62E+01	9.19E+02	**1.01E+03**
CWOA	1.26E+03	7.72E+01	1.09E+03	1.42E+03	1.02E+03	5.43E+01	9.31E+02	1.15E+03
OBWOA	1.28E+03	7.34E+01	1.06E+03	1.43E+03	1.02E+03	3.99E+01	9.65E+02	1.11E+03
ACWOA	1.25E+03	5.99E+01	1.08E+03	1.35E+03	1.01E+03	2.69E+01	9.72E+02	1.07E+03
BMWOA	1.25E+03	7.36E+01	1.11E+03	1.36E+03	1.01E+03	3.10E+01	9.49E+02	1.08E+03
IWOA	1.15E+03	8.53E+01	**9.42E+02**	**1.35E+03**	9.90E+02	4.39E+01	9.37E+02	1.12E+03
BWOA	1.26E+03	7.46E+01	1.07E+03	**1.35E+03**	9.77E+02	**2.19E+01**	9.30E+02	1.02E+03
CCMWOA	1.28E+03	7.24E+01	1.13E+03	1.40E+03	1.05E+03	2.94E+01	9.85E+02	1.10E+03
LWOA	**1.12E+03**	9.05E+01	9.80E+02	**1.35E+03**	1.01E+03	5.87E+01	**9.12E+02**	1.17E+03

Table 4 (continued)

	F9				F10			
	Avg	Std	Min	Max	Avg	Std	Min	Max
VCSWOA	**5.33E+03**	**4.40E+02**	4.31E+03	**6.22E+03**	**4.81E+03**	6.57E+02	3.72E+03	**6.59E+03**
CWOA	9.41E+03	3.82E+03	4.80E+03	1.83E+04	6.44E+03	7.92E+02	4.92E+03	7.83E+03
OBWOA	7.06E+03	9.82E+02	5.05E+03	8.94E+03	6.26E+03	6.46E+02	4.66E+03	7.84E+03
ACWOA	7.36E+03	9.72E+02	5.68E+03	9.65E+03	6.84E+03	9.43E+02	4.94E+03	8.57E+03
BMWOA	7.73E+03	1.08E+03	4.98E+03	9.97E+03	7.37E+03	**5.99E+02**	5.85E+03	8.24E+03
IWOA	7.03E+03	2.35E+03	4.01E+03	1.33E+04	5.73E+03	7.03E+02	4.21E+03	7.07E+03
BWOA	6.25E+03	8.00E+02	4.77E+03	7.88E+03	6.33E+03	8.37E+02	4.61E+03	7.84E+03
CCMWOA	7.77E+03	1.24E+03	4.91E+03	1.05E+04	7.30E+03	6.07E+02	6.52E+03	8.81E+03
LWOA	6.64E+03	1.75E+03	**3.52E+03**	1.24E+04	5.25E+03	8.54E+02	**3.32E+03**	7.29E+03
	F11				F12			
	Avg	Std	Min	Max	Avg	Std	Min	Max
VCSWOA	**1.20E+03**	**3.51E+01**	1.14E+03	**1.27E+03**	**2.77E+06**	**1.50E+06**	**2.60E+05**	**6.63E+06**
CWOA	3.29E+03	1.12E+03	1.47E+03	5.41E+03	1.02E+08	1.11E+08	1.45E+07	4.60E+08
OBWOA	1.70E+03	2.85E+02	1.37E+03	2.86E+03	5.32E+07	3.33E+07	1.35E+07	1.30E+08
ACWOA	2.76E+03	6.67E+02	1.81E+03	4.29E+03	5.01E+08	3.26E+08	9.16E+07	1.51E+09
BMWOA	1.70E+03	1.76E+02	1.37E+03	2.13E+03	7.54E+07	4.72E+07	7.58E+06	1.98E+08
IWOA	1.36E+03	1.10E+02	1.23E+03	1.85E+03	7.74E+06	6.35E+06	1.69E+06	2.59E+07
BWOA	1.82E+03	2.42E+02	1.51E+03	2.67E+03	1.17E+08	9.68E+07	1.30E+07	3.65E+08
CCMWOA	3.39E+03	8.42E+02	1.83E+03	6.36E+03	2.62E+09	1.72E+09	4.83E+08	6.35E+09
LWOA	1.28E+03	5.82E+01	**1.13E+03**	1.38E+03	4.02E+06	2.38E+06	7.13E+05	1.06E+07
	F13				F14			
	Avg	Std	Min	Max	Avg	Std	Min	Max
VCSWOA	4.20E+04	2.22E+04	**9.34E+03**	**9.82E+04**	**2.24E+04**	**1.41E+04**	3.30E+03	**5.49E+04**
CWOA	1.20E+05	7.45E+04	2.59E+04	3.25E+05	1.33E+06	1.15E+06	5.74E+04	4.89E+06
OBWOA	2.88E+05	1.29E+05	1.01E+05	5.78E+05	7.32E+05	7.33E+05	2.86E+04	2.68E+06
ACWOA	1.69E+08	5.14E+08	6.59E+06	2.06E+09	1.30E+06	8.25E+05	5.85E+04	2.86E+06
BMWOA	4.16E+05	5.36E+05	6.07E+04	2.71E+06	7.32E+05	7.08E+05	1.48E+04	3.16E+06
IWOA	**2.58E+04**	**1.78E+04**	9.79E+03	9.21E+04	6.28E+05	5.59E+05	2.50E+04	1.79E+06
BWOA	2.16E+05	1.01E+05	7.65E+04	4.60E+05	1.39E+06	1.21E+06	2.69E+04	4.48E+06
CCMWOA	6.86E+07	7.81E+07	6.40E+06	4.25E+08	1.43E+06	1.21E+06	4.56E+04	4.27E+06
LWOA	1.73E+05	1.01E+05	5.16E+04	5.02E+05	2.39E+04	1.70E+04	**2.12E+03**	8.18E+04
	F15				F16			
	Avg	Std	Min	Max	Avg	Std	Min	Max
VCSWOA	1.88E+04	**1.08E+04**	5.11E+03	5.26E+04	**2.85E+03**	3.79E+02	**2.08E+03**	3.64E+03
CWOA	2.44E+06	8.22E+06	3.64E+04	4.38E+07	3.60E+03	**3.70E+02**	2.99E+03	4.41E+03
OBWOA	7.75E+05	1.44E+06	2.82E+04	5.96E+06	3.58E+03	4.74E+02	2.70E+03	4.72E+03
ACWOA	6.41E+06	6.14E+06	7.01E+05	3.17E+07	3.90E+03	4.01E+02	3.01E+03	4.53E+03
BMWOA	9.00E+04	7.84E+04	1.37E+04	4.23E+05	3.44E+03	4.52E+02	2.63E+03	4.57E+03
IWOA	**1.61E+04**	1.12E+04	**3.97E+03**	**4.27E+04**	3.05E+03	3.40E+02	2.34E+03	**3.61E+03**
BWOA	1.62E+05	2.45E+05	1.90E+04	1.33E+06	3.74E+03	5.07E+02	2.66E+03	4.43E+03
CCMWOA	4.00E+06	5.21E+06	5.04E+04	2.08E+07	3.82E+03	5.09E+02	3.10E+03	4.92E+03
LWOA	6.89E+04	5.00E+04	1.82E+04	2.12E+05	2.96E+03	3.92E+02	2.41E+03	4.19E+03

Table 4 (continued)

	F17				F18			
	Avg	Std	Min	Max	Avg	Std	Min	Max
VCSWOA	**2.46E+03**	2.62E+02	1.97E+03	**2.97E+03**	2.10E+05	2.06E+05	**3.23E+04**	1.13E+06
CWOA	2.65E+03	2.91E+02	2.08E+03	3.28E+03	6.35E+06	5.16E+06	6.94E+04	1.75E+07
OBWOA	2.54E+03	2.42E+02	2.15E+03	3.11E+03	7.46E+05	6.46E+05	8.64E+04	2.92E+06
ACWOA	2.49E+03	2.70E+02	2.02E+03	3.03E+03	2.55E+06	3.23E+06	2.17E+05	1.68E+07
BMWOA	2.46E+03	**2.29E+02**	1.98E+03	3.10E+03	4.31E+06	5.27E+06	1.58E+05	2.58E+07
IWOA	2.43E+03	2.69E+02	1.97E+03	3.06E+03	**2.05E+06**	2.32E+06	2.03E+05	9.21E+06
BWOA	2.67E+03	2.85E+02	2.09E+03	3.33E+03	2.35E+06	2.68E+06	9.97E+04	1.15E+07
CCMWOA	2.69E+03	2.63E+02	2.15E+03	3.29E+03	1.14E+07	1.69E+07	2.33E+05	7.78E+07
LWOA	**2.46E+03**	2.57E+02	**1.91E+03**	**2.97E+03**	2.60E+05	**1.25E+05**	8.92E+04	**6.24E+05**
	F19				F20			
	Avg	Std	Min	Max	Avg	Std	Min	Max
VCSWOA	**1.06E+04**	**1.06E+04**	**2.09E+03**	**5.70E+04**	**2.54E+03**	1.82E+02	2.27E+03	**2.92E+03**
CWOA	3.31E+06	6.99E+06	9.49E+04	3.90E+07	2.78E+03	2.22E+02	2.37E+03	3.22E+03
OBWOA	2.23E+06	1.79E+06	3.22E+04	6.50E+06	2.69E+03	1.84E+02	**2.22E+03**	3.02E+03
ACWOA	1.11E+07	2.14E+07	1.63E+06	1.21E+08	2.66E+03	**1.53E+02**	2.39E+03	2.99E+03
BMWOA	6.50E+05	7.40E+05	1.27E+04	3.54E+06	2.74E+03	2.19E+02	2.31E+03	3.15E+03
IWOA	1.27E+04	1.52E+04	2.23E+03	7.85E+04	2.58E+03	1.74E+02	2.32E+03	3.04E+03
BWOA	4.07E+06	4.11E+06	1.16E+05	1.58E+07	2.71E+03	2.07E+02	2.34E+03	3.08E+03
CCMWOA	3.94E+06	4.54E+06	3.92E+05	1.87E+07	2.71E+03	1.71E+02	2.40E+03	3.02E+03
LWOA	2.31E+05	1.17E+05	4.48E+04	5.36E+05	2.71E+03	2.30E+02	2.27E+03	3.08E+03
	F21				F22			
	Avg	Std	Min	Max	Avg	Std	Min	Max
VCSWOA	**2.53E+03**	4.29E+01	2.44E+03	2.64E+03	6.35E+03	2.03E+03	**2.30E+03**	**8.41E+03**
CWOA	2.61E+03	5.48E+01	2.52E+03	2.74E+03	7.17E+03	1.89E+03	2.57E+03	9.57E+03
OBWOA	2.57E+03	6.01E+01	2.44E+03	2.68E+03	6.26E+03	2.39E+03	2.62E+03	9.23E+03
ACWOA	2.58E+03	**4.24E+01**	2.49E+03	2.71E+03	4.87E+03	2.17E+03	2.77E+03	9.15E+03
BMWOA	2.53E+03	4.73E+01	2.43E+03	2.60E+03	**4.83E+03**	3.11E+03	2.39E+03	9.99E+03
IWOA	2.54E+03	5.09E+01	2.45E+03	2.65E+03	5.93E+03	2.25E+03	2.31E+03	8.47E+03
BWOA	2.57E+03	7.57E+01	**2.24E+03**	2.67E+03	6.59E+03	2.01E+03	2.34E+03	9.37E+03
CCMWOA	2.64E+03	4.58E+01	2.58E+03	2.75E+03	7.79E+03	1.26E+03	4.58E+03	9.85E+03
LWOA	2.53E+03	4.43E+01	2.45E+03	**2.62E+03**	6.93E+03	**1.16E+03**	2.31E+03	8.56E+03
	F23				F24			
	Avg	Std	Min	Max	Avg	Std	Min	Max
VCSWOA	**2.97E+03**	9.02E+01	**2.80E+03**	3.21E+03	**3.11E+03**	8.03E+01	**2.95E+03**	3.32E+03
CWOA	3.09E+03	8.76E+01	2.92E+03	3.26E+03	3.22E+03	1.10E+02	3.03E+03	3.44E+03
OBWOA	3.07E+03	1.11E+02	2.87E+03	3.28E+03	3.13E+03	9.43E+01	**2.95E+03**	3.34E+03
ACWOA	3.06E+03	7.47E+01	2.90E+03	3.24E+03	3.19E+03	7.18E+01	3.07E+03	3.35E+03
BMWOA	2.98E+03	**6.15E+01**	2.86E+03	3.12E+03	3.08E+03	**6.56E+01**	**2.95E+03**	**3.22E+03**
IWOA	3.01E+03	8.57E+01	2.83E+03	3.24E+03	3.15E+03	9.02E+01	2.96E+03	3.33E+03
BWOA	3.06E+03	1.00E+02	2.86E+03	3.26E+03	3.20E+03	1.03E+02	3.00E+03	3.42E+03
CCMWOA	3.20E+03	1.04E+02	3.02E+03	3.37E+03	3.32E+03	9.79E+01	3.09E+03	3.56E+03
LWOA	2.99E+03	6.36E+01	2.91E+03	**3.16E+03**	3.19E+03	1.05E+02	2.98E+03	3.39E+03

Table 4 (continued)

	F25				F26			
	Avg	Std	Min	Max	Avg	Std	Min	Max
VCSWOA	2.91E+03	2.18E+01	**2.88E+03**	**2.95E+03**	7.23E+03	2.08E+03	**2.80E+03**	9.57E+03
CWOA	3.05E+03	8.44E+01	2.94E+03	3.42E+03	7.97E+03	1.02E+03	5.44E+03	9.55E+03
OBWOA	2.99E+03	4.11E+01	2.92E+03	3.13E+03	7.38E+03	1.27E+03	4.62E+03	9.50E+03
ACWOA	3.15E+03	1.10E+02	3.06E+03	3.48E+03	7.32E+03	1.07E+03	4.52E+03	**8.75E+03**
BMWOA	3.03E+03	4.64E+01	2.95E+03	3.14E+03	6.50E+03	1.54E+03	3.17E+03	8.81E+03
IWOA	2.93E+03	2.89E+01	2.89E+03	3.05E+03	7.13E+03	9.12E+02	5.37E+03	9.73E+03
BWOA	3.01E+03	4.95E+01	2.95E+03	3.10E+03	8.02E+03	1.12E+03	6.04E+03	1.02E+04
CCMWOA	3.35E+03	1.18E+02	3.12E+03	3.58E+03	8.86E+03	**8.31E+02**	6.62E+03	1.03E+04
LWOA	**2.90E+03**	**1.99E+01**	**2.88E+03**	**2.95E+03**	**6.28E+03**	1.26E+03	2.90E+03	7.64E+03
	F27				F28			
	Avg	Std	Min	Max	Avg	Std	Min	Max
VCSWOA	3.36E+03	7.04E+01	3.24E+03	3.55E+03	**3.20E+03**	3.45E+01	**3.10E+03**	**3.26E+03**
CWOA	3.40E+03	9.54E+01	3.28E+03	3.63E+03	3.50E+03	1.02E+02	3.30E+03	3.77E+03
OBWOA	3.40E+03	1.27E+02	3.24E+03	3.74E+03	3.37E+03	4.90E+01	3.30E+03	3.51E+03
ACWOA	3.46E+03	1.03E+02	3.26E+03	3.73E+03	3.70E+03	1.59E+02	3.48E+03	4.16E+03
BMWOA	3.34E+03	6.58E+01	3.23E+03	3.47E+03	3.41E+03	4.98E+01	3.34E+03	3.51E+03
IWOA	3.30E+03	7.80E+01	3.23E+03	3.65E+03	3.30E+03	2.63E+01	3.24E+03	3.37E+03
BWOA	3.39E+03	1.22E+02	3.27E+03	3.77E+03	3.40E+03	3.81E+01	3.33E+03	3.47E+03
CCMWOA	3.63E+03	2.03E+02	3.39E+03	4.37E+03	4.69E+03	3.86E+02	4.00E+03	5.56E+03
LWOA	**3.27E+03**	**4.04E+01**	**3.22E+03**	**3.38E+03**	3.23E+03	**2.46E+01**	3.19E+03	**3.26E+03**
	F29				F30			
	Avg	Std	Min	Max	Avg	Std	Min	Max
VCSWOA	4.34E+03	3.54E+02	**3.70E+03**	5.26E+03	**2.79E+05**	**2.73E+05**	**2.55E+04**	**1.05E+06**
CWOA	4.75E+03	3.69E+02	3.97E+03	5.86E+03	1.08E+07	8.12E+06	5.94E+05	2.99E+07
OBWOA	4.80E+03	4.25E+02	3.87E+03	5.56E+03	1.37E+07	8.53E+06	4.19E+06	4.59E+07
ACWOA	4.82E+03	3.71E+02	4.23E+03	5.65E+03	5.69E+07	4.15E+07	6.80E+06	1.53E+08
BMWOA	4.72E+03	3.68E+02	4.01E+03	5.59E+03	6.01E+06	4.00E+06	9.54E+05	2.02E+07
IWOA	**4.16E+03**	2.61E+02	3.66E+03	4.79E+03	6.12E+05	5.82E+05	1.58E+05	2.88E+06
BWOA	5.01E+03	4.38E+02	4.29E+03	5.84E+03	2.15E+07	1.55E+07	1.14E+06	5.25E+07
CCMWOA	5.36E+03	5.60E+02	4.32E+03	6.56E+03	5.91E+07	4.13E+07	3.35E+06	1.78E+08
LWOA	4.18E+03	**2.41E+02**	3.80E+03	**4.74E+03**	8.88E+05	3.82E+05	3.76E+05	2.32E+06

Bold are the best values

$g_2(x) = \left(4x_2^2 - x_1x_2/12,566\left(x_2x_1^3 - x_1^4\right) + \left(1/5108x_1^2\right)\right)$
$-10 \leq 0$

$g_3(x) = 1 - \left(140.45x_1/x_2^2x_3\right) \leq 0$

$g_4(x) = \left(x_2 + x_1\right)/1.5 - 1 \leq 0,$

Variable Range

$0.05 \leq x_1 \leq 2.00$

$0.25 \leq x_2 \leq 1.30$

$2.00 \leq x_3 \leq 15.00$

The statistical results to this problem are shown in Table 8 in which the proposed algorithm is compared with GA, WOA, MVO, GSA, PSO and MFO and it's noticed that VCSWOA has the best result.

5.2.4 Cantilever beam design problem

The last engineering problem introduced in this subsection is the Cantilever beam design problem which consists of 5 square hollow cross-sections. It intends to dwindle the Cantilever beam mass. The problem formulation is shown as follows:

Minimize:

$f(x) = 0.6224(x_1 + x_2 + x_3 + x_4 + x_5)$

Subject to:

$G(x) = 61/x_1^3 + 37/x_2^3 + 19/x_3^3 + 7/x_4 + 1/x_5^3$

Variable Range

$0.1 \leq x_i \leq 100, \qquad i = 1, 2, 3, 4, 5$

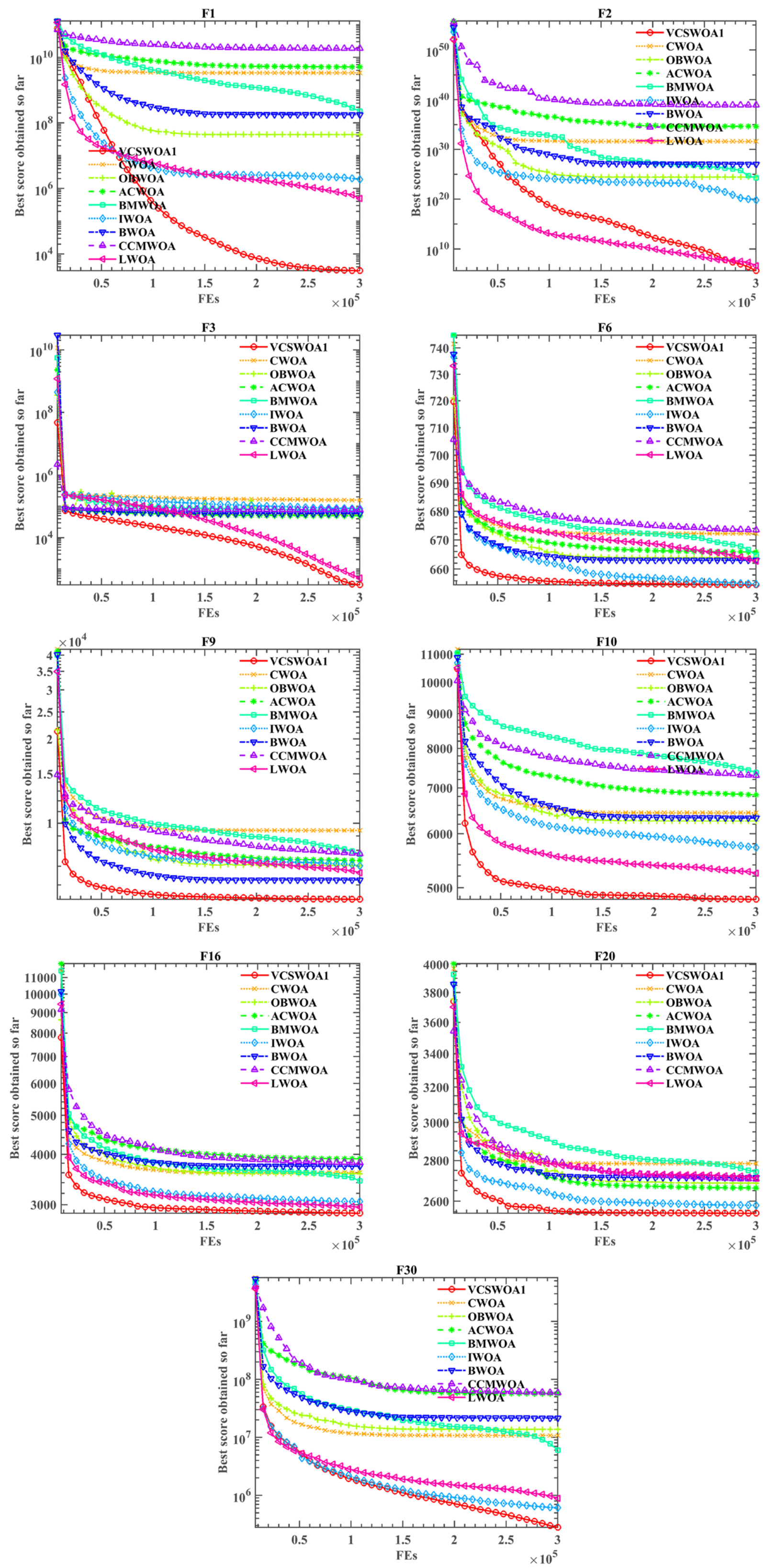

Fig. 2 Unimodal and multi-modal functions convergence curve

Table 5 The calculated p values from the signed-rank test

F.	CWOA	OBWOA	ACWOA	BMWOA	IWOA	BWOA	CCMWOA	LWOA
F1	1.73E−06	1.73E−06	1.73E−06	1.73E−06	1.73E−06	1.73E−06	1.73E−06	1.73E−06
F2	1.73E−06	1.73E−06	1.73E−06	1.73E−06	1.73E−06	1.73E−06	1.73E−06	5.45E−02
F3	1.73E−06	1.73E−06	1.73E−06	1.73E−06	1.73E−06	1.73E−06	1.73E−06	1.73E−06
F4	1.73E−06	1.73E−06	1.73E−06	1.73E−06	8.92E−05	1.73E−06	1.73E−06	3.93E−01
F5	1.48E−03	5.67E−03	5.67E−03	1.20E−01	1.71E−01	8.29E−01	1.13E−05	2.71E−01
F6	4.72E−06	1.36E−04	2.37E−05	1.06E−04	6.88E−01	1.15E−04	1.73E−06	2.96E−03
F7	0.95E−01	3.18E−01	2.29E−01	6.00E−01	4.29E−06	9.75E−01	4.05E−01	1.97E−05
F8	2.61E−04	6.98E−06	2.60E−05	4.90E−04	1.41E−01	2.54E−01	1.92E−06	1.66E−02
F9	5.75E−06	3.88E−06	1.92E−06	1.92E−06	1.04E−03	2.60E−05	2.13E−06	4.53E−04
F10	1.73E−06	6.98E−06	1.92E−06	1.73E−06	1.36E−04	1.02E−05	1.73E−06	5.45E−02
F11	1.73E−06	1.73E−06	1.73E−06	1.73E−06	1.73E−06	1.73E−06	1.73E−06	2.16E−05
F12	1.73E−06	1.73E−06	1.73E−06	1.73E−06	1.25E−04	1.73E−06	1.73E−06	5.45E−02
F13	9.31E−06	1.73E−06	1.73E−06	1.73E−06	1.59E−03	1.73E−06	1.73E−06	1.73E−06
F14	1.73E−06	2.13E−06	1.73E−06	1.92E−06	1.92E−06	1.73E−06	1.73E−06	6.73E−01
F15	1.73E−06	1.92E−06	1.73E−06	5.22E−06	1.20E−01	1.92E−06	1.73E−06	2.35E−06
F16	7.69E−06	1.97E−05	2.88E−06	1.36E−04	6.27E−02	3.88E−06	6.34E−06	5.30E−01
F17	2.41E−03	1.85E−01	6.73E−01	9.26E−01	7.50E−01	2.43E−02	4.11E−03	8.77E−01
F18	2.12E−06	1.89E−04	1.73E−06	1.73E−06	5.75E−06	6.98E−06	2.13E−06	4.28E−02
F19	1.73E−06	1.73E−06	1.73E−06	1.73E−06	5.86E−01	1.73E−06	1.73E−06	1.73E−06
F20	1.59E−03	1.85E−02	1.11E−02	5.29E−04	3.18E−01	6.04E−03	4.99E−03	4.39E−03
F21	2.84E−05	1.71E−03	1.49E−05	6.73E−01	2.71E−01	1.38E−03	2.35E−06	6.14E−01
F22	1.15E−01	8.13E−01	1.11E−02	5.19E−02	2.71E−01	7.19E−01	3.85E−03	2.62E−01
F23	1.05E−04	1.48E−03	6.16E−04	2.21E−01	2.18E−02	6.84E−03	4.29E−06	3.09E−01
F24	7.15E−04	1.85E−01	3.06E−04	1.59E−01	4.72E−02	1.48E−03	3.18E−06	5.67E−03
F25	1.73E−06	1.73E−06	1.73E−06	1.73E−06	4.90E−04	1.73E−06	1.73E−06	3.49E−01
F26	7.52E−02	8.29E−01	7.50E−01	6.27E−02	2.71E−01	3.18E−01	7.71E−04	3.33E−02
F27	1.58E−01	2.62E−01	1.60E−04	1.71E−01	1.48E−03	6.14E−01	2.60E−06	1.36E−05
F28	1.73E−06	1.73E−06	1.73E−06	1.73E−06	1.73E−06	1.73E−06	1.73E−06	6.16E−04
F29	1.60E−04	8.31E−04	4.20E−04	3.59E−04	3.87E−02	7.69E−06	2.35E−06	2.21E−01
F30	1.73E−06	1.73E−06	1.73E−06	1.73E−06	2.26E−03	1.73E−06	1.73E−06	1.13E−05

Table 6 Optimization results for pressure vessel design problem

Algorithm	Optimization results			Cost	
	T_s	T_h	R	L	Cost
VCSWOA	0.87451	0.430244	45.24849	142.4528	5515.211
SMA [12]	0.8125	0.4375	42.09844	176.6366	6059.715
WOA [88]	0.812500	0.4375	42.0982	176.638	6059.7410
GWO [89]	0.8125	0.4345	42.0892	176.7587	6051.5639
MFO [90]	0.8125	0.4375	42.0984	176.6366	6059.7143
ACO [91]	0.8125	0.4375	42.1036	176.5727	6059.0888
HPSO [92]	0.8125	0.4375	42.0984	176.6366	6059.7143
BA [93]	0.8125	0.4375	42.0984	176.6366	6059.7143

Table 9 compares VCSWOA with many algorithms MFO, SOS, CS, MMA, and GCA. It is seen that VCSWOA achieved the best result. As per results, we can find the potential of the proposed WOA-based method is not limited to these cases and it can be applied to more complex cases such as image classification [95, 96].

Table 7 Optimization results for welded beam design problem

Algorithm	Optimization results				Cost
	h	l	t	b	
VCSWOA	0.18885	3.5685	9.025806	0.207104	1.72003
CSA	0.2054	3.2589	9.0384	0.2068	1.73604
WOA	0.205	3.4842	9.0374	0.2062	1.73049
MVO	0.2054	3.4731	9.0445	0.2056	1.72645
MFO	0.2057	3.4703	9.0364	0.2057	1.72452
SSA [94]	0.2057	3.4714	9.0366	0.2057	1.72491

5.3 Image segmentation

In literature, many techniques are existed to segment images such as Otsu [97], Kapur [98], etc which are used to divide

Table 8 Optimization results for the Tension/compression design problem

Algorithm	Optimization results			Cost
	d	D	N	
VCSWOA	0.05169	0.356736	11.28791	0.012665
GA	0.05010	0.31011	14.0000	0.013036
WOA	0.05120	0.34521	12.0040	0.012676
MVO	0.05251	0.37602	10.3351	0.012790
GSA	0.05027	0.32368	13.5254	0.012702
PSO	0.05000	0.31041	15.0000	0.013192
MFO	0.05000	0.31350	14.0327	0.012753

image histogram to different groups based on threshold values. Figure 3 shows the flowchart of Berkeley image segmentation(MIS) for 241,004. Here, to validate our algorithm VCSWOA, 8 images from BSDS500 are used namely: 291,000, 38,092, 86,068, 170,057, 61,060, 175,032, 223,061, and 19,021. Figure 4 shows these images and their 2D histogram. Different metaheuristic algorithms are used in order to compare their results with VCSWOA: WOA, BA, CS, CBA, SCA, BLPSO, IGWO, IWOA, and SCADE. Finally, Peak Signal to Noise Ratio (PSNR) [99], Structural Similarity Index (SSIM) [100], and Feature Similarity Index (FSIM) [101] are used to evaluate image segmentation

Table 9 Optimization results for cantilever beam problem

Algorithm	Optimization results					Cost
	x_1	x_2	x_3	x_4	x_5	
VCSWOA	6.015106	5.307156	4.499152	3.49513	2.157171	1.33996
MFO	5.9830	5.3167	4.4973	3.5136	2.1616	1.33998
SOS	6.0188	5.3034	4.4959	3.4990	2.1556	1.33996
CS	6.0089	5.3049	4.5023	3.5077	2.1504	1.33999
MMA	6.0100	5.3000	4.4900	3.4900	2.1500	1.3400
GCA	6.0100	5.3000	4.4900	3.4900	2.1500	1.3400

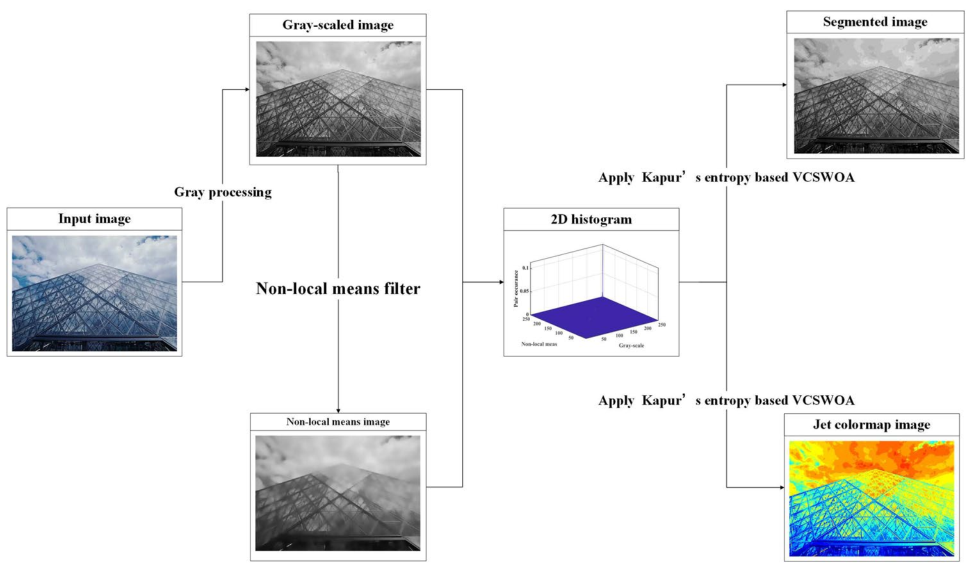

Fig. 3 Flowchart of MIS for 241,004

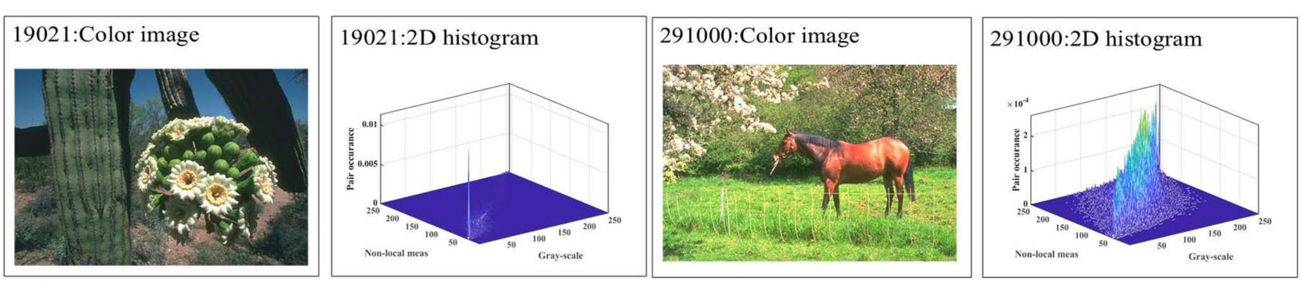

Fig. 4 Three-dimension view about 2D histograms of 19,021 and 291,000

Table 10 The PSNR comparison results of VCSWOA and other methods

Image	Thres.	Item	VCSWOA	WOA	BA	CS	CBA
291,000	2	AVG	**1.5469E+01**	1.4139E+01	1.3897E+01	1.4769E+01	1.4254E+01
		STD	1.4761E+00	2.1959E+00	2.4638E+00	1.8668E+00	1.7854E+00
	4	AVG	1.7513E+01	1.7192E+01	1.7589E+01	1.7643E+01	1.7404E+01
		STD	1.2496E+00	1.9756E+00	1.2213E+00	1.4215E+00	1.6360E+00
	6	AVG	**2.0709E+01**	2.0247E+01	1.9773E+01	2.0307E+01	2.0642E+01
		STD	9.5755E−01	1.6762E+00	2.1459E+00	1.3320E+00	1.6209E+00
	12	AVG	**2.6933E+01**	2.5977E+01	2.6811E+01	2.5762E+01	2.6791E+01
		STD	**3.6690E−01**	1.0349E+00	5.0902E−01	9.7953E−01	6.7301E−01
	16	AVG	**2.9321E+01**	2.8230E+01	2.8879E+01	2.8027E+01	2.8797E+01
		STD	**3.4656E−01**	8.1473E−01	5.9989E−01	8.9664E−01	7.5941E−01
	18	AVG	**3.0097E+01**	2.9088E+01	2.9594E+01	2.8607E+01	2.9684E+01
		STD	**3.9234E−01**	7.2479E−01	1.0276E+00	1.1026E+00	8.7337E−01
38,092	2	AVG	1.5387E+01	1.5384E+01	1.5215E+01	1.5382E+01	1.5351E+01
		STD	4.3936E−02	3.8515E−02	1.2991E+00	4.7546E−02	7.4480E−01
	4	AVG	**2.0529E+01**	2.0395E+01	2.0206E+01	2.0125E+01	2.0273E+01
		STD	**2.0084E−01**	2.8220E−01	1.2453E+00	3.8400E−01	8.0005E−01
	6	AVG	**2.3475E+01**	2.3283E+01	2.2896E+01	2.2677E+01	2.2158E+01
		STD	**8.3431E−02**	4.2648E−01	8.7902E−01	6.1763E−01	2.3798E+00
	12	AVG	**2.6377E+01**	2.5152E+01	2.6043E+01	2.5512E+01	2.6331E+01
		STD	**6.6003E−01**	7.9456E−01	2.6720E+00	7.1953E−01	8.0805E−01
	16	AVG	**2.9265E+01**	2.7852E+01	2.8393E+01	2.7846E+01	2.8177E+01
		STD	**4.4913E−01**	8.9518E−01	1.2202E+00	9.0842E−01	9.9741E−01
	18	AVG	**3.0408E+01**	2.8551E+01	2.9355E+01	2.8475E+01	2.9228E+01
		STD	**3.5656E−01**	1.0112E+00	1.0705E+00	1.0019E+00	1.4376E+00
86,068	2	AVG	1.5408E+01	1.5386E+01	1.5121E+01	1.5403E+01	1.5401E+01
		STD	**7.2269E−15**	3.6534E−02	7.4762E−01	5.9756E−03	4.7379E−02
	4	AVG	**1.9891E+01**	1.9796E+01	1.8567E+01	1.9638E+01	1.9081E+01
		STD	**2.9325E−01**	2.9573E−01	2.5709E+00	3.3398E−01	7.2704E−01
	6	AVG	**2.1871E+01**	2.1561E+01	2.1677E+01	2.1716E+01	2.1774E+01
		STD	**9.7778E−02**	3.6714E−01	1.0208E+00	2.9527E−01	2.4534E−01
	12	AVG	**2.6344E+01**	2.3444E+01	2.6248E+01	2.3161E+01	2.5491E+01
		STD	2.4088E+00	2.6082E+00	2.4976E+00	2.8482E+00	2.8115E+00
	16	AVG	**2.9412E+01**	2.5078E+01	2.8657E+01	2.6035E+01	2.7680E+01
		STD	**6.3045E−01**	2.9563E+00	2.2350E+00	2.3166E+00	3.2288E+00
	18	AVG	**2.9456E+01**	2.6956E+01	2.8479E+01	2.6916E+01	2.7836E+01
		STD	**1.2954E+00**	2.4324E+00	2.6393E+00	2.2689E+00	2.7271E+00
170,057	2	AVG	1.3852E+01	1.3751E+01	1.3791E+01	1.3603E+01	1.3921E+01
		STD	2.0594E−01	9.5548E−01	1.0196E+00	9.2202E−01	9.1945E−01
	4	AVG	1.8865E+01	1.8325E+01	1.8256E+01	**1.9270E+01**	1.8254E+01
		STD	**2.8104E−01**	1.3948E+00	1.5323E+00	7.7237E−01	1.5720E+00
	6	AVG	**2.1849E+01**	2.1050E+01	2.1672E+01	2.1564E+01	2.1592E+01
		STD	**7.6181E−01**	1.3121E+00	9.2326E−01	8.3760E−01	1.1731E+00
	12	AVG	**2.7977E+01**	2.6917E+01	2.6576E+01	2.6004E+01	2.6967E+01
		STD	**7.0969E−01**	1.1501E+00	1.9470E+00	1.1942E+00	1.3415E+00
	16	AVG	**3.0352E+01**	2.9215E+01	2.8094E+01	2.7853E+01	2.9023E+01
		STD	**5.3477E−01**	1.3431E+00	2.4247E+00	1.3126E+00	1.2279E+00
	18	AVG	**3.1418E+01**	2.9568E+01	2.9102E+01	2.8827E+01	2.9675E+01
		STD	**5.3128E−01**	1.4872E+00	2.2030E+00	1.3816E+00	1.7367E+00

Table 10 (continued)

Image	Thres.	Item	VCSWOA	WOA	BA	CS	CBA
61,060	2	AVG	1.4356E+01	1.4049E+01	1.4032E+01	1.4234E+01	1.4139E+01
		STD	**1.1816E−01**	6.7220E−01	6.6207E−01	2.8012E−01	2.9366E−01
	4	AVG	1.8815E+01	1.8423E+01	1.8813E+01	1.8539E+01	**1.8862E+01**
		STD	**2.4711E−01**	8.3974E−01	7.6752E−01	3.6267E−01	3.4265E−01
	6	AVG	2.1473E+01	2.1380E+01	2.1197E+01	2.1126E+01	**2.1474E+01**
		STD	**3.3790E−01**	5.2729E−01	1.6500E+00	7.2119E−01	3.9212E−01
	12	AVG	**2.6133E+01**	2.5162E+01	2.5128E+01	2.5321E+01	2.5634E+01
		STD	**8.3500E−01**	1.3203E+00	2.2377E+00	1.1990E+00	1.5028E+00
	16	AVG	**2.8816E+01**	2.7887E+01	2.7648E+01	2.7137E+01	2.8255E+01
		STD	**1.0001E+00**	1.6246E+00	1.6622E+00	1.5419E+00	1.0464E+00
	18	AVG	**2.9906E+01**	2.8653E+01	2.8864E+01	2.8714E+01	2.8606E+01
		STD	1.1216E+00	1.2467E+00	1.6273E+00	**9.9666E−01**	1.2067E+00
175032	2	AVG	1.3812E+01	1.3835E+01	1.2815E+01	1.3847E+01	1.3253E+01
		STD	1.7202E−01	**1.4738E−02**	1.6036E+00	1.4902E−02	1.1813E+00
	4	AVG	1.8419E+01	1.8385E+01	1.8259E+01	1.8336E+01	1.8320E+01
		STD	**1.2114E−01**	1.7594E−01	8.2320E−01	1.7005E−01	8.0605E−01
	6	AVG	2.1213E+01	2.1003E+01	2.1209E+01	2.0931E+01	2.1055E+01
		STD	**1.6797E−01**	6.5009E−01	7.4971E−01	3.4788E−01	1.1952E+00
	12	AVG	**2.8808E+01**	2.7681E+01	2.6606E+01	2.6680E+01	2.7890E+01
		STD	**4.6737E−01**	1.2573E+00	3.1113E+00	9.7908E−01	8.5450E−01
	16	AVG	**3.1056E+01**	3.0001E+01	2.8702E+01	2.8608E+01	2.8856E+01
		STD	**6.8160E−01**	8.3821E−01	1.7951E+00	1.0730E+00	1.5784E+00
	18	AVG	**3.2171E+01**	2.9859E+01	2.8629E+01	2.9102E+01	2.9760E+01
		STD	**3.6441E−01**	1.8403E+00	2.6881E+00	1.9095E+00	2.4370E+00
223,061	2	AVG	**1.6721E+01**	1.5206E+01	1.5525E+01	1.5585E+01	1.6131E+01
		STD	4.2365E−01	2.2905E+00	2.1146E+00	2.8287E+00	8.8540E−01
	4	AVG	**2.0451E+01**	1.9366E+01	1.9038E+01	1.6999E+01	1.9424E+01
		STD	1.3275E+00	1.7030E+00	3.4719E+00	3.6009E+00	2.1386E+00
	6	AVG	**2.2436E+01**	1.9660E+01	2.0656E+01	1.9185E+01	2.0641E+01
		STD	2.3760E+00	3.7313E+00	3.0777E+00	3.6299E+00	3.5669E+00
	12	AVG	**2.7966E+01**	2.6284E+01	2.6744E+01	2.6247E+01	2.6837E+01
		STD	**1.8689E−01**	1.1467E+00	1.2547E+00	7.5128E−01	1.5959E+00
	16	AVG	**3.0086E+01**	2.8589E+01	2.8515E+01	2.8092E+01	2.8809E+01
		STD	**3.1224E−01**	9.1802E−01	2.0070E+00	8.3237E−01	1.1132E+00
	18	AVG	**3.1237E+01**	2.9520E+01	2.9461E+01	2.8892E+01	2.9660E+01
		STD	**1.2594E−01**	8.5945E−01	1.2496E+00	7.5785E−01	1.0214E+00
19,021	2	AVG	**1.6238E+01**	1.6036E+01	1.5678E+01	1.6014E+01	1.5379E+01
		STD	**9.9054E−02**	8.8069E−01	1.4377E+00	3.5023E−01	1.4737E+00
	4	AVG	**1.9356E+01**	1.9011E+01	1.9246E+01	1.8680E+01	1.9125E+01
		STD	5.7631E−01	4.8208E−01	6.4570E−01	**3.5639E−01**	9.8518E−01
	6	AVG	**2.2709E+01**	2.1677E+01	2.1817E+01	2.1411E+01	2.1857E+01
		STD	**2.4533E−01**	1.1769E+00	1.6717E+00	1.1426E+00	1.1902E+00
	12	AVG	2.6861E+01	2.6606E+01	2.6950E+01	2.6774E+01	**2.7311E+01**
		STD	**5.2986E−01**	1.1172E+00	1.1677E+00	6.7277E−01	8.2237E−01
	16	AVG	**2.9153E+01**	2.8754E+01	2.8813E+01	2.8531E+01	2.8813E+01
		STD	**5.3685E−01**	1.2670E+00	2.4828E+00	1.1967E+00	1.5402E+00
	18	AVG	3.0062E+01	2.9528E+01	2.9770E+01	2.9300E+01	**3.0362E+01**
		STD	**5.7887E−01**	1.3410E+00	1.7697E+00	1.0482E+00	9.2978E−01

Bold are the best values

Table 11 The PSNR comparison results of VCSWOA and other methods

Image	Thres.	Item	VCSWOA	WOA	BA	CS	CBA
291,000	2	AVG	1.1540E+01	1.4249E+01	1.4272E+01	1.4199E+01	1.4009E+01
		STD	2.7555E+00	2.4146E−01	2.8738E−01	**2.0941E−01**	5.4376E−01
	4	AVG	1.5859E+01	1.8789E+01	**1.8579E+01**	1.7861E+01	1.6217E+01
		STD	1.8047E+00	**2.8304E−01**	3.4108E−01	9.0971E−01	1.2937E+00
	6	AVG	1.6921E+01	2.0607E+01	2.0686E+01	2.0446E+01	1.8123E+01
		STD	1.7870E+00	7.6795E−01	**7.2809E−01**	8.9592E−01	1.3799E+00
	12	AVG	2.2402E+01	2.4778E+01	2.4480E+01	2.5059E+01	2.2004E+01
		STD	1.8687E+00	1.0563E+00	1.0990E+00	1.0182E+00	1.7773E+00
	16	AVG	2.4270E+01	2.6785E+01	2.5787E+01	2.6458E+01	2.4438E+01
		STD	1.7749E+00	9.4010E−01	1.5702E+00	1.2329E+00	1.9780E+00
	18	AVG	2.5003E+01	2.7446E+01	2.6855E+01	2.6773E+01	2.5366E+01
		STD	2.3659E+00	1.1111E+00	1.5033E+00	2.3238E+00	1.5514E+00
38,092	2	AVG	**1.5402E+01**	1.2963E+01	1.3846E+01	1.3546E+01	1.3705E+01
		STD	7.6257E−01	4.0976E−01	**1.0417E−02**	4.5647E−01	2.1328E−01
	4	AVG	1.8406E+01	1.8066E+01	1.8335E+01	1.7927E+01	1.6334E+01
		STD	1.8150E+00	8.0144E−01	2.3587E−01	7.5284E−01	1.1044E+00
	6	AVG	1.9858E+01	2.0521E+01	2.0417E+01	1.9891E+01	1.7911E+01
		STD	1.7718E+00	9.8209E−01	5.6960E−01	1.1738E+00	1.6814E+00
	12	AVG	2.1656E+01	2.4457E+01	2.3778E+01	2.4082E+01	2.2171E+01
		STD	1.6223E+00	9.0147E−01	1.6145E+00	1.6152E+00	1.6195E+00
	16	AVG	2.4075E+01	2.6534E+01	2.5590E+01	2.6587E+01	2.4074E+01
		STD	1.6939E+00	1.2584E+00	1.2455E+00	1.2201E+00	1.9278E+00
	18	AVG	2.5049E+01	2.6977E+01	2.6481E+01	2.6554E+01	2.5369E+01
		STD	2.0921E+00	9.0452E−01	1.2262E+00	1.2410E+00	1.6953E+00
86,068	2	AVG	1.5178E+01	1.6710E+01	**1.6731E+01**	1.6019E+01	1.5724E+01
		STD	3.3427E−01	2.6455E−01	1.1641E−01	1.0228E+00	1.2836E+00
	4	AVG	1.7427E+01	1.9875E+01	1.9536E+01	1.9578E+01	1.7006E+01
		STD	1.7686E+00	2.0890E+00	1.9036E+00	1.4426E+00	3.1604E+00
	6	AVG	1.9143E+01	2.0526E+01	1.9740E+01	2.0408E+01	1.7993E+01
		STD	1.8736E+00	2.6564E+00	3.3539E+00	3.0873E+00	3.0954E+00
	12	AVG	2.1071E+01	2.4087E+01	2.1381E+01	2.2957E+01	2.1852E+01
		STD	2.5240E+00	1.6310E+00	2.7945E+00	2.4905E+00	2.7815E+00
	16	AVG	2.2750E+01	2.5571E+01	2.4100E+01	2.4791E+01	2.4665E+01
		STD	3.6002E+00	1.9866E+00	2.0990E+00	2.6484E+00	2.4248E+00
	18	AVG	2.4333E+01	2.6632E+01	2.5276E+01	2.6121E+01	2.4252E+01
		STD	2.2138E+00	1.5505E+00	2.6093E+00	2.5882E+00	3.1475E+00
170,057	2	AVG	1.3505E+01	1.3619E+01	**1.6233E+01**	1.5743E+01	1.5989E+01
		STD	1.1268E+00	1.3194E+00	**1.7764E−01**	9.1626E−01	8.0962E−01
	4	AVG	1.7908E+01	1.8248E+01	1.9210E+01	1.7810E+01	1.8220E+01
		STD	1.6775E+00	1.5512E+00	6.7226E−01	1.4543E+00	1.9514E+00
	6	AVG	1.9306E+01	2.0350E+01	2.1469E+01	2.0503E+01	1.9188E+01
		STD	1.7152E+00	1.2832E+00	1.3550E+00	1.6392E+00	1.9084E+00
	12	AVG	2.3672E+01	2.4131E+01	2.5379E+01	2.4856E+01	2.2474E+01
		STD	2.1226E+00	1.9157E+00	1.8850E+00	2.1013E+00	2.6435E+00
	16	AVG	2.4800E+01	2.6165E+01	2.6705E+01	2.7230E+01	2.5273E+01
		STD	1.8292E+00	1.6078E+00	2.1586E+00	1.6927E+00	1.7392E+00
	18	AVG	2.5049E+01	2.7035E+01	2.7071E+01	2.8110E+01	2.5473E+01
		STD	2.3897E+00	1.4866E+00	1.4915E+00	1.5644E+00	2.4709E+00

Table 11 (continued)

Image	Thres.	Item	VCSWOA	WOA	BA	CS	CBA
61,060	2	AVG	1.3884E+01	1.3183E+01	1.4867E+01	1.3281E+01	1.2860E+01
		STD	5.4384E−01	1.6621E+00	1.3692E+00	2.0230E+00	2.0075E+00
	4	AVG	1.6508E+01	1.7109E+01	1.6907E+01	1.7027E+01	1.5479E+01
		STD	1.3925E+00	1.3877E+00	1.4644E+00	1.8427E+00	2.5192E+00
	6	AVG	1.8484E+01	1.8822E+01	1.9271E+01	1.8890E+01	1.8108E+01
		STD	1.2882E+00	1.7603E+00	1.5250E+00	1.9604E+00	2.0635E+00
	12	AVG	2.2464E+01	2.4174E+01	2.4230E+01	2.3987E+01	2.2343E+01
		STD	2.1438E+00	2.1911E+00	1.3344E+00	1.6406E+00	3.1568E+00
	16	AVG	2.3939E+01	2.6533E+01	2.6404E+01	2.5781E+01	2.5068E+01
		STD	2.9817E+00	2.0090E+00	1.4375E+00	2.4686E+00	1.9827E+00
	18	AVG	2.5627E+01	2.7636E+01	2.7320E+01	2.7151E+01	2.5723E+01
		STD	2.2776E+00	1.5247E+00	1.2747E+00	2.1666E+00	2.0443E+00
175,032	2	AVG	1.3524E+01	1.4766E+01	1.5383E+01	1.5272E+01	**1.5537E+01**
		STD	3.8959E−01	1.2054E+00	3.7511E−02	3.3892E−01	5.9322E−01
	4	AVG	1.5754E+01	1.8646E+01	**2.0356E+01**	1.9651E+01	1.8942E+01
		STD	1.6555E+00	1.5270E+00	2.9627E−01	8.4606E−01	1.6884E+00
	6	AVG	1.7960E+01	2.1199E+01	2.3097E+01	2.2207E+01	2.0319E+01
		STD	1.8154E+00	1.2152E+00	6.8594E−01	1.1725E+00	1.9910E+00
	12	AVG	2.3648E+01	2.3977E+01	2.5698E+01	2.6197E+01	2.3586E+01
		STD	1.9610E+00	1.6781E+00	1.6910E+00	1.4663E+00	1.9628E+00
	16	AVG	2.5858E+01	2.6156E+01	2.7215E+01	2.7661E+01	2.4820E+01
		STD	1.9990E+00	1.3185E+00	2.0427E+00	2.1651E+00	1.9969E+00
	18	AVG	2.5432E+01	2.7299E+01	2.7602E+01	2.8041E+01	2.6381E+01
		STD	2.0126E+00	1.2310E+00	1.6108E+00	1.8014E+00	1.6936E+00
223,061	2	AVG	1.5080E+01	1.5402E+01	1.5403E+01	1.5369E+01	1.5253E+01
		STD	1.6679E+00	1.7161E−02	**1.4723E−02**	1.0240E−01	1.8501E−01
	4	AVG	1.6531E+01	1.9020E+01	1.9640E+01	1.9489E+01	1.7854E+01
		STD	3.0394E+00	4.8091E−01	**3.2839E−01**	4.5413E−01	1.2589E+00
	6	AVG	1.6743E+01	2.1258E+01	2.1421E+01	2.1104E+01	1.8141E+01
		STD	3.3762E+00	**4.9606E−01**	7.2741E−01	1.0828E+00	1.9674E+00
	12	AVG	2.3033E+01	2.4495E+01	2.5389E+01	2.5219E+01	2.2500E+01
		STD	1.4262E+00	1.5994E+00	1.1023E+00	1.1338E+00	1.9331E+00
	16	AVG	2.4610E+01	2.6106E+01	2.6615E+01	2.6965E+01	2.4468E+01
		STD	1.8484E+00	1.2718E+00	1.6195E+00	1.5873E+00	1.5348E+00
	18	AVG	2.5363E+01	2.7304E+01	2.6930E+01	2.7834E+01	2.5219E+01
		STD	1.4702E+00	1.3278E+00	8.1205E−01	1.2441E+00	1.8808E+00
19,021	2	AVG	1.5450E+01	1.4130E+01	1.3846E+01	1.3931E+01	1.3626E+01
		STD	9.1065E−01	4.2569E−01	3.0575E−01	7.0591E−01	1.0463E+00
	4	AVG	1.6878E+01	1.8872E+01	1.8946E+01	1.8744E+01	1.7852E+01
		STD	2.4115E+00	9.4882E−01	1.1093E+00	9.1329E−01	1.3193E+00
	6	AVG	1.8983E+01	2.1017E+01	2.1098E+01	2.0980E+01	1.8807E+01
		STD	2.1188E+00	9.6586E−01	1.1209E+00	1.5207E+00	1.7535E+00
	12	AVG	2.2867E+01	2.4693E+01	2.4628E+01	2.4482E+01	2.3319E+01
		STD	2.3472E+00	1.4290E+00	1.7702E+00	1.5539E+00	1.3545E+00
	16	AVG	2.5079E+01	2.7020E+01	2.6847E+01	2.7504E+01	2.5438E+01
		STD	2.0556E+00	1.3793E+00	1.8186E+00	1.2652E+00	1.9875E+00
	18	AVG	2.6227E+01	2.8093E+01	2.6960E+01	2.7801E+01	2.5510E+01
		STD	1.6849E+00	1.4210E+00	1.7548E+00	2.0122E+00	2.1284E+00

Bold are the best values

Table 12 The SSIM comparison results of VCSWOA and other methods

Image	Thres.	Item	SCA	BLPSO	IGWO	IWOA	SCADE
291,000	2	AVG	**7.0750E+01**	6.8577E−01	6.9009E−01	7.0093E−01	7.0022E−01
		STD	4.0932E−02	4.4047E−02	7.9963E−02	4.4785E−02	4.0458E−02
	4	AVG	7.8451E−01	7.7853E−01	7.8563E−01	7.8200E−01	7.7637E−01
		STD	2.9222E−02	4.0825E−02	3.2227E−02	3.4994E−02	4.1429E−02
	6	AVG	8.2647E−01	8.2891E−01	8.2036E−01	8.2539E−01	8.3739E−01
		STD	**1.3973E−02**	2.7519E−02	5.6508E−02	3.5432E−02	3.6554E−02
	12	AVG	**9.6328E−01**	9.5016E−01	9.6195E−01	9.4784E−01	9.6094E−01
		STD	**3.0024E−03**	1.3255E−02	4.0376E−03	1.2800E−02	5.0739E−03
	16	AVG	**9.7680E−01**	9.6795E−01	9.7410E−01	9.6552E−01	9.7308E−01
		STD	**1.8180E−03**	6.2520E−03	3.2901E−03	7.8420E−03	4.7776E−03
	18	AVG	**9.8019E−01**	9.7320E−01	9.7599E−01	9.6795E−01	9.7666E−01
		STD	**1.5076E−03**	5.9712E−03	9.6273E−03	1.0099E−02	5.1768E−03
38,092	2	AVG	**6.2308E−01**	6.2288E−01	6.0298E−01	6.2272E−01	6.1547E−01
		STD	2.4614E−03	2.1863E−03	8.6580E−02	2.6885E−03	4.5442E−02
	4	AVG	**8.3939E−01**	8.3607E−01	8.2633E−01	8.2707E−01	8.3190E−01
		STD	**5.7686E−03**	7.0205E−03	5.4741E−02	1.1822E−02	2.4842E−02
	6	AVG	**9.0610E−01**	9.0314E−01	8.9403E−01	8.8821E−01	8.6704E−01
		STD	**1.8303E−03**	8.4161E−03	2.0440E−02	1.4146E−02	9.1687E−02
	12	AVG	**9.2602E−01**	9.0919E−01	9.0245E−01	8.9843E−01	9.1824E−01
		STD	**5.7827E−03**	1.9579E−02	8.0001E−02	1.2397E−02	8.6744E−03
	16	AVG	**9.4331E−01**	9.2835E−01	9.3737E−01	9.2707E−01	9.3673E−01
		STD	**3.7487E−03**	1.1904E−02	1.1511E−02	9.5202E−03	9.9155E−03
	18	AVG	**9.5197E−01**	9.3895E−01	9.4432E−01	9.3188E−01	9.4418E−01
		STD	**3.5307E−03**	1.1701E−02	7.4438E−03	1.0033E−02	1.4255E−02
86,068	2	AVG	**5.9149E−01**	5.8995E−01	5.7178E−01	5.9107E−01	5.9094E−01
		STD	**0.0000E+00**	2.9551E−03	5.1163E−02	4.9198E−04	5.6689E−03
	4	AVG	**7.3581E−01**	7.3535E−01	6.8994E−01	7.2221E−01	7.1168E−01
		STD	2.0623E−02	2.2504E−02	1.0607E−01	1.8031E−02	**1.4961E−02**
	6	AVG	8.0293E−01	8.0109E−01	7.9468E−01	8.0326E−01	**8.0416E−01**
		STD	**5.3442E−03**	1.4904E−02	3.8238E−02	7.1383E−03	1.1158E−02
	12	AVG	**8.8515E−01**	8.0882E−01	8.8426E−01	8.0364E−01	8.6052E−01
		STD	5.8698E−02	7.2453E−02	5.0091E−02	8.1405E−02	7.8881E−02
	16	AVG	**9.3622E−01**	8.4816E−01	9.1945E−01	8.7446E−01	8.9950E−01
		STD	**8.4199E−03**	7.6800E−02	5.2352E−02	5.1664E−02	7.4478E−02
	18	AVG	**9.3468E−01**	8.8587E−01	9.1062E−01	8.8884E−01	9.0655E−01
		STD	**1.8505E−02**	5.2156E−02	6.0175E−02	4.8963E−02	5.1292E−02
170,057	2	AVG	3.0783E−01	3.0303E−01	3.0515E−01	2.9158E−01	3.1472E−01
		STD	1.3500E−02	6.5662E−02	6.7872E−02	6.0551E−02	6.3481E−02
	4	AVG	5.9428E−01	5.7925E−01	5.7007E−01	**6.3169E−01**	5.7648E−01
		STD	**1.9756E−02**	9.2155E−02	8.5237E−02	5.7476E−02	1.0435E−01
	6	AVG	7.5435E−01	7.2196E−01	7.4046E−01	**7.6859E−01**	7.3305E−01
		STD	6.1642E−02	7.3403E−02	6.9059E−02	5.1298E−02	8.0715E−02
	12	AVG	**8.7523E−01**	8.5637E−01	8.4788E−01	8.3779E−01	8.5440E−01
		STD	**1.4766E−02**	2.2417E−02	4.2398E−02	2.3517E−02	3.0003E−02
	16	AVG	**9.1676E−01**	8.9721E−01	8.7888E−01	8.7322E−01	8.9544E−01
		STD	**8.5209E−03**	2.6442E−02	4.5063E−02	2.5155E−02	2.0110E−02
	18	AVG	**9.3128E−01**	9.0198E−01	8.9513E−01	8.8833E−01	9.0643E−01
		STD	**7.7082E−03**	2.5766E−02	3.9526E−02	2.4795E−02	2.6755E−02

Table 12 (continued)

Image	Thres.	Item	SCA	BLPSO	IGWO	IWOA	SCADE
61,060	2	AVG	6.1249E−01	5.9833E−01	6.0373E−01	6.0785E−01	5.9648E−01
		STD	**5.3193E−03**	3.1855E−02	3.1901E−02	1.1648E−02	3.4409E−02
	4	AVG	**8.2624E−01**	8.0688E−01	8.2157E−01	8.1638E−01	8.2428E−01
		STD	**6.0356E−03**	3.0819E−02	2.6377E−02	1.0649E−02	9.2444E−03
	6	AVG	8.9253E−01	8.8783E−01	8.8081E−01	8.8214E−01	**8.9307E−01**
		STD	**6.9314E−03**	1.2132E−02	6.4144E−02	1.7825E−02	8.7795E−03
	12	AVG	8.9537E−01	8.8738E−01	8.8872E−01	8.8321E−01	**8.9549E−01**
		STD	**1.1862E−02**	1.5930E−02	2.7100E−02	1.8845E−02	1.5305E−02
	16	AVG	**9.1822E−01**	9.0873E−01	9.1197E−01	9.0453E−01	9.1614E−01
		STD	**7.2328E−03**	1.8396E−02	1.7480E−02	1.6677E−02	1.0762E−02
	18	AVG	**9.2993E−01**	9.2100E−01	9.2380E−01	9.1697E−01	9.1827E−01
		STD	**6.4478E−03**	1.2494E−02	1.9422E−02	1.1379E−02	1.0356E−02
175,032	2	AVG	5.8057E−01	5.8009E−01	5.5525E−01	5.7998E−01	5.6445E−01
		STD	**2.1412E−04**	9.9839E−04	7.2444E−02	1.2530E−03	5.5825E−02
	4	AVG	7.4176E−01	7.3965E−01	7.3603E−01	7.4345E−01	7.3374E−01
		STD	**1.9383E−03**	8.0498E−03	1.8426E−02	7.1059E−03	2.6450E−02
	6	AVG	8.2938E−01	8.2192E−01	8.2516E−01	8.2321E−01	8.2380E−01
		STD	**8.8811E−03**	1.5585E−02	1.6730E−02	1.6116E−02	2.0313E−02
	12	AVG	**9.6968E−01**	9.5804E−01	9.3703E−01	9.4757E−01	9.6226E−01
		STD	**5.2624E−03**	1.5741E−02	6.4654E−02	1.4190E−02	9.4679E−03
	16	AVG	**9.8180E−01**	9.7513E−01	9.6484E−01	9.6418E−01	9.6687E−01
		STD	**3.6244E−03**	6.1267E−03	1.5769E−02	1.0701E−02	1.4065E−02
	18	AVG	**9.8587E−01**	9.7146E−01	9.5867E−01	9.6566E−01	9.6926E−01
		STD	**1.7245E−03**	1.5078E−02	4.0355E−02	1.8742E−02	2.3520E−02
223,061	2	AVG	5.0820E−01	4.4229E−01	4.6267E−01	4.4419E−01	4.8709E−01
		STD	7.3582E−03	1.1271E−01	1.0247E−01	1.4086E−01	2.6769E−02
	4	AVG	7.1793E−01	6.6357E−01	6.4474E−01	5.4944E−01	6.6839E−01
		STD	6.2271E−02	8.4107E−02	1.5357E−01	1.6765E−01	9.9450E−02
	6	AVG	7.8055E−01	6.7863E−01	7.1514E−01	6.4804E−01	7.2012E−01
		STD	8.3824E−02	1.3973E−01	1.1921E−01	1.5406E−01	1.3017E−01
	12	AVG	**9.0960E−01**	8.8953E−01	8.9052E−01	8.9069E−01	8.9661E−01
		STD	**4.6542E−03**	1.7343E−02	2.6912E−02	8.7706E−03	1.4244E−02
	16	AVG	**9.3546E−01**	9.2143E−01	9.1809E−01	9.1640E−01	9.2192E−01
		STD	**2.8794E−03**	9.2572E−03	2.7222E−02	9.8862E−03	1.0409E−02
	18	AVG	**9.4638E−01**	9.3282E−01	9.2849E−01	9.2252E−01	9.3089E−01
		STD	**2.1149E−03**	1.0176E−02	1.5405E−02	1.0511E−02	1.0858E−02
19,021	2	AVG	5.0150E−01	4.9367E−01	4.8862E−01	**5.2260E−01**	4.8417E−01
		STD	**1.0962E−02**	2.6513E−02	6.4508E−02	2.8011E−02	6.9677E−02
	4	AVG	6.3442E−01	6.2631E−01	**6.3445E−01**	6.1553E−01	6.3290E−01
		STD	2.0514E−02	1.6180E−02	2.5335E−02	**1.1524E−02**	2.8441E−02
	6	AVG	**7.3927E−01**	7.2084E−01	7.1990E−01	7.0949E−01	7.1848E−01
		STD	**8.8549E−03**	3.0854E−02	4.0684E−02	2.7736E−02	3.4378E−02
	12	AVG	8.9878E−01	8.8927E−01	8.9460E−01	8.9343E−01	**9.0646E−01**
		STD	**1.3060E−02**	3.0974E−02	3.8897E−02	1.9555E−02	2.1584E−02
	16	AVG	**9.2831E−01**	9.2337E−01	9.1942E−01	9.1776E−01	9.2031E−01
		STD	**1.0435E−02**	2.4393E−02	5.6828E−02	2.1612E−02	3.3894E−02
	18	AVG	9.3914E−01	9.3316E−01	9.3077E−01	9.2745E−01	**9.4220E−01**
		STD	**1.0910E−02**	2.2138E−02	4.0618E−02	1.8392E−02	1.3422E−02

Bold are the best values

Table 13 The SSIM comparison results of VCSWOA and other methods

Image	Thres.	Item	SCA	BLPSO	IGWO	IWOA	SCADE
291,000	2	AVG	6.1946E−01	6.0962E−01	6.0573E−01	6.1313E−01	5.7531E−01
		STD	9.9228E−02	1.1589E−02	1.3046E−02	1.0378E−02	3.8211E−02
	4	AVG	7.3921E−01	8.2417E−01	**8.1523E−01**	7.8385E−01	6.9818E−01
		STD	4.5514E−02	**8.2364E−03**	1.0249E−02	4.5811E−02	7.2511E−02
	6	AVG	7.6770E−01	8.6577E−01	**8.7099E−01**	8.6335E−01	7.7685E−01
		STD	5.2197E−02	2.0964E−02	2.1715E−02	2.0962E−02	6.0402E−02
	12	AVG	8.8554E−01	9.3329E−01	9.2718E−01	9.3822E−01	8.7807E−01
		STD	4.3002E−02	1.5064E−02	1.8303E−02	1.3806E−02	4.4532E−02
	16	AVG	9.1604E−01	9.5259E−01	9.4131E−01	9.4968E−01	9.1819E−01
		STD	3.1284E−02	1.0160E−02	2.1185E−02	1.6484E−02	3.5560E−02
	18	AVG	9.2403E−01	9.5773E−01	9.5130E−01	9.4874E−01	9.3249E−01
		STD	4.5679E−02	1.0511E−02	1.6941E−02	4.3992E−02	2.2788E−02
38,092	2	AVG	6.2244E−01	5.6425E−01	5.8037E−01	5.7453E−01	5.7753E−01
		STD	4.3249E−02	4.5159E−02	**3.8395E−04**	1.0258E−02	1.0849E−02
	4	AVG	7.5602E−01	7.1492E−01	7.4841E−01	7.2640E−01	6.9008E−01
		STD	8.5241E−02	3.0235E−02	8.9293E−03	2.4957E−02	5.2709E−02
	6	AVG	8.1024E−01	7.9673E−01	8.2543E−01	7.9136E−01	7.4565E−01
		STD	6.3805E−02	2.7558E−02	1.6421E−02	3.2382E−02	4.2548E−02
	12	AVG	8.4203E−01	8.8224E−01	8.8065E−01	8.8065E−01	8.4099E−01
		STD	3.3746E−02	1.7476E−02	2.6199E−02	3.0004E−02	4.1269E−02
	16	AVG	8.7294E−01	9.0736E−01	9.0275E−01	9.1150E−01	8.7610E−01
		STD	3.3762E−02	1.4946E−02	2.0977E−02	1.9038E−02	3.0696E−02
	18	AVG	8.9236E−01	9.1429E−01	9.1733E−01	9.1195E−01	8.8960E−01
		STD	3.2714E−02	1.3605E−02	1.7159E−02	2.2826E−02	2.4152E−02
86,068	2	AVG	5.9060E−01	5.0924E−01	5.0634E−01	4.7694E−01	4.6222E−01
		STD	3.1461E−02	3.7387E−03	5.5275E−03	5.3351E−02	5.1335E−02
	4	AVG	7.0262E−01	6.9369E−01	6.7428E−01	6.7969E−01	5.4352E−01
		STD	4.6485E−02	8.3645E−02	7.2661E−02	6.3391E−02	1.4312E−01
	6	AVG	7.6044E−01	7.1886E−01	6.7936E−01	7.0111E−01	5.9677E−01
		STD	4.9403E−02	1.0052E−01	1.3245E−01	1.1952E−01	1.3037E−01
	12	AVG	7.2788E−01	8.2104E−01	7.4037E−01	7.9400E−01	7.6571E−01
		STD	9.5552E−02	**4.7243E−02**	1.0278E−01	7.2176E−02	8.2964E−02
	16	AVG	7.7526E−01	8.6185E−01	8.1914E−01	8.4280E−01	8.3317E−01
		STD	1.0349E−01	4.5636E−02	6.1815E−02	7.3580E−02	6.5863E−02
	18	AVG	8.2417E−01	8.8461E−01	8.4393E−01	8.6901E−01	8.2128E−01
		STD	6.2206E−02	2.6121E−02	7.2092E−02	5.7395E−02	8.9906E−02
170,057	2	AVG	2.9228E−01	4.4150E−01	5.0363E−01	4.9095E−01	**5.0893E−01**
		STD	8.8439E−02	7.8113E−02	**1.3179E−02**	1.8736E−02	2.1368E−02
	4	AVG	6.1598E−01	6.0809E−01	6.3059E−01	5.9935E−01	6.2060E−01
		STD	1.1359E−01	4.4607E−02	2.4905E−02	4.4062E−02	5.3154E−02
	6	AVG	6.8010E−01	6.8036E−01	7.1607E−01	6.9188E−01	6.6296E−01
		STD	8.4881E−02	3.7774E−02	3.1906E−02	4.3949E−02	4.9811E−02
	12	AVG	7.8294E−01	7.9229E−01	8.2281E−01	8.1267E−01	7.5666E−01
		STD	5.0065E−02	4.4907E−02	3.9594E−02	4.6353E−02	6.3464E−02
	16	AVG	8.0790E−01	8.3700E−01	8.4904E−01	8.6385E−01	8.2014E−01
		STD	4.2569E−02	3.3225E−02	4.1804E−02	3.1851E−02	3.8581E−02
	18	AVG	8.1488E−01	8.5308E−01	8.5741E−01	8.7637E−01	8.2242E−01
		STD	5.2113E−02	2.9931E−02	2.7588E−02	3.0477E−02	5.4885E−02

Table 13 (continued)

Image	Thres.	Item	SCA	BLPSO	IGWO	IWOA	SCADE
61,060	2	AVG	5.6909E−01	6.8293E−01	**6.9395E−01**	6.7246E−01	6.5617E−01
		STD	3.5898E−02	3.7547E−02	3.2108E−02	5.5533E−02	5.5491E−02
	4	AVG	7.1777E−01	7.5946E−01	7.5537E−01	7.6000E−01	7.2231E−01
		STD	6.2687E−02	3.4992E−02	4.3028E−02	3.0975E−02	6.0069E−02
	6	AVG	7.8982E−01	8.0834E−01	8.1478E−01	8.0187E−01	7.7633E−01
		STD	5.3734E−02	3.8980E−02	3.1489E−02	3.9574E−02	5.2972E−02
	12	AVG	8.5813E−01	8.7735E−01	8.7750E−01	8.7378E−01	8.5724E−01
		STD	3.6994E−02	2.6488E−02	2.2433E−02	2.2273E−02	3.3585E−02
	16	AVG	8.7319E−01	8.9806E−01	8.9826E−01	8.9485E−01	8.8762E−01
		STD	4.0437E−02	2.3194E−02	1.6524E−02	2.8387E−02	2.2206E−02
	18	AVG	8.9267E−01	9.1142E−01	9.0682E−01	9.0403E−01	8.8765E−01
		STD	2.6672E−02	1.5608E−02	1.6757E−02	2.2163E−02	2.8638E−02
175,032	2	AVG	5.7654E−01	5.7659E−01	6.2279E−01	6.1642E−01	**6.2996E−01**
		STD	1.4813E−02	8.1274E−02	2.1352E−03	1.8952E−02	3.1700E−02
	4	AVG	6.7135E−01	7.6775E−01	**8.3382E−01**	8.0864E−01	7.8047E−01
		STD	5.6142E−02	6.4600E−02	8.8566E−03	2.9843E−02	7.2086E−02
	6	AVG	7.5544E−01	8.4872E−01	8.9854E−01	8.7711E−01	8.1874E−01
		STD	3.8021E−02	3.6189E−02	1.4764E−02	3.1345E−02	7.0547E−02
	12	AVG	8.9911E−01	9.0691E−01	9.3376E−01	9.4105E−01	8.9900E−01
		STD	4.4068E−02	3.3551E−02	2.4482E−02	1.9067E−02	4.7434E−02
	16	AVG	9.3458E−01	9.3965E−01	9.4798E−01	9.5134E−01	9.1543E−01
		STD	2.9545E−02	1.6755E−02	2.4440E−02	3.3991E−02	3.9050E−02
	18	AVG	9.2402E−01	9.5289E−01	9.5186E−01	9.5695E−01	9.3896E−01
		STD	3.8323E−02	1.3194E−02	1.7363E−02	1.8245E−02	2.7126E−02
223,061	2	AVG	4.3255E−01	5.9101E−01	5.9125E−01	5.9020E−01	**5.9181E−01**
		STD	8.5152E−02	**1.2020E−03**	1.7262E−03	5.0076E−03	2.3584E−02
	4	AVG	5.1063E−01	7.0411E−01	7.2625E−01	7.3405E−01	7.2174E−01
		STD	1.3311E−01	1.5043E−02	2.0017E−02	2.5265E−02	4.7389E−02
	6	AVG	5.5316E−01	7.9430E−01	7.9417E−01	7.8915E−01	7.2293E−01
		STD	1.2672E−01	1.6546E−02	2.5729E−02	2.8980E−02	6.1359E−02
	12	AVG	8.4524E−01	8.6297E−01	8.7568E−01	8.8219E−01	8.3590E−01
		STD	3.2835E−02	2.8562E−02	2.1970E−02	1.8716E−02	3.6741E−02
	16	AVG	8.7860E−01	8.9577E−01	8.9501E−01	9.0154E−01	8.6872E−01
		STD	2.3706E−02	1.9861E−02	2.3738E−02	2.2749E−02	3.2460E−02
	18	AVG	8.8383E−01	9.0938E−01	9.0298E−01	9.1203E−01	8.8178E−01
		STD	2.8633E−02	1.7344E−02	1.2031E−02	1.6716E−02	2.9742E−02
19,021	2	AVG	4.9638E−01	3.2640E−01	3.0758E−01	3.1489E−01	2.9347E−01
		STD	3.3653E−02	2.8324E−02	2.0051E−02	4.9948E−02	6.9040E−02
	4	AVG	5.8309E−01	6.1460E−01	6.1863E−01	6.1424E−01	6.2140E−01
		STD	6.3368E−02	4.7882E−02	7.8348E−02	6.3777E−02	9.0202E−02
	6	AVG	6.5350E−01	7.2726E−01	7.3746E−01	7.3561E−01	6.5244E−01
		STD	5.6019E−02	5.4658E−02	6.8044E−02	7.1856E−02	9.6081E−02
	12	AVG	8.0363E−01	8.3915E−01	8.4465E−01	8.4439E−01	8.1150E−01
		STD	9.1751E−02	4.8262E−02	5.5329E−02	4.3168E−02	5.0831E−02
	16	AVG	8.4832E−01	8.8766E−01	8.8663E−01	9.0301E−01	8.6395E−01
		STD	5.7471E−02	2.8272E−02	4.7704E−02	3.0503E−02	4.9316E−02
	18	AVG	8.7734E−01	9.0627E−01	8.8445E−01	8.9725E−01	8.5547E−01
		STD	3.9458E−02	3.0534E−02	4.6023E−02	5.2585E−02	5.7292E−02

Bold are the best values

Table 14 The FSIM comparison results of VCSWOA and other methods

Image	Thres.	Item	VCSWOA	WOA	BA	CS	CBA
291,000	2	AVG	7.0070E−01	6.9890E−01	6.9549E−01	7.0450E−01	7.0290E−01
		STD	1.1661E−02	9.4608E−03	5.1055E−02	**7.9145E−03**	2.4177E−02
	4	AVG	7.7925E−01	7.7417E−01	7.7789E−01	7.7352E−01	7.7117E−01
		STD	2.3654E−02	3.0673E−02	3.0574E−02	3.2551E−02	3.1773E−02
	6	AVG	8.1991E−01	8.2828E−01	8.1425E−01	8.2040E−01	8.3567E−01
		STD	**1.6554E−02**	2.1939E−02	4.9927E−02	3.0920E−02	2.9815E−02
	12	AVG	9.5748E−01	9.5302E−01	9.5986E−01	9.5118E−01	**9.6234E−01**
		STD	**4.3092E−03**	1.1912E−02	6.0902E−03	1.0445E−02	5.4623E−03
	16	AVG	9.7197E−01	9.6682E−01	9.7320E−01	9.6783E−01	**9.7397E−01**
		STD	**3.5724E−03**	8.2113E−03	4.5181E−03	8.4288E−03	6.3335E−03
	18	AVG	9.7550E−01	9.7340E−01	9.7713E−01	9.7320E−01	**9.7795E−01**
		STD	**4.7209E−03**	6.1495E−03	7.0184E−03	6.5624E−03	6.1864E−03
38,092	2	AVG	7.8783E−01	7.8765E−01	7.7250E−01	7.8747E−01	7.8254E−01
		STD	5.0869E−04	1.7996E−03	5.8843E−02	2.1247E−03	2.8013E−02
	4	AVG	**9.1677E−01**	9.1325E−01	9.1084E−01	9.1059E−01	9.0919E−01
		STD	**2.1157E−03**	8.0268E−03	2.6569E−02	8.1979E−03	1.6676E−02
	6	AVG	**9.4553E−01**	9.4298E−01	9.4023E−01	9.3557E−01	9.2596E−01
		STD	**8.7705E−04**	4.0596E−03	9.3801E−03	8.9414E−03	4.7719E−02
	12	AVG	**9.5018E−01**	9.3429E−01	9.3533E−01	9.2988E−01	9.4605E−01
		STD	**4.5188E−03**	1.6393E−02	5.4889E−02	9.4892E−03	5.8335E−03
	16	AVG	**9.6563E−01**	9.5312E−01	9.6076E−01	9.5154E−01	9.5948E−01
		STD	**3.3109E−03**	8.8835E−03	8.9581E−03	7.6994E−03	9.5660E−03
	18	AVG	**9.7156E−01**	9.6001E−01	9.6568E−01	9.5441E−01	9.6485E−01
		STD	**2.4592E−03**	7.8032E−03	6.7922E−03	9.1200E−03	1.2665E−02
86,068	2	AVG	6.9772E−01	6.9756E−01	6.8708E−01	6.9776E−01	6.9753E−01
		STD	**4.5168E−16**	1.3138E−03	2.7579E−02	5.4580E−05	4.1799E−03
	4	AVG	**8.1103E−01**	8.0925E−01	7.7829E−01	8.0213E−01	7.9413E−01
		STD	1.2264E−02	1.2592E−02	7.2398E−02	1.0679E−02	**1.0241E−02**
	6	AVG	**8.6375E−01**	8.6105E−01	8.5829E−01	8.6319E−01	8.6342E−01
		STD	**3.8694E−03**	9.2373E−03	2.6310E−02	5.4492E−03	6.9830E−03
	12	AVG	**9.2535E−01**	8.6999E−01	9.2520E−01	8.6717E−01	9.0718E−01
		STD	4.2958E−02	**5.3628E−02**	3.5500E−02	5.8894E−02	5.8320E−02
	16	AVG	**9.6238E−01**	8.9641E−01	9.5029E−01	9.1650E−01	9.3599E−01
		STD	**5.5611E−03**	5.6312E−02	3.6110E−02	3.8206E−02	5.5433E−02
	18	AVG	**9.6211E−01**	9.2558E−01	9.4269E−01	9.2796E−01	9.4129E−01
		STD	**1.1611E−02**	3.6864E−02	4.2241E−02	3.6018E−02	3.8895E−02
170,057	2	AVG	6.4696E−01	6.4337E−01	6.4547E−01	6.4142E−01	**6.4752E−01**
		STD	5.3170E−03	2.0947E−02	2.2744E−02	2.1008E−02	2.0341E−02
	4	AVG	**7.9878E−01**	7.7579E−01	7.7825E−01	7.8679E−01	7.7892E−01
		STD	1.4397E−02	3.3107E−02	4.3738E−02	1.9850E−02	3.5195E−02
	6	AVG	**8.5724E−01**	8.3689E−01	8.5337E−01	8.4393E−01	8.5500E−01
		STD	**8.5633E−03**	3.4431E−02	1.3274E−02	2.0593E−02	1.8953E−02
	12	AVG	**9.2135E−01**	8.9727E−01	8.8950E−01	8.7737E−01	9.0005E−01
		STD	**1.1982E−02**	2.4365E−02	4.7029E−02	2.4043E−02	2.5985E−02
	16	AVG	**9.5452E−01**	9.3156E−01	9.1476E−01	9.0949E−01	9.3388E−01
		STD	**7.0951E−03**	2.4275E−02	4.4259E−02	2.3961E−02	1.7933E−02
	18	AVG	**9.6466E−01**	9.3480E−01	9.2970E−01	9.2304E−01	9.3848E−01
		STD	**4.9502E−03**	2.3498E−02	3.7675E−02	2.3890E−02	2.6902E−02

Table 14 (continued)

Image	Thres.	Item	VCSWOA	WOA	BA	CS	CBA
61,060	2	AVG	7.1748E−01	**7.0891E−01**	7.2519E−01	7.1445E−01	7.1589E−01
		STD	**8.1343E−03**	3.5622E−02	1.9980E−02	1.2501E−02	2.9874E−02
	4	AVG	**8.5331E−01**	8.3927E−01	8.4565E−01	8.4551E−01	8.5010E−01
		STD	**7.3224E−03**	1.9380E−02	1.8130E−02	9.1219E−03	1.1118E−02
	6	AVG	8.9331E−01	8.9483E−01	8.8594E−01	8.9435E−01	**9.0592E−01**
		STD	**1.2214E−02**	1.4995E−02	3.8322E−02	1.5642E−02	1.4075E−02
	12	AVG	8.9958E−01	8.9836E−01	8.9630E−01	8.9632E−01	**9.0489E−01**
		STD	1.4515E−02	1.5846E−02	3.0335E−02	**1.3909E−02**	2.0093E−02
	16	AVG	9.3040E−01	9.2195E−01	9.2595E−01	9.1989E−01	**9.3237E−01**
		STD	1.2679E−02	1.9575E−02	1.6986E−02	1.4124E−02	**1.1164E−02**
	18	AVG	**9.4228E−01**	9.3336E−01	9.3606E−01	9.3493E−01	9.3582E−01
		STD	1.1868E−02	1.3914E−02	2.5076E−02	**8.8969E−03**	9.6902E−03
175,032	2	AVG	6.8060E−01	6.8074E−01	6.5587E−01	6.8073E−01	6.6627E−01
		STD	2.3246E−03	5.7789E−04	5.0062E−02	**5.0307E−04**	3.7293E−02
	4	AVG	8.2631E−01	8.2370E−01	8.2037E−01	8.2639E−01	8.1918E−01
		STD	**8.7769E−04**	6.2964E−03	1.5501E−02	4.8918E−03	1.9267E−02
	6	AVG	8.8953E−01	8.7890E−01	8.8554E−01	8.7925E−01	8.7873E−01
		STD	**4.3267E−03**	1.4926E−02	1.3150E−02	1.1055E−02	2.3207E−02
	12	AVG	**9.7563E−01**	9.6847E−01	9.5743E−01	9.6348E−01	9.7316E−01
		STD	**5.8186E−03**	1.1149E−02	3.5995E−02	1.0838E−02	7.7710E−03
	16	AVG	**9.8546E−01**	9.8014E−01	9.7494E−01	9.7393E−01	9.7665E−01
		STD	**3.3522E−03**	7.3528E−03	1.2420E−02	6.7361E−03	1.0546E−02
	18	AVG	**9.8897E−01**	9.7948E−01	9.6929E−01	9.7513E−01	9.7841E−01
		STD	**2.1669E−03**	1.0156E−02	3.1243E−02	1.2187E−02	1.4986E−02
223,061	2	AVG	6.5119E−01	6.0015E−01	6.2876E−01	6.1073E−01	6.3239E−01
		STD	2.5413E−03	7.3998E−02	5.7373E−02	7.7352E−02	3.8263E−02
	4	AVG	7.9614E−01	7.4998E−01	7.4249E−01	6.7030E−01	7.5887E−01
		STD	4.0972E−02	6.9305E−02	9.7403E−02	1.0828E−01	7.0548E−02
	6	AVG	8.4644E−01	7.7189E−01	7.9972E−01	7.4799E−01	8.0293E−01
		STD	4.8518E−02	9.3150E−02	8.2070E−02	9.2415E−02	9.1564E−02
	12	AVG	**9.5067E−01**	9.3027E−01	9.3434E−01	9.3194E−01	9.3919E−01
		STD	**2.6151E−03**	1.5993E−02	2.2934E−02	7.7854E−03	1.3703E−02
	16	AVG	**9.6754E−01**	9.5286E−01	9.5179E−01	9.4867E−01	9.5570E−01
		STD	**2.3170E−03**	6.3910E−03	2.6621E−02	8.6569E−03	1.1097E−02
	18	AVG	**9.7397E−01**	9.6039E−01	9.5962E−01	9.5361E−01	9.6165E−01
		STD	**1.0467E−03**	7.2699E−03	1.3577E−02	7.6458E−03	1.0427E−02
19,021	2	AVG	6.1058E−01	6.0635E−01	6.0220E−01	6.0841E−01	5.9866E−01
		STD	**7.0456E−04**	1.5484E−02	2.1174E−02	4.2819E−03	2.0878E−02
	4	AVG	7.1348E−01	7.0338E−01	7.0856E−01	6.9980E−01	7.0737E−01
		STD	**1.0369E−02**	1.2482E−02	1.9192E−02	1.0697E−02	2.0816E−02
	6	AVG	7.9887E−01	7.7742E−01	7.7921E−01	7.6760E−01	7.7818E−01
		STD	**5.4582E−03**	2.7674E−02	4.2613E−02	2.9266E−02	2.7107E−02
	12	AVG	9.3434E−01	9.2946E−01	9.3415E−01	9.3145E−01	**9.3910E−01**
		STD	**5.6745E−03**	1.4145E−02	1.2954E−02	1.0225E−02	9.6392E−03
	16	AVG	**9.5381E−01**	9.5062E−01	9.4684E−01	9.4839E−01	9.5237E−01
		STD	**4.2524E−03**	1.2688E−02	4.2393E−02	1.3163E−02	1.4745E−02
	18	AVG	9.6131E−01	9.5524E−01	9.5745E−01	9.5494E−01	**9.6447E−01**
		STD	**4.3954E−03**	1.4416E−02	1.6545E−02	1.0629E−02	7.7567E−03

Bold are the best values

Table 15 The FSIM comparison results of VCSWOA and other methods

Image	Thres.	Item	SCA	BLPSO	IGWO	IWOA	SCADE
291,000	2	AVG	6.8504E−01	7.1725E−01	7.0959E−01	**7.2611E−01**	6.9056E−01
		STD	3.9609E−02	1.3296E−02	1.7158E−02	1.5747E−02	3.5720E−02
	4	AVG	7.3226E−01	**8.4928E−01**	8.4130E−01	8.2290E−01	7.6658E−01
		STD	4.3904E−02	**7.8390E−03**	1.0009E−02	3.0863E−02	4.3329E−02
	6	AVG	7.6460E−01	**8.8770E−01**	8.8268E−01	8.7471E−01	8.3043E−01
		STD	5.3785E−02	1.7816E−02	1.9311E−02	1.8018E−02	4.0168E−02
	12	AVG	9.1006E−01	9.4548E−01	9.3861E−01	9.4394E−01	9.0064E−01
		STD	3.1633E−02	1.3812E−02	1.6379E−02	1.3462E−02	3.0314E−02
	16	AVG	9.3217E−01	9.6036E−01	9.5001E−01	9.5710E−01	9.3348E−01
		STD	2.1568E−02	1.0207E−02	1.8272E−02	1.4109E−02	2.5438E−02
	18	AVG	9.3986E−01	9.6506E−01	9.5995E−01	9.5404E−01	9.4730E−01
		STD	3.2963E−02	8.9836E−03	1.1006E−02	3.2786E−02	1.5031E−02
38,092	2	AVG	**7.8788E−01**	6.5818E−01	6.8094E−01	6.7485E−01	6.7698E−01
		STD	3.2519E−02	2.7284E−02	**1.9469E−04**	8.1337E−03	5.5071E−03
	4	AVG	8.5056E−01	7.8815E−01	8.2923E−01	8.0362E−01	7.5312E−01
		STD	5.8036E−02	2.9217E−02	4.4658E−03	2.7607E−02	4.8267E−02
	6	AVG	8.8231E−01	8.5112E−01	8.7198E−01	8.4097E−01	7.9134E−01
		STD	4.2566E−02	2.5614E−02	1.5645E−02	3.2772E−02	3.4630E−02
	12	AVG	8.7283E−01	9.1330E−01	9.1122E−01	9.0927E−01	8.7771E−01
		STD	2.9843E−02	1.4335E−02	2.0066E−02	2.7314E−02	3.6543E−02
	16	AVG	9.0118E−01	9.3464E−01	9.2872E−01	9.3779E−01	9.0212E−01
		STD	3.3386E−02	1.4774E−02	1.6655E−02	1.5460E−02	3.0410E−02
	18	AVG	9.1941E−01	9.3920E−01	9.3943E−01	9.3621E−01	9.1739E−01
		STD	2.8801E−02	1.1480E−02	1.2827E−02	1.9982E−02	2.1468E−02
86,068	2	AVG	**6.9817E−01**	6.5155E−01	6.4658E−01	6.2517E−01	6.0191E−01
		STD	2.4264E−02	7.0345E−03	8.4831E−03	4.4489E−02	4.8406E−02
	4	AVG	7.7075E−01	7.7119E−01	7.5884E−01	7.6311E−01	6.5990E−01
		STD	4.0727E−02	6.4022E−02	5.1197E−02	4.7038E−02	8.8118E−02
	6	AVG	8.1552E−01	8.0059E−01	7.7385E−01	7.8179E−01	7.0825E−01
		STD	4.4406E−02	6.0239E−02	8.8061E−02	8.0707E−02	8.9830E−02
	12	AVG	8.1078E−01	8.7711E−01	8.2187E−01	8.5489E−01	8.3247E−01
		STD	6.5279E−02	3.8091E−02	7.4580E−02	5.2587E−02	6.8163E−02
	16	AVG	8.3807E−01	9.0701E−01	8.7482E−01	8.9038E−01	8.8604E−01
		STD	8.4103E−02	3.2650E−02	4.4935E−02	5.4829E−02	4.6049E−02
	18	AVG	8.7553E−01	9.2209E−01	8.9527E−01	9.1039E−01	8.7737E−01
		STD	4.8306E−02	2.0764E−02	5.3433E−02	4.2872E−02	6.6435E−02
170,057	2	AVG	6.3280E−01	5.6354E−01	6.1072E−01	6.0318E−01	6.1039E−01
		STD	2.7164E−02	**1.5082E−02**	1.0571E−03	1.5745E−02	9.8482E−03
	4	AVG	7.3469E−01	6.8375E−01	7.0728E−01	6.8063E−01	6.7538E−01
		STD	4.4299E−02	3.4373E−02	**1.3411E−02**	2.5465E−02	4.4694E−02
	6	AVG	7.8061E−01	7.3831E−01	7.6842E−01	7.4922E−01	7.0686E−01
		STD	5.1478E−02	3.5289E−02	3.4131E−02	3.7340E−02	4.3564E−02
	12	AVG	8.2199E−01	8.3324E−01	8.6113E−01	8.4981E−01	7.9377E−01
		STD	4.5864E−02	4.1669E−02	3.9118E−02	4.7835E−02	5.5509E−02
	16	AVG	8.4286E−01	8.7519E−01	8.8293E−01	8.9642E−01	8.5377E−01
		STD	4.0296E−02	3.2778E−02	4.2345E−02	3.0496E−02	3.4664E−02
	18	AVG	8.4958E−01	8.8883E−01	8.8822E−01	9.0903E−01	8.5540E−01
		STD	4.8137E−02	2.8999E−02	2.7299E−02	2.8287E−02	4.7737E−02

Table 15 (continued)

Image	Thres.	Item	SCA	BLPSO	IGWO	IWOA	SCADE
61,060	2	AVG	6.8124E−01	7.0455E−01	6.8972E−01	6.9770E−01	6.9219E−01
		STD	3.3539E−02	1.2719E−02	1.7646E−02	1.5637E−02	2.3358E−02
	4	AVG	7.7451E−01	7.5495E−01	7.5170E−01	7.5331E−01	7.3314E−01
		STD	4.3350E−02	3.2929E−02	3.7290E−02	2.8240E−02	4.6566E−02
	6	AVG	8.3365E−01	8.0619E−01	8.1301E−01	8.1011E−01	7.8026E−01
		STD	3.3729E−02	3.5709E−02	3.2194E−02	3.6639E−02	5.4715E−02
	12	AVG	8.6080E−01	8.8946E−01	8.8433E−01	8.8246E−01	8.6747E−01
		STD	3.2775E−02	2.3408E−02	2.2919E−02	1.7405E−02	3.0230E−02
	16	AVG	8.8404E−01	9.1038E−01	9.0786E−01	9.0678E−01	8.9510E−01
		STD	3.4109E−02	2.0798E−02	1.5007E−02	2.8825E−02	2.4979E−02
	18	AVG	9.0008E−01	9.2321E−01	9.1954E−01	9.1852E−01	8.9836E−01
		STD	2.8883E−02	1.4348E−02	1.3571E−02	1.9475E−02	2.8358E−02
175,032	2	AVG	6.7289E−01	7.6164E−01	7.8741E−01	7.8519E−01	**7.9197E−01**
		STD	1.0620E−02	5.3794E−02	1.5850E−03	1.4197E−02	2.0773E−02
	4	AVG	7.2743E−01	8.7155E−01	9.1364E−01	8.9343E−01	8.6866E−01
		STD	5.6077E−02	4.2053E−02	6.1767E−03	2.3350E−02	4.9100E−02
	6	AVG	7.9945E−01	9.1370E−01	**9.3703E−01**	9.2388E−01	8.8326E−01
		STD	4.2175E−02	2.1585E−02	1.2234E−02	2.1068E−02	5.1686E−02
	12	AVG	9.3592E−01	9.4048E−01	9.5315E−01	9.5670E−01	9.3800E−01
		STD	2.9879E−02	2.1350E−02	1.5712E−02	1.1687E−02	2.4527E−02
	16	AVG	9.5400E−01	9.6008E−01	9.6393E−01	9.6712E−01	9.4663E−01
		STD	2.3395E−02	1.1611E−02	1.6449E−02	1.9518E−02	2.1149E−02
	18	AVG	9.5251E−01	9.6783E−01	9.6597E−01	9.6881E−01	9.5988E−01
		STD	2.1760E−02	8.2453E−03	1.1766E−02	1.1373E−02	1.4608E−02
223,061	2	AVG	5.8882E−01	6.9772E−01	6.9806E−01	6.9561E−01	**6.9891E−01**
		STD	7.1601E−02	**4.3030E−04**	1.2765E−03	7.7364E−03	1.9142E−02
	4	AVG	6.3998E−01	7.8809E−01	8.0422E−01	**8.0588E−01**	7.8421E−01
		STD	7.8363E−02	**9.3914E−03**	1.0819E−02	1.6162E−02	3.6719E−02
	6	AVG	6.7012E−01	**8.5355E−01**	8.5329E−01	8.4834E−01	7.8462E−01
		STD	9.3119E−02	**1.3016E−02**	2.1119E−02	2.4915E−02	5.1957E−02
	12	AVG	8.8270E−01	9.0529E−01	9.1626E−01	9.1839E−01	8.7667E−01
		STD	2.8263E−02	2.4384E−02	1.7842E−02	1.7963E−02	3.1097E−02
	16	AVG	9.0938E−01	9.2622E−01	9.2868E−01	9.3361E−01	9.0203E−01
		STD	2.3454E−02	1.8472E−02	2.2655E−02	2.1025E−02	3.1211E−02
	18	AVG	9.1604E−01	9.3827E−01	9.3255E−01	9.4110E−01	9.1249E−01
		STD	2.7712E−02	1.6411E−02	1.1320E−02	1.4023E−02	2.7069E−02
19,021	2	AVG	6.0140E−01	**6.5356E−01**	6.4706E−01	6.4792E−01	6.4120E−01
		STD	1.2928E−02	9.9495E−03	7.0396E−03	1.4862E−02	2.4277E−02
	4	AVG	6.4593E−01	7.6776E−01	**7.8351E−01**	7.7538E−01	7.3994E−01
		STD	5.1147E−02	3.4036E−02	2.2740E−02	2.7825E−02	4.6925E−02
	6	AVG	7.0133E−01	8.2950E−01	**8.3456E−01**	8.3222E−01	7.7088E−01
		STD	4.6472E−02	2.4903E−02	3.0463E−02	4.0733E−02	5.3160E−02
	12	AVG	8.6153E−01	9.0051E−01	8.9191E−01	8.9564E−01	8.7273E−01
		STD	4.8497E−02	2.2729E−02	3.3421E−02	2.7298E−02	3.0208E−02
	16	AVG	8.9911E−01	9.2804E−01	9.2647E−01	9.3556E−01	9.0567E−01
		STD	3.3839E−02	2.0246E−02	2.3065E−02	1.6082E−02	3.3119E−02
	18	AVG	9.1525E−01	9.4142E−01	9.2670E−01	9.3858E−01	9.0330E−01
		STD	2.6264E−02	1.4152E−02	2.1946E−02	1.9481E−02	3.5614E−02

Bold are the best values

Table 16 The PSNR comparison results of VCSWOA and other methods

Thres.	VCSWOA	WOA	BA	CS	CBA
2					
+/−/=		3/0/5	5/0/3	3/0/5	5/0/3
Mean	3.0000	5.8750	6.8750	4.3750	5.1250
Rank	1	5	9	3	4
4					
+/−/=		3/0/5	1/0/7	6/1/1	2/0/6
Mean	2.5000	4.6250	5.2500	5.2500	4.8750
Rank	1	3	6	6	4
6					
+/−/=		4/0/4	3/0/5	6/0/2	4/0/4
Mean	1.3750	5.1250	4.1250	5.3750	3.5000
Rank	1	5	3	6	2
12					
+/−/=		7/0/1	4/0/4	7/0/1	3/1/4
Mean	1.2500	4.1250	3.2500	4.5000	2.1250
Rank	1	4	3	5	2
16					
+/−/=		7/0/1	6/0/2	8/0/0	7/0/1
Mean	1.0000	3.5000	3.0000	4.8750	2.7500
Rank	1	4	3	5	2
18					
+/−/=		7/0/1	6/0/2	8/0/0	7/0/1
Mean	1.1250	3.5000	3.1250	4.6250	2.6250
Rank	1 4		3	5	2

Thres.	SCA	BLPSO	IGWO	IWOA	SCADE
2					
+/−/=	6/0/2	6/2/0	4/4/0	5/3/0	5/2/1
Mean	7.5000	6.3750	3.6250	5.8750	6.3750
Rank	10	7	2	5	7
4					
+/−/=	8/0/0	3/1/4	3/3/2	5/1/2	6/1/1
Mean	9.1250	5.1250	4.1250	5.7500	8.3750
Rank	10	5	2	8	9
6					
+/−/=	8/0/0	6/0/2	5/1/2	6/1/1	7/0/1
Mean	9.3750	5.8750	4.6250	6.0000	9.6250
Rank	9	7	4	8	10
12					
+/−/=	8/0/0	8/0/0	8/0/0	8/0/0	8/0/0
Mean	9.3750	6.7500	7.1250	7.0000	9.5000
Rank	9	6	8	7	10
16					
+/−/=	8/0/0	8/0/0	8/0/0	8/0/0	8/0/0
Mean	9.6250	6.8750	7.6250	6.5000	9.2500
Rank	10	7	8	6	9
18					
+/−/=	8/0/0	8/0/0	8/0/0	8/0/0	8/0/0
Mean	9.6250	6.6250	7.5000	6.8750	9.3750
Rank	10	6	8	7	9

Table 17 The SSIM comparison results of VCSWOA and other methods

Thres.	VCSWOA	WOA	BA	CS	CBA
2					
+/−/=		4/0/4	1/0/7	4/1/3	1/0/7
Mean	3.1250	5.7500	6.5000	4.7500	5.7500
Rank	1	5	9	2	5
4					
+/−/=		2/0/6	2/0/6	5/1/2	2/0/6
Mean	3.2500	5.2500	5.6250	4.8750	5.5000
Rank	1	4	6	3	5
6					
+/−/=		3/0/5	3/0/5	4/0/4	3/0/5
Mean	2.8750	5.0000	5.2500	5.2500	4.2500
Rank	1	4	6	6 3	
12					
+/−/=		6/0/2	4/0/4	7/0/1	4/0/4
Mean	1.2500	3.8750	3.5000	4.6250	2.1250
Rank	1	4	3	5	2
16					
+/−/=		7/0/1 5/0/3	8/0/0	6/0/2	
Mean	1.0000	3.3750	3.1250	4.8750	2.7500
Rank	1	4	3	5	2
18					
+/−/=		7/0/1	5/0/3	8/0/0	7/0/1
Mean	1.1250	3.2500	3.2500	4.7500	2.6250
Rank	1	3	3	5	2

Thres.	SCA	BLPSO	IGWO	IWOA	SCADE
2					
3/0/5	4/3/1	4/4/0	4/4/0	4/4/0	
Mean	6.7500	6.0000	5.0000	5.7500	5.6250
Rank	10	8	3	5 4	
4					
+/−/=	7/1/0	5/2/1	3/3/2	3/1/4	4/2/2
Mean	8.0000	5.6250	4.6250	5.6250	6.6250
Rank	10	6 2	6 9		
6					
+/−/=	8/0/0	4/2/2	4/2/2	4/2/2	7/0/1
Mean	8.7500	5.0000	4.1250	5.3750	9.1250
Rank	9	4	2	8	10
12					
+/−/=	8/0/0	8/0/0	8/0/0	8/0/0	8/0/0
Mean	9.2500	7.0000	7.1250	6.6250	9.6250
Rank	9	7	8	6	10
16					
+/−/=	8/0/0	8/0/0	8/0/0	8/0/0	8/0/0
Mean	9.7500	6.8750	7.6250	6.5000	9.1250
Rank	10	7	8	6	9
18					
+/−/=	8/0/0	8/0/0	8/0/0	8/0/0	8/0/0
Mean	9.3750	6.6250	7.3750	7.0000	9.6250
Rank	9	6	8	7	10

Table 18 The FSIM comparison results of VCSWOA and other methods

Thres.	VCSWOA	WOA	BA	CS	CBA
2					
+/−/=		1/0/7	2/1/5	2/2/4	3/1/4
Mean	4.0000	5.5000	6.1250	4.8750	5.5000
Rank	1	5	8	2	5
4					
+/−/=		6/0/2	4/0/4	6/0/2	4/0/4
Mean	2.7500	5.2500	5.2500	5.3750	5.5000
Rank	1	5	5	7	8
6					
+/−/=		5/1/2	3/0/5	5/0/3	4/2/2
Mean	3.3750	5.2500	5.1250	5.7500	4.2500
Rank	1	6	4	8	2
12					
+/−/=		6/0/2	4/0/4	6/0/2	3/2/3
Mean	1.5000	4.0000	3.3750	4.6250	1.7500
Rank	1	4	3	5	2
16					
+/−/=		6/0/2	5/0/3	7/0/1	5/0/3
Mean	1.3750	3.7500	3.2500	4.6250	2.1250
Rank	1	4	3	5	2
18					
+/−/=		6/0/2	5/1/2	7/0/1	6/0/2
Mean	1.3750	3.7500	3.0000	4.6250	2.2500
Rank	1	4	3	5	2
Thres.	SCA	BLPSO	IGWO	IWOA	SCADE
2					
+/−/=	6/0/2	4/4/0	4/4/0	4/4/0	4/3/1
Mean	6.8750	5.3750	5.1250	5.5000	6.1250
Rank	10	4	3	5	8
4					
+/−/=	8/0/0	4/3/1	4/3/1	4/3/1	4/2/2
Mean	8.1250	5.1250	4.7500	5.1250	7.7500
Rank	10	3	2	3	9
6					
+/−/=	8/0/0	4/3/1	4/3/1	4/3/1	6/0/2
Mean	8.0000	5.1250	4.5000	5.3750	8.2500
Rank	9	4	3	7	10
12					
+/−/=	8/0/0	8/0/0	8/0/0	8/0/0	8/0/0
Mean	9.6250	6.5000	7.3750	7.0000	9.2500
Rank	10	6	8	7	9
16					
+/−/=	8/0/0	8/0/0	8/0/0	8/0/0	8/0/0
Mean	9.7500	6.8750	7.6250	6.5000	9.1250
Rank	10	7	8	6	9
18					
+/−/=	8/0/0	8/0/0	8/0/0	8/0/0	8/0/0
Mean	9.5000	6.5000	7.5000	7.0000	9.5000
Rank	9	6	8	7	9

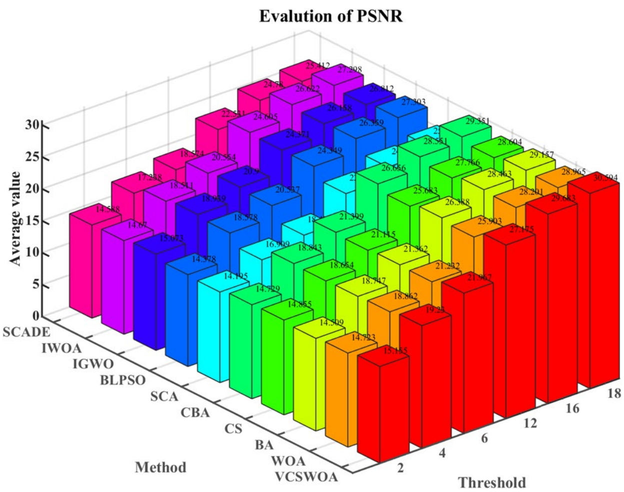

Fig. 5 Average of PSNR at each threshold level

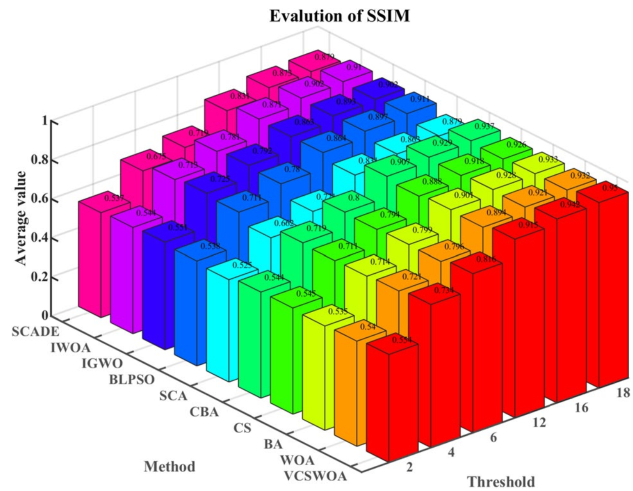

Fig. 7 Average of SSIM at each threshold level

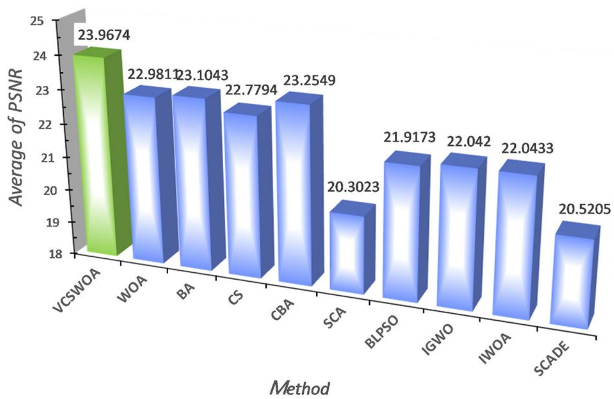

Fig. 6 Average of PSNR for all threshold levels

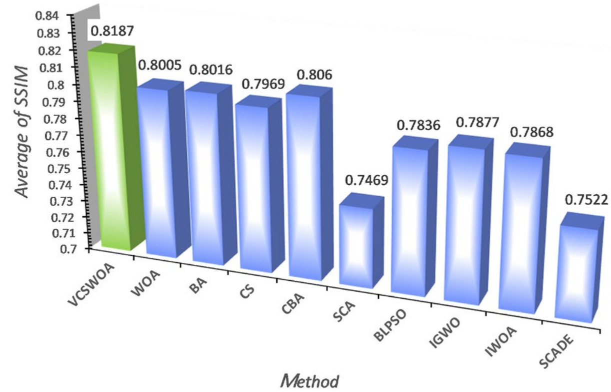

Fig. 8 Average of SSIM for all threshold levels

results. PSNR, SSIM, FSIM can be calculated from the following equations:

$$\mathrm{PSNR} = 20\log_{10}\left(\frac{255}{\sqrt{\frac{\sum_{i=1}^{n}\sum_{j=1}^{m}(I_{i,j}-I_{\mathrm{seq}})^2}{N.M}}}\right) \tag{22}$$

where I and I_{seg} refers to the original image and segmented one. $I_{i,j}$ refers to image gray level at (i, j)th pixel

$$\mathrm{SSIM}(I, I_{\mathrm{seg}}) = \frac{(2\mu_I\mu_{I_{\mathrm{seg}}} + c_1)(2\sigma_{I,I_{\mathrm{seg}}} + c_2)}{(\mu_I^2\mu_{I_{\mathrm{seg}}}^2 + c_1)(\sigma_I^1 + \sigma_{I_{\mathrm{seg}}}^2 + c_2)} \tag{23}$$

μ_I and $\mu_{I_{\mathrm{seg}}}$ refers to image mean intensity of I and I_{seg}, respectively and, σ_I and $\sigma_{I_{\mathrm{seg}}}$ refers to the standard deviation of I and I_{seg}, respectively.

$$\mathrm{FSIM} = \frac{\sum_{x\in\Omega} S_L(x).\mathrm{PC}_m(x)}{\sum_{x\in\Omega}\mathrm{PC}_m(x)} \tag{24}$$

where Ω refers to the spatial domain of the whole image and $S_L(x)$ and PC_m can be calculated as follows:

$$S_L(x) = [S_{\mathrm{PC}}(x)]^{\alpha}[S_G(x)]^{\beta} \tag{25}$$

where α, β refers to PC and GM relative important parameters and $S_G(x)$ can be calculated as follows:

$$S_G(x) = \frac{2G_1(x).G_2(x) + T_2}{G_1^2(x).G_2^2(x) + T_2} \tag{26}$$

$$S_{\mathrm{PC}} = \frac{2\mathrm{PC}_1(x).\mathrm{PC}_2(x) + T_1}{\mathrm{PC}_1^2(x).\mathrm{PC}_2^2(x) + T_1} \tag{27}$$

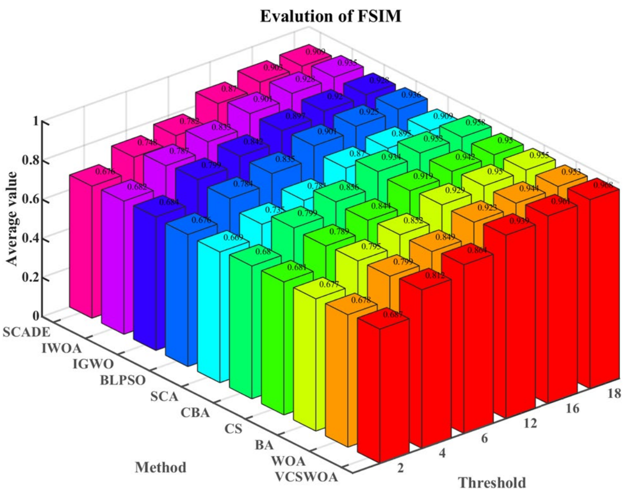

Fig. 9 Average of FSIM at each threshold level

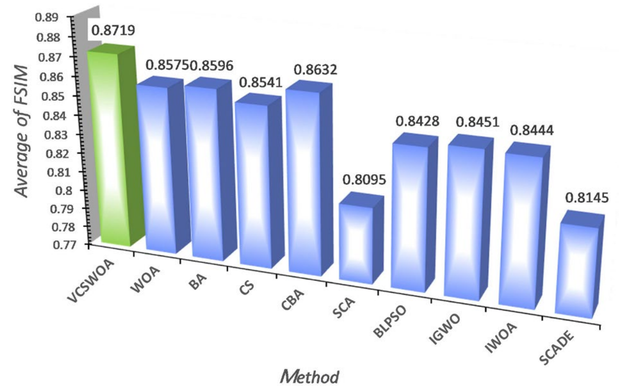

Fig. 10 Average of FSIM for all threshold levels

Fig. 11 Threshold values of 291,000 obtained by each algorithm at level 6

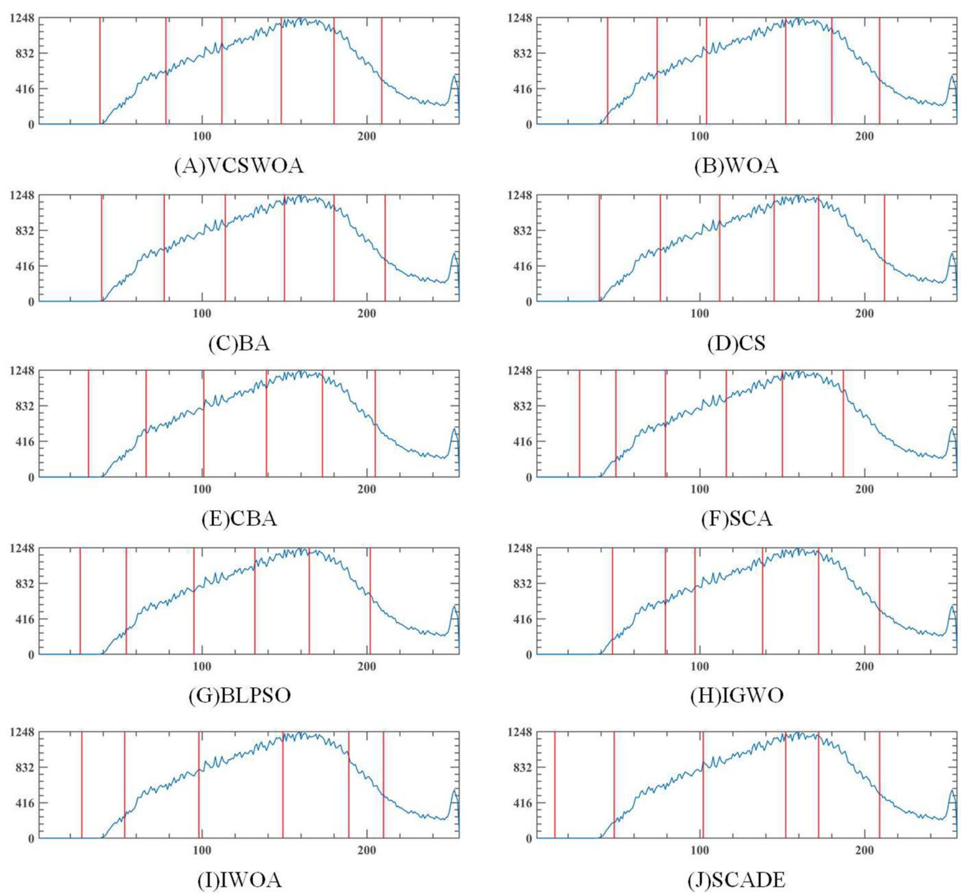

Furthermore, Figs. 5 and 6 respectively show the average PSNR for each threshold level and all threshold levels. Figures 7 and 8 respectively show the average SSIM for each threshold level and all threshold levels. Figures 9 and 10 respectively show the average FSIM for each threshold level and all threshold levels. And, Tables 10, 11, 12, 13, 14,

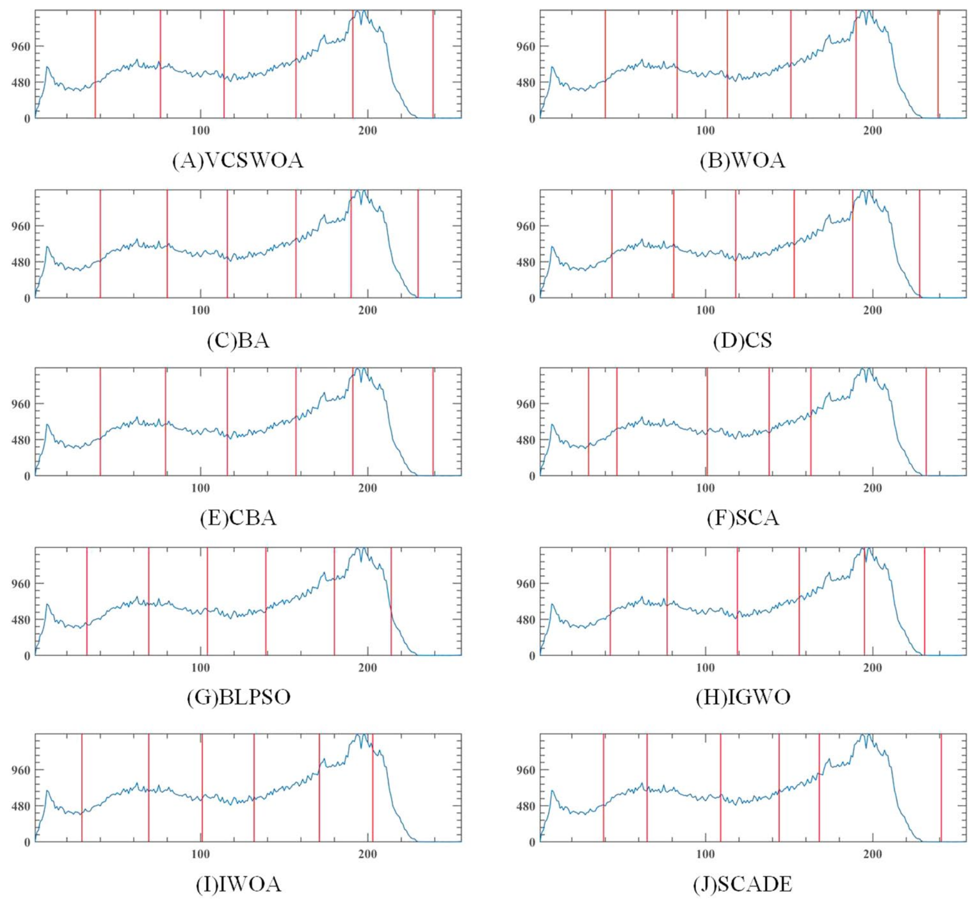

Fig. 12 Threshold values of 223,061 obtained by each algorithm at level 6

and 15 and Figs. 11, 12, 13, 14, 15, 16, 17, 18, 19, 20 and 21 show the results of VCSWOA compared with other metaheuristics algorithms.

Also, Tables 16, 17 and 18 show the ranking of compared algorithms. It can be noticed that the proposed algorithm ranked first in almost all images.

As said by our findings, the developed WOA-based technique has obtained enhanced results based on its core exploitative patterns in engineering and image processing tasks. Hence, we suggest the application of our WOA variant to problems on the evaluation of human lower limb motions [102], Lunar impact crater detection and age estimation [103], social recommendation and QoS-aware service composition [104–106], shape registration [107], and regression tasks [108]. Also, its continuous and binary variants can be applied to gate resource allocation [109, 110], and shape analysis [111, 112]. Also, we need to apply this variant of WOA to more real-world problems and investigate its full explorative features based on more cases such as brain function prediction [113, 114], covert communication system [115–117], epidemic prevention and control [118, 119], large scale network analysis [120], energy storage planning and scheduling [121], medical diagnosis [95, 122–124], pedestrian dead reckoning [125], image dehazing [126–128], and feature selection [129–131].

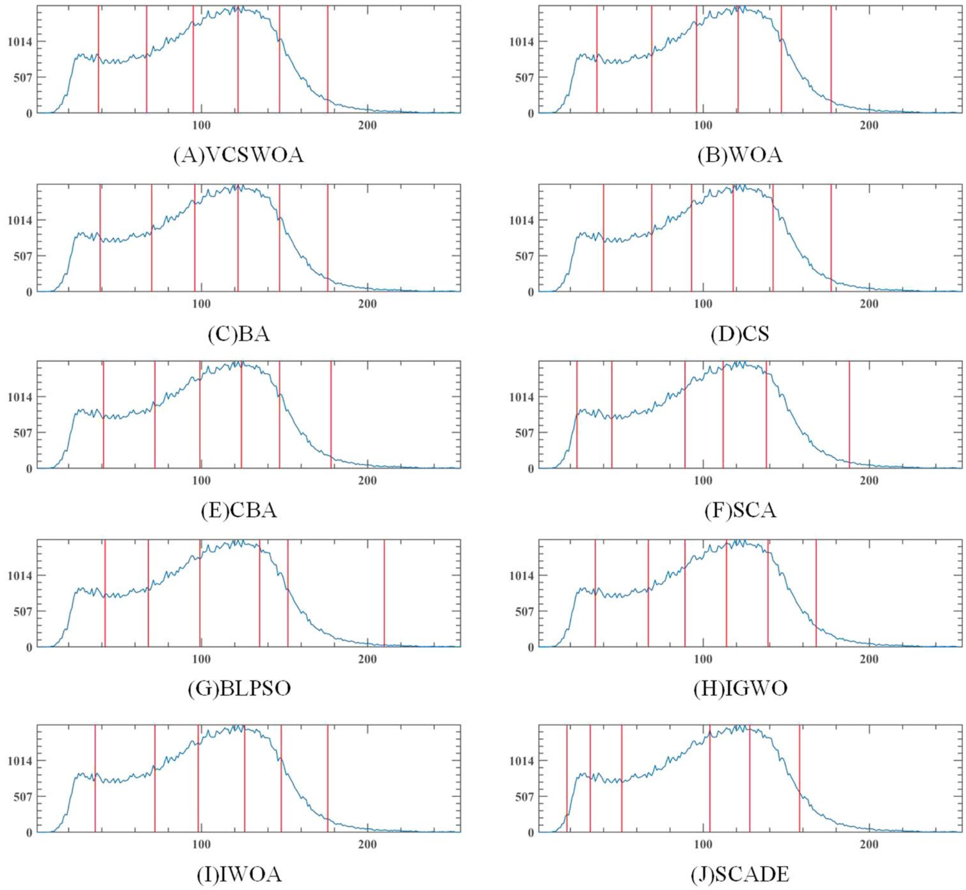

Fig. 13 Threshold values of 175,032 obtained by each algorithm at level 6

6 Conclusion and future works

As there are some core shortcomings for WOA, such as immature convergence and stagnation, we proposed an enhanced VCSWOA method with two active cores of the WOA and VCS optimizers as a new structure. We considered a set of functions from the IEEE CEC2017 competition, and four different engineering problems are utilized to validate the efficacy of the developed VCSWOA. Also, the VSCWOA has been verified in dealing with image segmentation problems over many threshold values. We observed that the VSCWOA achieves the best results than other WOA-based algorithms, namely CWOA, OBWOA, ACWOA, BMWOA, IWOA, BWOA, and CCMWOA. The proposed approach is also applied to several well-known methods of image cases. The results indicate the convergence speed and quality of searching has enhanced significantly based on the better balance amongst the essential diversification and intensification trends.

For future works, we intend to develop the binary and multi-objective version of the WOA-based method. Applying this variant to the training of neural networks is another valuable direction that is in line with the higher exploratory power of the VCSWOA.

Fig. 14 Threshold values of 170,057 obtained by each algorithm at level 6

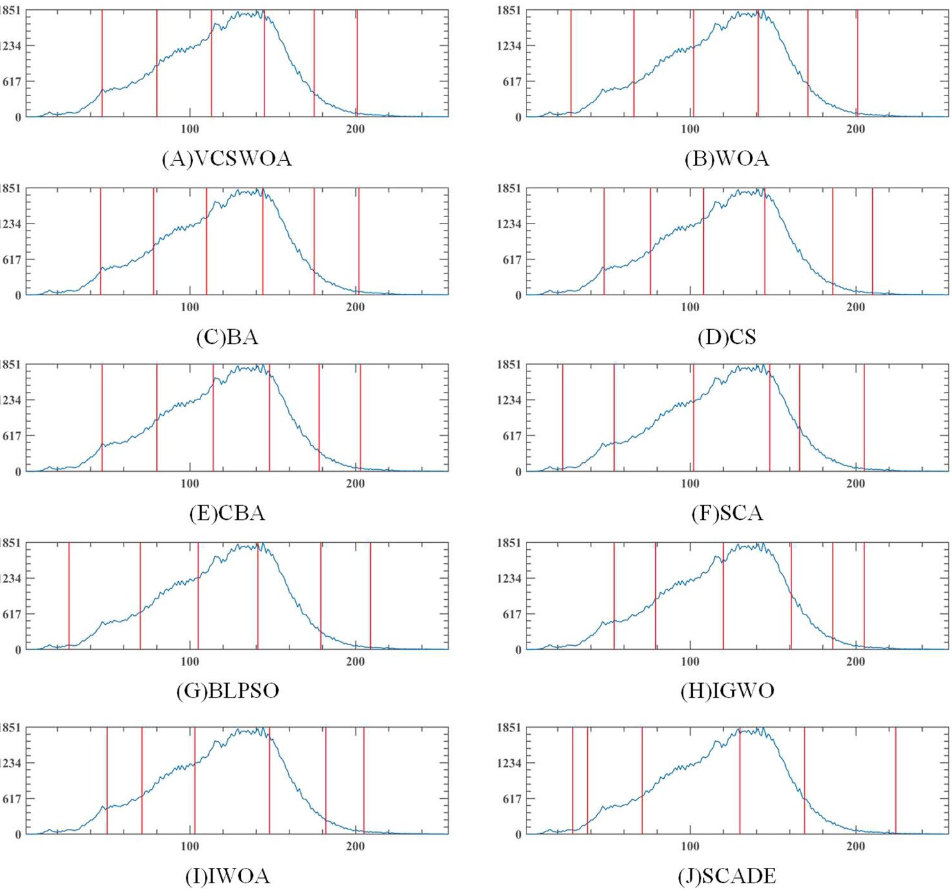

Fig. 15 Threshold values of 86,068 obtained by each algorithm at level 6

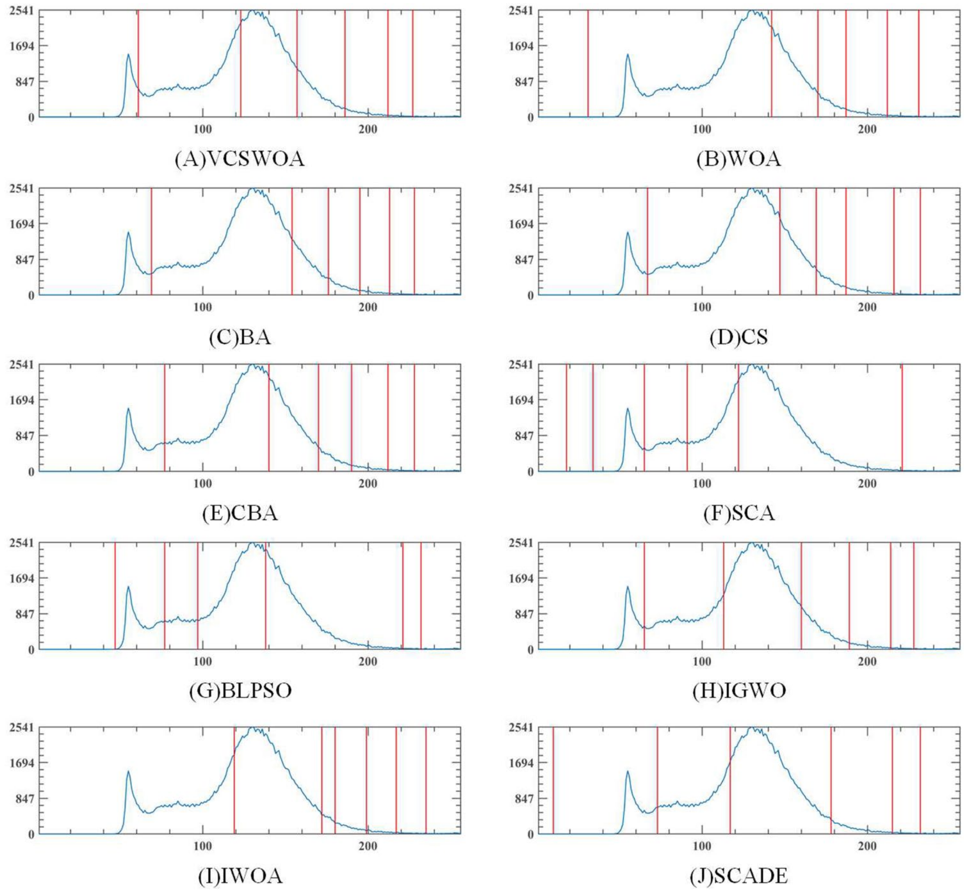

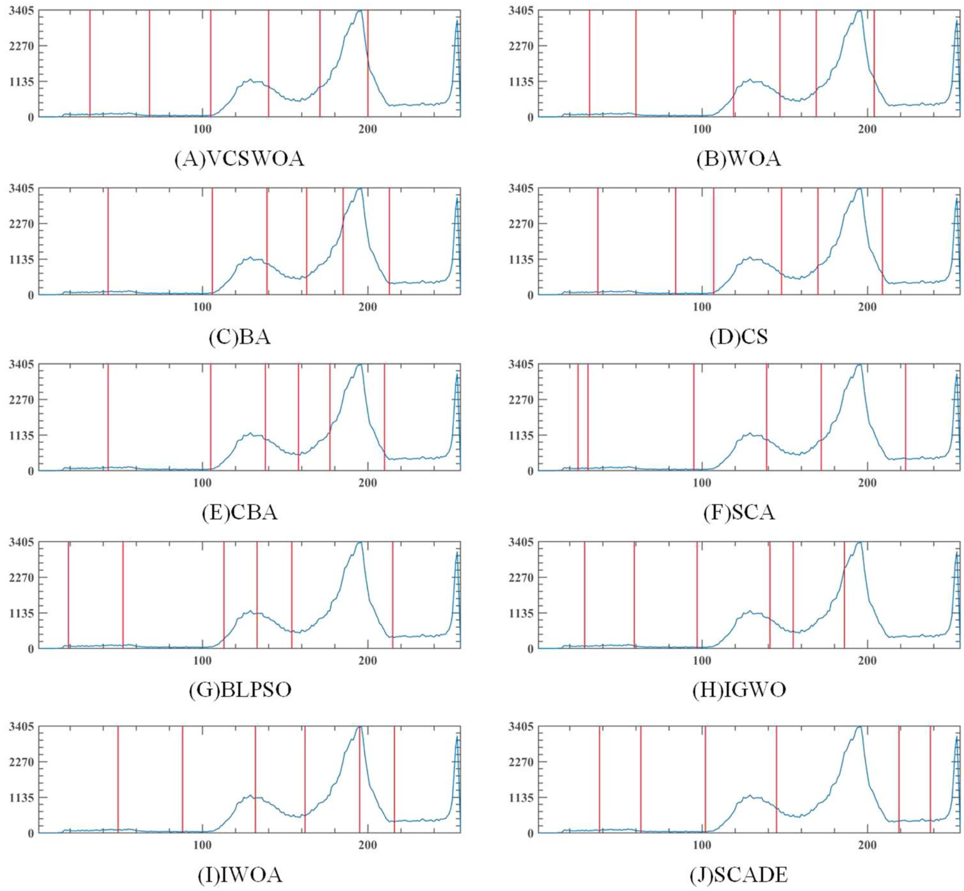

Fig. 16 Threshold values of 61,060 obtained by each algorithm at level 6

Fig. 17 Threshold values of 38,092 obtained by each algorithm at level 6

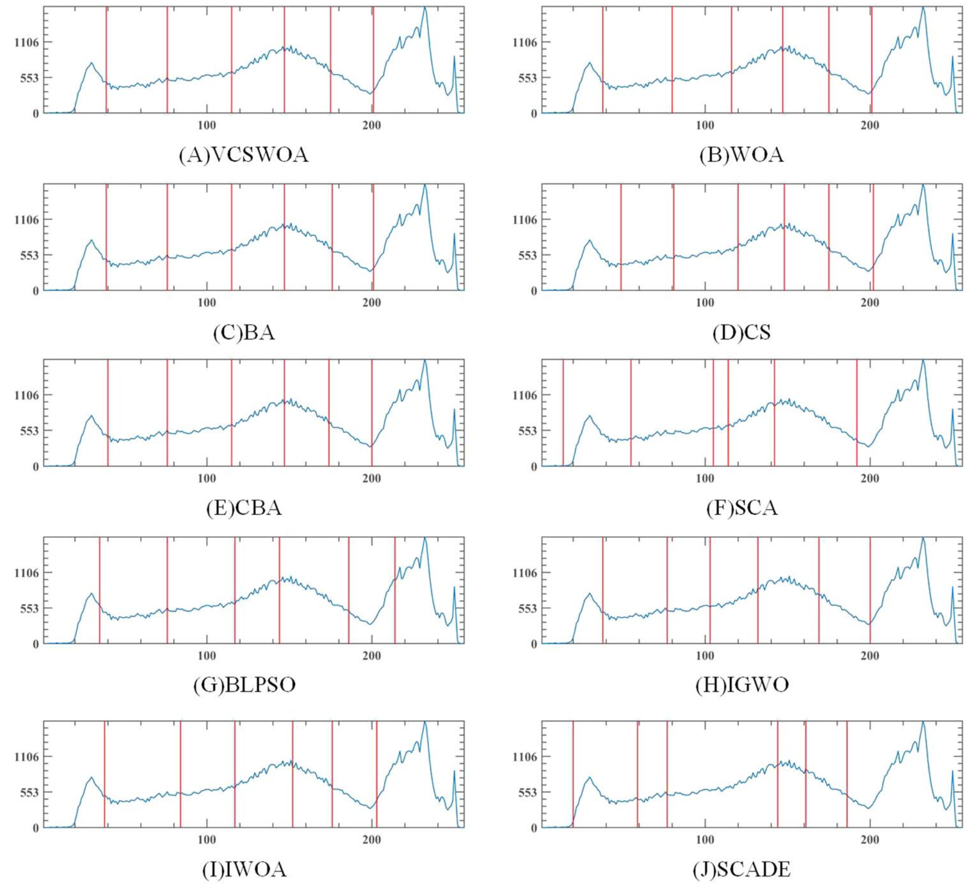

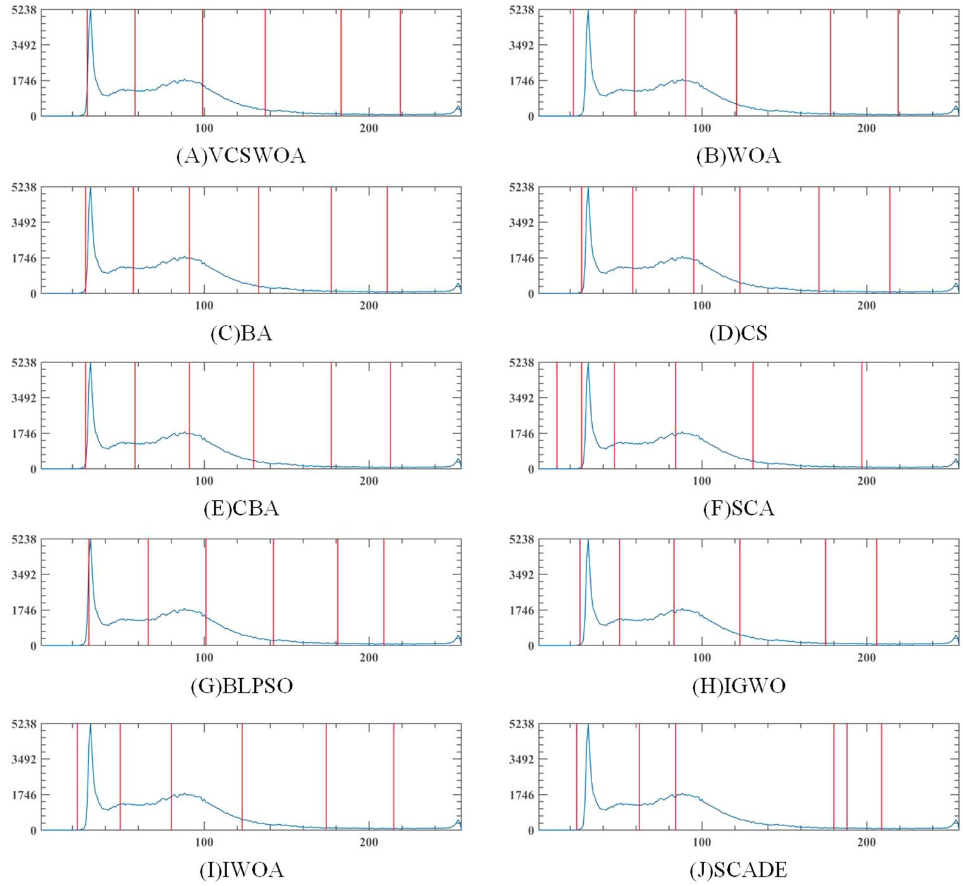

Fig. 18 Threshold values of 19,021 obtained by each algorithm at level 6

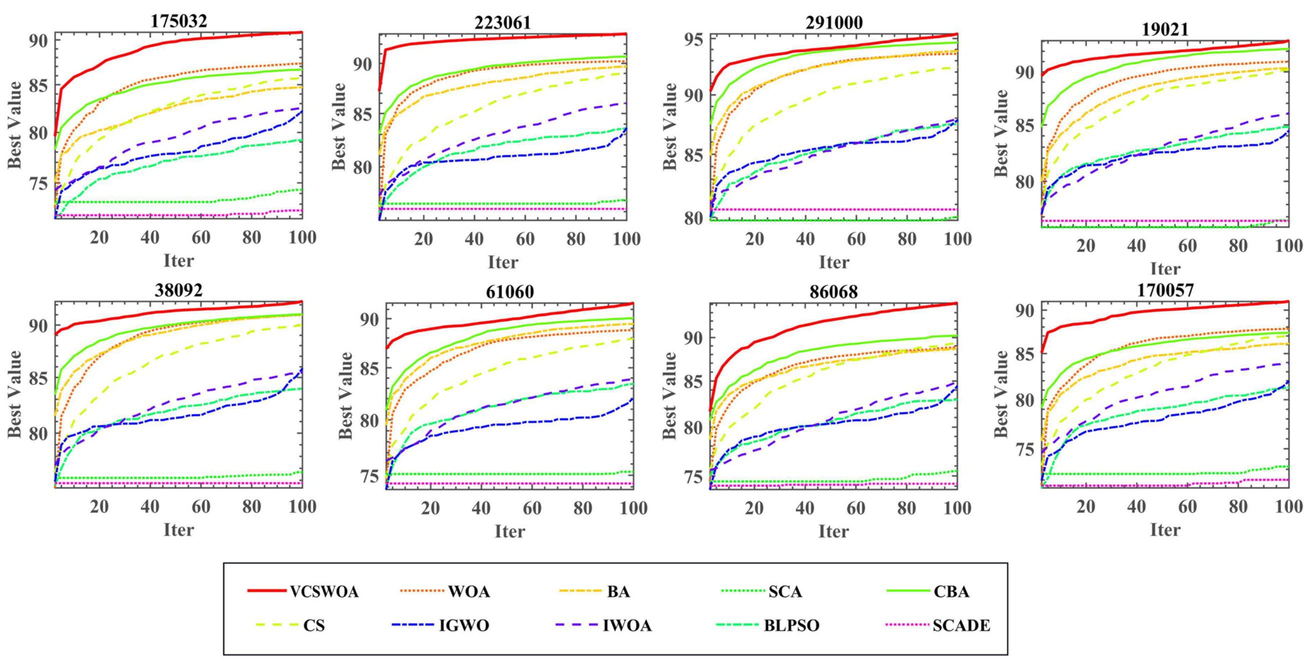

Fig. 19 Convergence curves of Kapur's entropy at threshold value 18

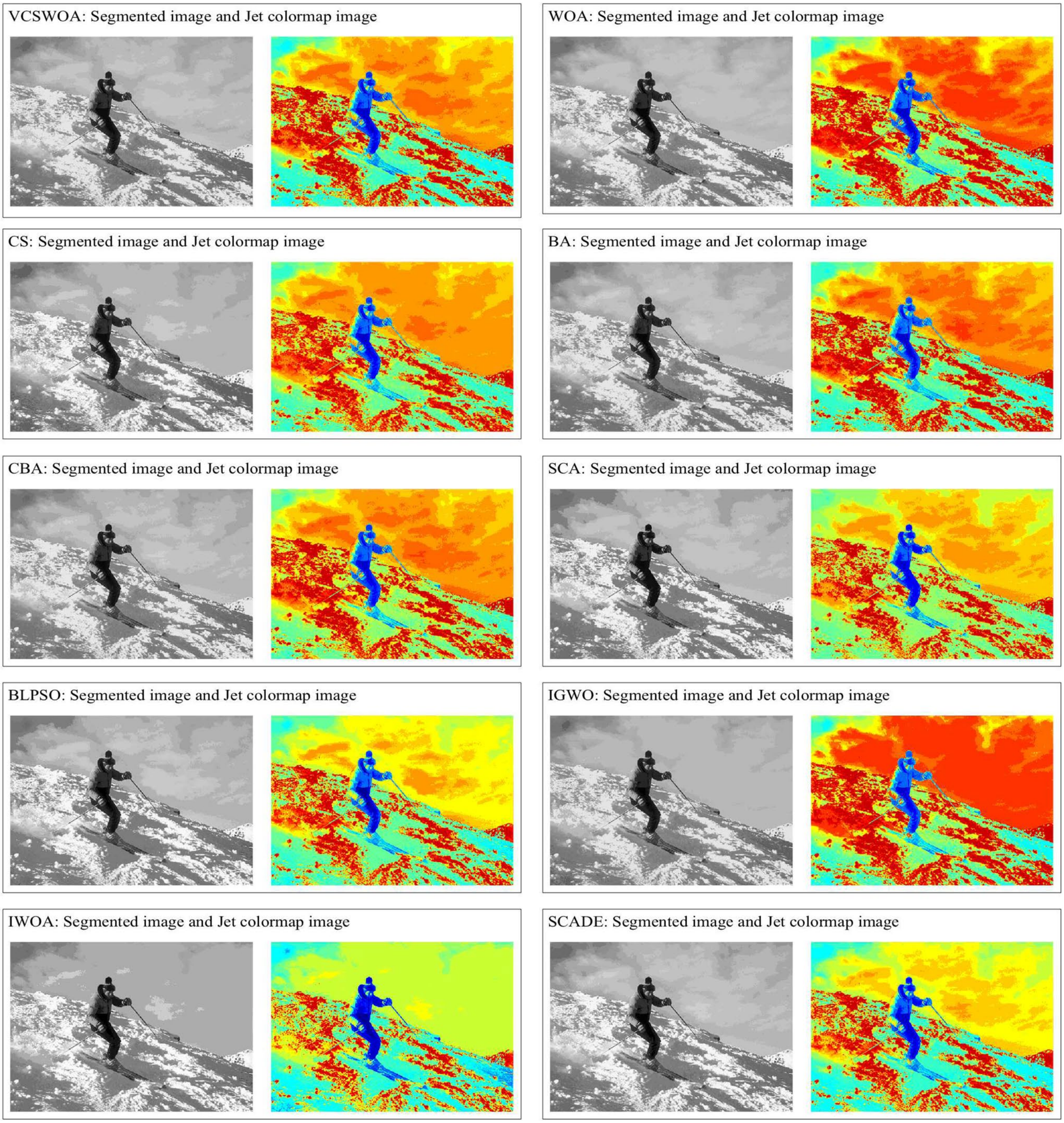

Fig. 20 Segmented results of 61,060 obtained by each algorithm at threshold value 18

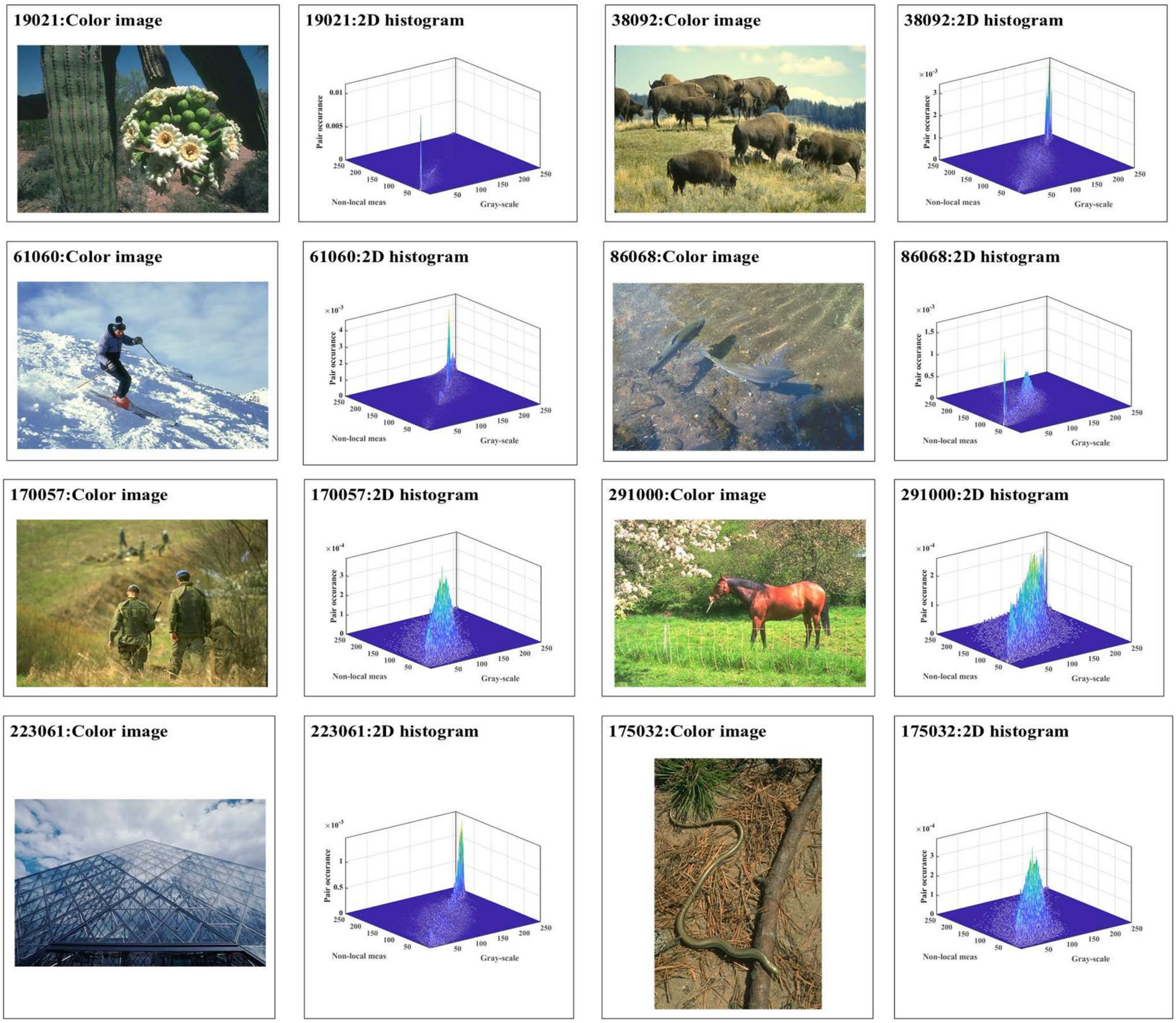

Fig. 21 Samples of the segmented images

Declarations

Conflict of interest The authors declare that they have no conflict of interest.

Ethical approval This article does not contain any studies with human participants or animals performed by any of the authors.

Informed consent Informed consent was obtained from all individual participants included in the study.

References

1. Simon D (2008) Biogeography-based optimization. IEEE Trans Evol Comput 12(6):702–713
2. Hassanien AE, Emary E (2018) Swarm intelligence: principles, advances, and applications. CRC Press, Boca Raton
3. Abualigah L, Gandomi AH, Elaziz MA, Hussien AG, Khasawneh AM, Alshinwan M, Houssein EH (2020) Nature-inspired optimization algorithms for text document clustering-a comprehensive analysis. Algorithms 13(12):345
4. Holland JH (1992) Genetic algorithms. Sci Am 267(1):66–73
5. Rechenberg I (1978) Evolutionsstrategien. In: Schneider B, Ranft U (eds) Simulationsmethoden in der Medizin und Biologie. Medizinische Informatik und Statistik, vol 8. Springer, Berlin, Heidelberg. Berthold Schneider, Ulrich Ranft. https://doi.org/10.1007/978-3-642-81283-5_8
6. Koza JR, Koza JR (1992) Genetic programming: on the programming of computers by means of natural selection, vol 1. MIT Press, Cambridge
7. Wang T, Liu W, Zhao J, Guo X, Terzija V (2020) A rough set-based bio-inspired fault diagnosis method for electrical

substations. Int J Elec Power Energy Syst 119:105961. https://doi.org/10.1016/j.ijepes.2020.105961
8. Kennedy J, Eberhart R (1995) Particle swarm optimization. In: Proceedings of ICNN'95-international conference on neural networks, vol 4. IEEE, pp 1942–1948
9. Dorigo M, Maniezzo V, Colorni A (1996) Ant system: optimization by a colony of cooperating agents. IEEE Trans Syst Man Cybern Part B (Cybern) 26(1):29–41
10. Heidari AA, Mirjalili S, Faris H, Aljarah I, Mafarja M, Chen H (2019) Harris hawks optimization: algorithm and applications. Future Gener Comput Syst 97:849–872
11. Li MD, Zhao H, Weng XW, Han T (2016) A novel nature-inspired algorithm for optimization: virus colony search. Adv Eng Softw 92:65–88
12. Li S, Chen H, Wang M, Heidari AA, Mirjalili S (2020) Slime mould algorithm: a new method for stochastic optimization. Future Gener Comput Syst 111:300–323
13. Yang Y, Chen H, Heidari AA, Gandomi AH (2021) Hunger games search: visions, conception, implementation, deep analysis, perspectives, and towards performance shifts. Expert Syst Appl 177:114864
14. Ahmadianfar I, Heidari AA, Gandomi AH, Chu X, Chen H (2021) Run beyond the metaphor: an efficient optimization algorithm based on runge kutta method. Expert Syst Appl 181:115079
15. Kirkpatrick S, Gelatt CD, Vecchi MP (1983) Optimization by simulated annealing. Science 220(4598):671–680
16. Rashedi E, Nezamabadi-Pour H, Saryazdi S (2009) GSA: a gravitational search algorithm. Inf Sci 179(13):2232–2248
17. Rao RV, Savsani VJ, Vakharia D (2012) Teaching-learning-based optimization: an optimization method for continuous non-linear large scale problems. Inf Sci 183(1):1–15
18. Glover F (1989) Tabu search-part i. ORSA J Comput 1(3):190–206
19. Ba AF, Huang H, Wang M, Ye X, Gu Z, Chen H, Cai X (2020) Levy-based antlion-inspired optimizers with orthogonal learning scheme. Eng Comput. https://doi.org/10.1007/s00366-020-01042-7
20. Liang X, Cai Z, Wang M, Zhao X, Chen H, Li C (2020) Chaotic oppositional sine–cosine method for solving global optimization problems. Eng Comput. https://doi.org/10.1007/s00366-020-01083-y
21. Hu L, Li H, Cai Z, Lin F, Hong G, Chen H, Lu Z (2017) A new machine-learning method to prognosticate paraquat poisoned patients by combining coagulation, liver, and kidney indices. PLoS One 12(10):e0186427
22. Huang H, Zhou S, Jiang J, Chen H, Li Y, Li C (2019) A new fruit fly optimization algorithm enhanced support vector machine for diagnosis of breast cancer based on high-level features. BMC Bioinform 20(8):1–14
23. Li C, Hou L, Sharma BY, Li H, Chen C, Li Y, Zhao X, Huang H, Cai Z, Chen H (2018) Developing a new intelligent system for the diagnosis of tuberculous pleural effusion. Comput Methods Programs Biomed 153:211–225
24. Zhao X, Zhang X, Cai Z, Tian X, Wang X, Huang Y, Chen H, Hu L (2019) Chaos enhanced grey wolf optimization wrapped elm for diagnosis of paraquat-poisoned patients. Comput Biol Chem 78:481–490
25. Pang J, Zhou H, Tsai Y-C, Chou F-D (2018) A scatter simulated annealing algorithm for the bi-objective scheduling problem for the wet station of semiconductor manufacturing. Comput Ind Eng 123:54–66. https://doi.org/10.1016/j.cie.2018.06.017
26. Zhou H, Pang J, Chen P-K, Chou F-D (2018) A modified particle swarm optimization algorithm for a batch-processing machine scheduling problem with arbitrary release times and non-identical job sizes. Comput Ind Eng 123:67–81. https://doi.org/10.1016/j.cie.2018.06.018
27. Li Q, Chen H, Huang H, Zhao X, Cai Z, Tong C, Liu W, Tian X (2017) An enhanced grey wolf optimization based feature selection wrapped kernel extreme learning machine for medical diagnosis. Comput Math Methods Med. https://doi.org/10.1155/2017/9512741
28. Liu T, Hu L, Ma C, Wang Z-Y, Chen H-L (2015) A fast approach for detection of erythemato-squamous diseases based on extreme learning machine with maximum relevance minimum redundancy feature selection. Int J Syst Sci 46(5):919–931
29. Zhang Y, Liu R, Wang X et al (2021) Boosted binary Harris hawks optimizer and feature selection. Eng Comput 37:3741–3770
30. Chen M, Zeng G, Lu K, Weng J (2019) A two-layer nonlinear combination method for short-term wind speed prediction based on elm, enn, and lstm. IEEE Internet Things J 6(4):6997–7010. https://doi.org/10.1109/JIOT.2019.2913176
31. Ba AF, Huang H, Wang M, Ye X, Gu Z, Chen H, Cai X (2020) Levy-based antlion-inspired optimizers with orthogonal learning scheme. Eng Comput 1–22. https://doi.org/10.1007/s00366-020-01042-7
32. Liang X, Cai Z, Wang M, Zhao X, Chen H, Li C (2020) Chaotic oppositional sine–cosine method for solving global optimization problems. Eng Comput 1–17
33. Zhang H, Cai Z, Ye X, Wang M, Kuang F, Chen H, Li C, Li Y (2020) A multi-strategy enhanced salp swarm algorithm for global optimization. Eng Comput 1–27
34. Zeng G-Q, Lu Y-Z, Mao W-J (2011) Modified extremal optimization for the hard maximum satisfiability problem. J Zhejiang Univ Sci C 12(7):589–596
35. Zeng G, Lu Y, Dai Y, Wu Z, Mao W, Zhang Z, Zheng CJI-JICIC (2012) Backbone guided extremal optimization for the hard maximum satisfiability problem. Int J Innov Comput Inf Control 8(12):8355–8366
36. Cai Z, Gu J, Luo J, Zhang Q, Chen H, Pan Z, Li Y, Li C (2019) Evolving an optimal kernel extreme learning machine by using an enhanced grey wolf optimization strategy. Expert Syst Appl 138:112814
37. Yu C, Chen M, Cheng K, Zhao X, Ma C, Kuang F, Chen H (2021) SGOA: annealing-behaved grasshopper optimizer for global tasks. Eng Comput. https://doi.org/10.1007/s00366-020-01234-1
38. Shen L, Chen H, Yu Z, Kang W, Zhang B, Li H, Yang B, Liu D (2016) Evolving support vector machines using fruit fly optimization for medical data classification. Knowl Based Syst 96:61–75
39. Wang M, Chen H (2020) Chaotic multi-swarm whale optimizer boosted support vector machine for medical diagnosis. Appl Soft Comput 88:105946
40. Wang M, Chen H, Yang B, Zhao X, Hu L, Cai Z, Huang H, Tong C (2017) Toward an optimal kernel extreme learning machine using a chaotic moth-flame optimization strategy with applications in medical diagnoses. Neurocomputing 267:69–84
41. Zeng G-Q, Chen J, Dai Y-X, Li L-M, Zheng C-W, Chen M-RJN (2015) Design of fractional order pid controller for automatic regulator voltage system based on multi-objective extremal optimization. Neurocomputing 160:173–184
42. Zeng G-Q, Lu K-D, Dai Y-X, Zhang Z-J, Chen M-R, Zheng C-W, Wu D, Peng W-WJN (2014) Binary-coded extremal optimization for the design of pid controllers. Neurocomputing 138:180–188
43. Zeng G-Q, Xie X-Q, Chen M-R, Weng J (2019) Adaptive population extremal optimization-based pid neural network for multivariable nonlinear control systems. Swarm Evol Comput 44:320–334. https://doi.org/10.1016/j.swevo.2018.04.008

44. Zhao X, Li D, Yang B, Chen H, Yang X, Yu C, Liu S (2015) A two-stage feature selection method with its application. Comput Electr Eng 47:114–125
45. Zhao X, Li D, Yang B, Ma C, Zhu Y, Chen H (2014) Feature selection based on improved ant colony optimization for online detection of foreign fiber in cotton. Appl Soft Comput 24:585–596
46. Pei H, Yang B, Liu J, Chang K (2020) Active surveillance via group sparse Bayesian learning. IEEE Trans Pattern Anal Mach Intell. https://doi.org/10.1109/TPAMI.2020.3023092
47. Xue X, Chen Z, Wang S, Feng Z, Duan Y, Zhou Z (2020) Value entropy: a systematic evaluation model of service ecosystem evolution. IEEE Trans Serv Comput. https://doi.org/10.1109/TSC.2020.3016660
48. Xue X, Wang SF, Zhan LJ, Feng ZY, Guo YD (2019) Social learning evolution (sle): computational experiment-based modeling framework of social manufacturing. IEEE Trans Ind Inform 15(6):3343–3355. https://doi.org/10.1109/tii.2018.2871167
49. Li J, Soladie C, Seguier R (2020) Local temporal pattern and data augmentation for micro-expression spotting. IEEE Trans Affect Comput. https://doi.org/10.1109/TAFFC.2020.3023821
50. Wang S-J, He Y, Li J, Fu X (2011) Mesnet: a convolutional neural network for spotting multi-scale micro-expression intervals in long videos. IEEE Trans Image Process. https://doi.org/10.1109/TIP.2021.3064258
51. Tu J, Lin A, Chen H, Li Y, Li C (2019) Predict the entrepreneurial intention of fresh graduate students based on an adaptive support vector machine framework. Math Probl Eng 2019:1–16
52. Wei Y, Ni N, Liu D, Chen H, Wang M, Li Q, Cui X, Ye H (2017) An improved grey wolf optimization strategy enhanced svm and its application in predicting the second major. Math Probl Eng 2017:1–12
53. Mirjalili S, Lewis A (2016) The whale optimization algorithm. Adv Eng Softw 95:51–67
54. Hussien AG, Hassanien AE, Houssein EH, Amin M, Azar AT (2019) New binary whale optimization algorithm for discrete optimization problems. Eng Optim 1–15
55. Aljarah I, Faris H, Mirjalili S (2018) Optimizing connection weights in neural networks using the whale optimization algorithm. Soft Comput 22(1):1–15
56. Elaziz MA, Mirjalili S (2019) A hyper-heuristic for improving the initial population of whale optimization algorithm. Knowl Based Syst 172:42–63
57. Emary E, Zawbaa HM, Sharawi M (2019) Impact of lèvy flight on modern meta-heuristic optimizers. Appl Soft Comput 75:775–789
58. Oliva D, El Aziz MA, Hassanien AE (2017) Parameter estimation of photovoltaic cells using an improved chaotic whale optimization algorithm. Appl Energy 200:141–154
59. Xiong G, Zhang J, Shi D, He Y (2018) Parameter extraction of solar photovoltaic models using an improved whale optimization algorithm. Energy Convers Manag 174:388–405
60. Chen H, Xu Y, Wang M, Zhao X (2019) A balanced whale optimization algorithm for constrained engineering design problems. Appl Math Model 71:45–59
61. Mafarja MM, Mirjalili S (2017) Hybrid whale optimization algorithm with simulated annealing for feature selection. Neurocomputing 260:302–312
62. Abdel-Basset M, El-Shahat D, El-Henawy I, Sangaiah AK, Ahmed SH (2018) A novel whale optimization algorithm for cryptanalysis in Merkle–Hellman cryptosystem. Mob Netw Appl 23(4):723–733
63. Jadhav AN, Gomathi N (2018) Wgc: hybridization of exponential grey wolf optimizer with whale optimization for data clustering. Alex Eng J 57(3):1569–1584
64. Agrawal R, Kaur B, Sharma S (2020) Quantum based whale optimization algorithm for wrapper feature selection. Appl Soft Comput 89:106092
65. Salgotra R, Singh U, Saha S (2019) On some improved versions of whale optimization algorithm. Arabian J Sci Eng 44(11):9653–9691
66. Hussien AG, Houssein EH, Hassanien AE (2017) A binary whale optimization algorithm with hyperbolic tangent fitness function for feature selection. In: 2017 Eighth international conference on intelligent computing and information systems (ICICIS). IEEE, pp 166–172
67. Hussien AG, Hassanien AE, Houssein EH, Bhattacharyya S, Amin M (2019) S-shaped binary whale optimization algorithm for feature selection. In: Recent trends in signal and image processing. Springer, pp 79–87
68. Hemasian-Etefagh F, Safi-Esfahani F (2019) Group-based whale optimization algorithm. Soft Comput 1–27
69. Hassib EM, El-Desouky AI, Labib LM, El-kenawy E-SM (2019) Woa+ brnn: an imbalanced big data classification framework using whale optimization and deep neural network. Soft Comput 1–20
70. Liu M, Yao X, Li Y (2020) Hybrid whale optimization algorithm enhanced with lévy flight and differential evolution for job shop scheduling problems. Appl Soft Comput 87:105954
71. Jiang R, Yang M, Wang S, Chao T (2020) An improved whale optimization algorithm with armed force program and strategic adjustment. Appl Math Model 81:603–623
72. Guo W, Liu T, Dai F, Xu P (2020) An improved whale optimization algorithm for forecasting water resources demand. Appl Soft Comput 86:105925
73. Got A, Moussaoui A, Zouache D (2020) A guided population archive whale optimization algorithm for solving multiobjective optimization problems. Expert Syst Appl 141:112972
74. Abdel-Basset M, Manogaran G, El-Shahat D, Mirjalili S (2018) Integrating the whale algorithm with tabu search for quadratic assignment problem: a new approach for locating hospital departments. Appl Soft Comput 73:530–546
75. Tharwat A, Moemen YS, Hassanien AE (2017) Classification of toxicity effects of biotransformed hepatic drugs using whale optimized support vector machines. J Biomed Inform 68:132–149
76. Zhao D, Liu H, Zheng Y, He Y, Lu D, Lyu C (2019) Whale optimized mixed kernel function of support vector machine for colorectal cancer diagnosis. J Biomed Inform 92:103124
77. Gharehchopogh FS, Gholizadeh H (2019) A comprehensive survey: Whale optimization algorithm and its applications. Swarm Evol Comput 48:1–24
78. Shahinzadeh H, Gharehpetian GB, Moazzami M, Moradi J, Hosseinian SH (2017) Unit commitment in smart grids with wind farms using virus colony search algorithm and considering adopted bidding strategy. In: 2017 Smart Grid Conference (SGC). IEEE, pp 1–9
79. Jayasena KPN, Li L, Elaziz MA, Xiong S (2018) Multi-objective energy efficient resource allocation using virus colony search (vcs) algorithm. In: 2018 IEEE 20th international conference on high performance computing and communications; IEEE 16th international conference on smart city; IEEE 4th international conference on data science and systems (HPCC/SmartCity/DSS). IEEE, pp 766–773
80. Hosseini S, Moradian M, Shahinzadeh H, Ahmadi S (2018) Optimal placement of distributed generators with regard to reliability assessment using virus colony search algorithm. Int J Renew Energy Res (IJRER) 8(2):714–723
81. Yousri D, Allam D, Eteiba M (2019) Chaotic whale optimizer variants for parameters estimation of the chaotic behavior in permanent magnet synchronous motor. Appl Soft Comput 74:479–503

82. Elaziz MA, Oliva D (2018) Parameter estimation of solar cells diode models by an improved opposition-based whale optimization algorithm. Energy Convers Manag 171:1843–1859
83. Elhosseini MA, Haikal AY, Badawy M, Khashan N (2019) Biped robot stability based on an a-c parametric whale optimization algorithm. J Comput Sci 31:17–32
84. Tubishat M, Abushariah MA, Idris N, Aljarah I (2019) Improved whale optimization algorithm for feature selection in arabic sentiment analysis. Appl Intell 49(5):1688–1707
85. He Y, Dai L, Zhang H (2020) Multi-branch deep residual learning for clustering and beamforming in user-centric network. IEEE Commun Lett 24(10):2221–2225. https://doi.org/10.1109/LCOMM.2020.3005947
86. Yan J, Meng Y, Yang X, Luo X, Guan X (2021) Privacy-preserving localization for underwater sensor networks via deep reinforcement learning. IEEE Trans Inform Forensics Secur 16:1880–1895. https://doi.org/10.1109/TIFS.2020.3045320
87. García S, Molina D, Lozano M, Herrera F (2009) A study on the use of non-parametric tests for analyzing the evolutionary algorithms' behaviour: a case study on the cec'2005 special session on real parameter optimization. J Heuristics 15(6):617
88. Hussien AG, Oliva D, Houssein EH, Juan AA, Yu X (2020) Binary whale optimization algorithm for dimensionality reduction. Mathematics 8(10):1821
89. Mirjalili S, Mirjalili SM, Lewis A (2014) Grey wolf optimizer. Adv Eng Softw 69:46–61
90. Hussien AG, Amin M, Abd El Aziz M (2020) A comprehensive review of moth-flame optimisation: variants, hybrids, and applications. J Exp Theor Artif Intell 1–21
91. Kaveh A, Talatahari S (2010) An improved ant colony optimization for constrained engineering design problems. Eng Comput. https://doi.org/10.1108/02644401011008577
92. He Q, Wang L (2007) A hybrid particle swarm optimization with a feasibility-based rule for constrained optimization. Appl Math Comput 186(2):1407–1422
93. Gandomi AH, Yang X-S, Alavi AH, Talatahari S (2013) Bat algorithm for constrained optimization tasks. Neural Comput Appl 22(6):1239–1255
94. Hussien AG (2021) An enhanced opposition-based salp swarm algorithm for global optimization and engineering problems. J Ambient Intell Humaniz Comput 1–22
95. Liu Y, Zhang Z, Liu X, Wang L, Xia X (2021) Efficient image segmentation based on deep learning for mineral image classification. Adv Powder Technol 32(10):3885–3903
96. Liu Y, Zhang Z, Liu X, Wang L, Xia X (2021) Ore image classification based on small deep learning model: Evaluation and optimization of model depth, model structure and data size. Miner Eng 172:107020. https://doi.org/10.1016/j.mineng.2021.107020
97. Otsu N (1979) A threshold selection method from gray-level histograms. IEEE Trans Syst Man Cybern 9(1):62–66
98. Kapur JN, Sahoo PK, Wong AK (1985) A new method for gray-level picture thresholding using the entropy of the histogram. Comput Vis Graph Image Process 29(3):273–285
99. Huynh-Thu Q, Ghanbari M (2008) Scope of validity of psnr in image/video quality assessment. Electron Lett 44(13):800–801
100. Wang Z, Bovik AC, Sheikh HR, Simoncelli EP (2004) Image quality assessment: from error visibility to structural similarity. IEEE Trans Image Process 13(4):600–612
101. Zhang L, Zhang L, Mou X, Zhang D (2011) Fsim: a feature similarity index for image quality assessment. IEEE Trans Image Process 20(8):2378–2386
102. Qiu S, Wang Z, Zhao H, Hu H (2016) Using distributed wearable sensors to measure and evaluate human lower limb motions. IEEE Tran Instrum Meas 65(4):939–950
103. Yang C, Zhao H, Bruzzone L, Benediktsson JA, Liang Y, Liu B, Zeng X, Guan R, Li C, Ouyang Z (2020) Lunar impact crater identification and age estimation with Chang'e data by deep and transfer learning. Nat Commun 11(1):6358. https://doi.org/10.1038/s41467-020-20215-y
104. Li J, Chen C, Chen H, Tong C (2017) Towards context-aware social recommendation via individual trust. Knowl Based Syst 127:58–66. https://doi.org/10.1016/j.knosys.2017.02.032
105. Li J, Lin J (2020) A probability distribution detection based hybrid ensemble qos prediction approach. Inf Sci 519:289–305. https://doi.org/10.1016/j.ins.2020.01.046
106. Li J, Zheng X-L, Chen S-T, Song W-W, Chen D-R (2014) An efficient and reliable approach for quality-of-service-aware service composition. Inf Sci 269:238–254. https://doi.org/10.1016/j.ins.2013.12.015
107. Jin L, Wen Z, Hu Z (2020) Topology-preserving nonlinear shape registration on the shape manifold. Multimed Tools Appl 1–13
108. Wu X, Xu X, Liu J, Wang H, Hu B, Nie FJ (2020) Supervised feature selection with orthogonal regression and feature weighting. IEEE Trans Neural Netw Learn Syst. https://doi.org/10.1109/TNNLS.2020.2991336
109. Deng W, Xu J, Zhao H, Song Y (2020) A novel gate resource allocation method using improved pso-based qea. IEEE Trans Intell Transp Syst. https://doi.org/10.1109/TITS.2020.3025796
110. W D, JJ X, YJ S, HM Z (2020) An effective improved co-evolution ant colony optimization algorithm with multi-strategies and its application. Int J Bioinspired Comput 16(3):158–170
111. Wang X, Bennamoun M, Sohel F, Lei H (2021) Diffusion geometry derived keypoints and local descriptors for 3d deformable shape analysis. J Circuits Syst Comput 30(01):2150016
112. Wang X, Sohel F, Bennamoun M, Guo Y, Lei H (2017) Scale space clustering evolution for salient region detection on 3d deformable shapes. Pattern Recognit 71:414–427
113. Feng C, Zhu Z, Cui Z, Ushakov V, Dreher J, Luo W, Gu R, Wu X, Krueger F (2021) Prediction of trust propensity from intrinsic brain morphology and functional connectome. Hum Brain Mapp 42(1):175–191
114. Li Q, Wu X, Liu T (2021) Differentiable neural architecture search for optimal spatial/temporal brain function network decomposition. Med Image Anal 69:101974. https://doi.org/10.1016/j.media.2021.101974
115. Zhang L, Zhang Z, Wang W, Jin Z, Su Y, Chen H (2021) Research on a covert communication model realized by using smart contracts in blockchain environment. IEEE Syst J. https://doi.org/10.1109/JSYST.2021.3057333
116. Zhang L, Zhang Z, Wang W, Waqas R, Zhao C, Kim S, Chen H (2020) A covert communication method using special bitcoin addresses generated by vanitygen. Comput Mater Continua 65(1):597–616 http://www.techscience.com/cmc/v65n1/39585
117. Zhang L, Zou Y, Wang W, Jin Z, Su Y, Chen H (2021) Resource allocation and trust computing for blockchain-enabled edge computing system. Comput Secur. https://doi.org/10.1016/j.cose.2021.102249
118. Chen H, Yang B, Liu J, Zhou X-N, Philip SY (2019) Mining spatiotemporal diffusion network: a new framework of active surveillance planning. IEEE Access 7:108458–108473
119. Luo J, Li M, Liu X, Tian W, Zhong S,... Shi K (2020) Stabilization analysis for fuzzy systems with a switched sampled-data control. J Franklin Inst 357(1):39–58. https://doi.org/10.1016/j.jfranklin.2019.09.029
120. Liu X, Yang B, Chen H, Musial K, Chen H, Li Y, Zuo W (2021) A scalable redefined stochastic blockmodel. ACM Trans Knowl Discov Data (TKDD) 15(3):1–28
121. Cao X, Cao T, Gao F, Guan X (2021) Risk-averse storage planning for improving res hosting capacity under uncertain siting choice. IEEE Trans Sustain Energy. https://doi.org/10.1109/TSTE.2021.3075615

122. Fei X, Wang J, Ying S, Hu Z, Shi J (2020) Projective parameter transfer based sparse multiple empirical kernel learning machine for diagnosis of brain disease. Neurocomputing 413:271–283. https://doi.org/10.1016/j.neucom.2020.07.008
123. Hu Z, Wang J, Zhang C, Luo Z, Luo X, Xiao L, Shi J, Uncertainty modeling for multi center autism spectrum disorder classification using takagi-sugeno-kang fuzzy systems. IEEE Trans Cogn Dev Syst
124. Saber A, Sakr M, Abo-Seida OM, Keshk A, Chen H (2021) A novel deep-learning model for automatic detection and classification of breast cancer using the transfer-learning technique. IEEE Access 9:71194–71209. https://doi.org/10.1109/ACCESS.2021.3079204
125. Qiu S, Wang Z, Zhao H, Qin K, Li Z, Hu H (2018) Inertial/magnetic sensors based pedestrian dead reckoning by means of multi-sensor fusion. Inf Fusion 39:108–119
126. Huang P, Zhao L, Jiang R, Wang T, Zhang X (2021) Self-filtering image dehazing with self-supporting module. Neurocomputing 432:57–69
127. Wang T, Zhao L, Huang P, Zhang X, Xu J (2021) Haze concentration adaptive network for image dehazing. Neurocomputing 439:75–85
128. Zhang X, Wang T, Wang J, Tang G, Zhao L (2020) Pyramid channel-based feature attention network for image dehazing. Comput Vis Image Underst 197–198:103003. https://doi.org/10.1016/j.cviu.2020.103003
129. Zhou W, Yu L, Zhou Y, Qiu W, Wu M,... Luo T (2018) Local and Global Feature Learning for Blind Quality Evaluation of Screen Content and Natural Scene Images. IEEE Trans Image Process 27(5):2086–2095. https://doi.org/10.1109/TIP.2018.2794207
130. Zhang X, Fan M, Wang D, Zhou P, Tao D Top-k feature selection framework using robust 0-1 integer programming. IEEE Trans Neural Netw Learn Syst
131. Zhang X, Li W, Ye X, Maybank S (2015) Robust hand tracking via novel multi-cue integration. Neurocomputing 157:296–305